AD-770 096

SAN FRANCISCO VESSEL TRAFFIC SYSTEM TEST OF THE AN/FPS-109 (XN-1) VESSEL TRAFFIC SYSTEM MANUAL RADAR

I. J. Shepperd

Johns Hopkins University

Prepared for:

Coast Guard
Department of the Navy

May 1973

Technical Report Documentation Page

1. Report No.	2. Government Accession No.	3. Recipient's Catalog No.
732222.02/02		AD 770 096

4. Title and Subtitle	5. Report Date
SAN FRANCISCO VESSEL TRAFFIC SYSTEM TEST OF THE AN/FPS-109 (XN-1) VESSEL TRAFFIC SYSTEM MANUAL RADAR - TEST RESULTS	May 1973
	6. Performing Organization Code
7. Author(s) I. J. Shepperd	8. Performing Organization Report No. MS-383
9. Performing Organization Name and Address The Johns Hopkins University Applied Physics Laboratory 8621 Georgia Avenue, Silver Spring, Maryland 20910	10. Work Unit No. (TRAIS) 732222.02
	11. Contract or Grant No. DOT-CG-03,301-B
12. Sponsoring Agency Name and Address Commandant (GDET/62) U. S. Coast Guard Headquarters Washington, D. C. 20590	13. Type of Report and Period Covered Test Results 3/2/73 - 4/30/73
	14. Sponsoring Agency Code

15. Supplementary Notes

16. Abstract

This report presents the results of engineering tests made on the U.S. Coast Guard Vessel Traffic System (VTS) radars, the AN/FPS-109 (XN-1), which are installed at Yerba Buena Island (YBI) in the San Francisco Bay and at Point Bonita (PTB) overlooking the seaward approach to the Bay. Two types of tests were conducted. The first type consisted of measurements of antenna beam patterns of the YBI antenna, radiated power, transmitter and receiver characteristics, display characteristics, and PTB/YBI data link performance. The second type of tests was concerned with performance measurements and included maximum detection range in clear and clutter environments, coverage as a function of elevation angle, realizable range and angle resolution, and the utility of the various radar and display operating modes.

It was found that the radars met or exceeded all significant performance and parameter specifications, except the receiver noise figures for all receivers were higher than specified and the cosecant-squared antenna pattern coverage of the YBI radar did not meet the specifications.

17. Key Words	18. Distribution Statement
Radar Performance Tests Navigation System Vessel Traffic System	Document is available to the public through the National Technical Information Service, Springfield, Virginia 22151

19. Security Classif. (of this report)	20. Security Classif. (of this page)	21. No. of Pages	22. Price
UNCLASSIFIED	UNCLASSIFIED	124	

Form DOT F 1700.7 (8-72) Reproduction of completed p

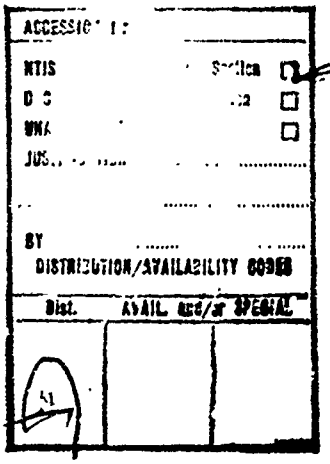

NOTICE

This document is disseminated under the sponsorship of the Department of Transportation in the interest of information exchange. The United States Government assumes no liability for its contents or use thereof.

MS-383
MAY 1973

SAN FRANCISCO VESSEL TRAFFIC SYSTEM
TEST OF THE AN/FPS-109 (XN-1)
VESSEL TRAFFIC SYSTEM MANUAL RADAR

I.J.Shepperd

THE JOHNS HOPKINS UNIVERSITY • APPLIED PHYSICS LABORATORY
8621 Georgia Avenue • Silver Spring, Maryland • 20910
Operating under Contract N00017 72-C-4401 with the Department of the Navy

UNITED STATES COAST GUARD
ENVIRONMENTAL AND TRANSPORTATION
TECHNOLOGY DIVISION REPORT

SAN FRANCISCO VESSEL TRAFFIC SYSTEM TEST OF THE AN/FPS-109 (XN-1) VESSEL TRAFFIC SYSTEM MANUAL RADAR

BY

I. J. SHEPPERD

THE JOHNS HOPKINS UNIVERSITY APPLIED PHYSICS LABORATORY
SILVER SPRING, MARYLAND

This report has been submitted under contract DOT-CG-03,301-B and is subject to the following qualifications:

W. E. Lehr
Commander, U. S. Coast Guard
Chief, Environmental and
Transportation Technology
Division
Washington, D. C. 20590

Dist: NTIS (10)
GDET (20)
DTSS (5)

ABSTRACT

This report presents the results of engineering tests made on the U. S. Coast Guard Vessel Traffic System (VTS) radars, the AN/FPS-109 (XN-1), which are installed at Yerba Buena Island (YBI) in the San Francisco Bay and at Point Bonita (PTB) overlooking the seaward approach to the Bay. Two types of tests were conducted. The first type consisted of measurements of antenna beam patterns of the YBI antenna, radiated power, transmitter and receiver characteristics, display characteristics, and PTB/YBI data link performance. The second type of tests was concerned with performance measurements and included maximum detection range in clear and clutter environments, coverage as a function of elevation angle, realizable range and angle resolution, and the utility of the various radar and display operating modes.

It was found that the radars met or exceeded all significant performance and parameter specifications, except the receiver noise figures for all receivers were higher than specified and the cosecant-squared antenna pattern coverage of the YBI radar did not meet the specifications.

SUMMARY

A series of engineering and operational tests was conducted on the AN/FPS-109(XN-1) Vessel Traffic System (VTS) radars manufactured by the Airborne Instrument Laboratories. These radars are installed at Yerba Buena Island (YBI) in the San Francisco Bay and at Point Bonita (PTB). The basic engineering qualities of the radars (i.e., radiated power, antenna beam patterns, etc.) were measured. In addition, the operational characteristics of the radars in monitoring ship traffic were assessed. The following paragraphs summarize the results of these tests.

Antenna Beam Patterns

The near and far field antenna patterns of the YBI radar were measured by AIL engineers. It was found that the patterns were essentially identical to the patterns measured at the manufacturer's test site.

It was noted that the sidelobe level and the feedhorn spill-over level are larger relative to the main beam as the elevation (depression) angle becomes larger. At large depression angles corresponding to short range (i.e., 1000 yards or less), the sidelobe level and feedhorn spill-over level are a relatively serious source of interference to tracking.

Radiated Power

Measurements of the radiated power were made for both the YBI and the PTB radars in the far field at Pier 45. It was found that the received power in the far field corresponded to within 1 to 2 dB with the computed power density at the receiving point based on measured transmitter power, line losses, and antenna gain.

Transmitted Pulse

The transmitted pulse shape of the radars was measured. The 50-nanosecond pulse was found to have a rise time of 35 nanoseconds, a fall time of 45 nanoseconds, and a 3-dB amplitude width of 50 nanoseconds. The 200-nanosecond pulse typically had a rise time of 45 nanoseconds and a 3-dB

width of 190 nanoseconds. The rise and fall shapes for both the 50- and 200-nanoseconds pulses was essentially exponential, which should minimize spectrum bandwidth requirements.

Receiver Pulse Response

The receiver pulse response was measured by injecting a test signal at the radar operating frequency and observing the receiver output pulse. A test pulse having a 60-nanosecond width at the 3-dB level, a 25-nanosecond rise time, and a 20-nanosecond fall time between the 10- and 90-percent amplitude levels was used.

The observed pulse output of the logarithmic receiver was approximately 95-nanoseconds in width corresponding to the expected value. With the 50-nanosecond transmitted pulse the output pulse width should be 80-nanoseconds which should give an intrinsic range resolution of 40-feet.

The observed pulse output of the experimental linear receiver was 70-nanoseconds in width which also corresponds to the expected value. With the 50-nanosecond radar pulse the linear receiver output pulse width should be 58-nanoseconds which corresponds to an intrinsic range resolution of 30-feet.

Receiver Bandwidths

It was found that the logarithmic receiver bandwidths for the narrow pulse mode of radar transmission at PTB were within the expected value. The logarithmic receiver at YBI was found to have a bandwidth that was slightly smaller than the expected value tolerance but this is not considered to be a serious deficiency. The bandwidth of one logarithmic receiver at YBI and one logarithmic receiver at PTB was measured for the wide pulse mode of transmission and found to be somewhat greater than the expected tolerance value. This is not considered to be a significant deficiency. Bandwidths of the experimental linear IF amplifier were measured after installation in transceiver #1 at YBI and #2 at PTB and were found to be considerably smaller than the expected value for both installations. Nevertheless, the bandwidths measured for the experimental linear IF are considered to be acceptable inasmuch as they are comparable to the expected and measured values for the normally installed logarithmic IF amplifiers in the narrow pulse mode.

Receiver Transfer Function

The logarithmic transfer functions of the receivers at YBI and PTB were measured by injecting a pulsed signal at the operating frequency into a transmission line bidirectional coupler. The receivers were found to have an essentially linear logarithmic transfer function between the input levels of -85 and -40 dBm.

PPI Characteristics

Qualitative tests were made to assess the performance of the PPI displays. Measurements were made of the relative accuracy of the range and bearing cursor and the quality of the display. The range cursor was found to be accurate to within approximately 40 yards. No apparent distortion or warpage of the displays were discovered.

Microwave and UHF Control Links

The fade margin of the microwave and UHF control links between PTB and YBI was measured. A fade margin of at least 30 dB was measured for the microwave link. The UHF control link was found to have a fade margin of at least 23 dB.

YBI Antenna Elevation Coverage

Tests were made to determine the effectiveness of the consecant-squared elevation pattern of the YBI antenna in maintaining a constant echo signal power into the receiver as a function of range. It was found that the receiver input power from a fixed size target was essentially constant within ± 3 dB for a range from 3000 to 8000 yards. At shorter ranges, the power dropped to 10 dB below the 3000-yard figure at 1400 yards. At longer ranges, the received power fell off inversely as the range to the fourth power.

This performance does not meet the specification requirements which call for equal received signal strength from equal size targets at 1200 feet and 8.0 nmi and received signal strengths that are not less than those levels for the same target size at ranges between the specified limits.

Maximum Detection Range

Maximum detection range tests were made in clear and sea state 3 conditions for the YBI radar. The experimental results show that the maximum detection range with linear polarization while the radar is tracking a 4 square meter target is 15.5 nmi, which exceeds the YBI specification requirements of 9.5 nmi and equals the PTB requirements of 15.5 nmi. With circular polarization, the maximum detection range was observed to be 13.3 nmi for a 4 square meter target and 11.8 nmi for a 1 square meter target, both measured figures exceeding the required YBI detection ranges of 9.5 for a 4.0 square meter target and 6.7 nmi for a 1 square meter target.

Sea state 3 detection measurements were made for the YBI and PTB radars using buoys whose equivalent cross section had been measured as targets. Blip-scan measurements on buoy number 1 at Hunters Point with the YBI radar averaged 0.8 for a series of tests. Buoy number 1 has an echoing cross section of 3.6 square meters and is at a range of 4.14 nmi, which is greater than the required detection range of 3.6 nmi for a 4 square meter target. Similarly, measurements from PTB of the return from channel marker number 8 showed an average blip-scan ratio of 0.8. Channel marker number 8 has an equivalent echoing area of 1.07 square meters and is at a range of 3.6 nmi, which is greater than the required 2.5 nmi for a 1 square meter target. The system requirements in sea state 3 are therefore considered to be met.

Tests of the circular polarization mode of the antenna indicated that rain clutter was very effectively reduced in amplitude and the detection of targets, which were otherwise masked when using linear polarization, was possible.

Angle Resolution

Tests of angle resolution were made by having the radar track two 40-foot cutters that were a known distance apart on a radial course toward the radar. When separation into two targets was observed on the PPI display, the range was recorded. Data points were collected at several ranges out to 14,000 yards. The data indicates a mean angular resolution of 0.35 degree. This compares favorably with the measured antenna beamwidth of 0.277 degree.

Range Resolution

Tests of apparent range resolution as observed on the PPI display by the operator were made by injecting 60-nanosecond pulse pairs at the receiver input frequency. The spacing between the pulse pairs was varied and the PPI display monitored for range separation. The range resolution was found to be nearly a direct function of the PPI range scale. The results of the test are summarized in the following table.

Range Resolution Observed on PPI Display

Range Scale (nmi)	Observed Resolution (feet)	
	Logarithmic IF	Linear IF
2	80	60
4	90	90
6	130	130
8	180	170
16	230	290

Sensitivity Time Control

The PPI displays are equipped with a three-position sensitivity time control (STC) arrangement. An operator can select the position that most effectively minimizes the display saturation by clutter. A series of tests of the operational characteristics of this control was made for YBI and PTB. The sample conditions observed showed the value of the STC in preventing saturation; at least one position was usually found to be useful in reducing the clutter saturation effects.

Test Targets

A number of buoys in the coverage areas of the PTB and YBI radars were calibrated as test targets. The receiver input power return from the buoys was measured and the equivalent echoing cross section computed from the radar equation. The known test target characteristics can be used for radar system operational tests conducted on a daily or regular basis.

MAJOR CONCLUSIONS

The VTS radars were found to be deficient in performance in the following areas. The cosecant-squared pattern coverage was not satisfactory at short ranges. The bandwidth of two of the four receivers was slightly less than the expected value. Noise figures for all receivers were higher than those specified. The latter two deficients are not considered to be serious.

Although the antenna beam patterns were essentially as designed and measured by the manufacturer, it is considered that the sidelobe levels and feedhorn spill-over levels are too high at the higher depression angles corresponding to short range. This causes spurious targets to be generated in the short range region, which can be particularly troublesome for the automatic detection system.

The remainder of the measurement characteristics and the performance levels are considered to be within the limits of the specification.

MAJOR RECOMMENDATIONS

Future specifications for VTS radars should emphasize the importance of minimizing the relative sidelobe levels at the higher depression angles of a cosecant-squared antenna.

It is recommended that the antenna elevation angle of the YBI radar be mechanically adjusted upward by 0.5 degree in order to reduce the magnitude of the variation of received signal strength from a target of fixed size as a function of range. It is expected that this adjustment would reduce the magnitude of the observed hole at 1400 yards by about 5.0 dB and that there would be only a slight reduction in antenna gain for targets at the maximum range of 16 nmi.

It is recommended that calibrated test targets be provided in the operating coverage area of the VTS radars as a means for measuring day-to-day system performance.

Future specifications for VTS radars should include requirements for an adequate number of test points in the equipment and built-in test equipment for maintenance purposes. Some difficulty was encountered during this testing period because of the lack of suitable points into which signals could be injected or monitored.

It is recommended that consideration be given to the use of a continuously variable type of STC control as an aid to the operator in lieu of the three-position type switch on the current PPI displays.

The multiple pulse repetition rates and the wide pulse mode of transmission are considered to be redundant features for the AN/FPS-109(XN-1) radars for the current application. Future specifications should stress the requirement for simplicity of design and functions.

It is recommended that future VTS radars include a circular antenna polarization option. Experience with the YBI and PTB radars has indicated the definite value of circular polarization in reducing the clutter caused by rainfall.

TABLE OF CONTENTS

TABLE OF CONTENTS (CONTINUED)

LIST OF ILLUSTRATIONS

LIST OF ILLUSTRATIONS (CONTINUED)

LIST OF ILLUSTRATIONS (CONTINUED)

LIST OF ILLUSTRATIONS (CONTINUED)

LIST OF TABLES

SECTION 1

INTRODUCTION

1.1 GENERAL

The Vessel Traffic System (VTS) installation in the San Francisco Bay area is the first in a series of such installations to be made by the U.S. Coast Guard in various U.S. ports. VTS is designed to provide the Coast Guard with accurate details of ship and craft movements in the approach and conjested areas of the San Francisco Bay. This system is currently being tested and evaluated by the Coast Guard with assistance from the Applied Physics Laboratory/The Johns Hopkins University (APL/JHU) to determine the operational parameters of the VTS and to establish the basic system performance capabilities. The determination of these qualities will enable not only a better understanding of the San Francisco installation but will also provide the basis for the requirements for future VTS installations in other ports.

The San Francisco VTS is being implemented in sequential steps, with the manual system being operational initially. The manual system involves manual tracking of targets on a standard real-video plan position indicator (PPI) display and voice communications of advisories with cooperative users. When the automatic system becomes operational, automated detection and tracking and synethetic displays will be implemented. In addition, in the automatic system, subsets of traffic analysis compuer routines will be available.

The radars associated with the San Francisco VTS are two AN/FPS-109(XN-1) installations, manufactured by the Airborne Instrument Laboratories. One radar is installed at Yerba Buena Island (YBI) and another at Point Bonita (PTB). These radars have replaced the Raytheon 1605 Harbor Advisory Radar (HAR) that was used previously for monitoring the vessel traffic in the bay area. The first test conducted on VTS involved a side-by-side comparison of the HAR and the FPS-109. The results of this test are presented in reference (a).

The second test, reported herein, involves a series of engineering tests conducted to determine the operational parameters of the manual system and to establish quantitatively the baseline performance of the manual operation of the VTS FPS-109 radars. (The automatic detection and

tracking system operation will be evaluated in subsequent test efforts as the automatic system is phased into operation.)

1.2 TEST APPROACH

The approach to the test was to conduct analysis of two types of data to isolate the critical radar parameters and to relate these to desired operational radar performance. In addition, various modes of radar operation were evaluated and related to desired operational performance. The data collected in the test was divided into two basic categories. The first was parametric in nature and was used to characterize the basic engineering qualities of the VTS radars. This data was analyzed to determine the degree to which the radars, after their installation, were operating within the designed specifications. The second type of data was radar system performance oriented measurements that were used to characterize the man/machine interface operability of the radars in monitoring the vessel traffic in the bay area.

The intent was to perform an evaluation of the system and to integrate the results obtained from the two categories of data to derive the basis for a radar specification to be used for future manual vessel traffic systems.

To carry out this approach, three major tests were conducted during the manual radar system test effort. First, various radar and target parameters were tested to determine the basic ranges and their significance. Second, the sensitivity of the control and composite video microwave links between PTB and YBI were evaluated to determine the effect of disruptions, malfunctions, and failures on the normal detection and tracking functions of the radar system. In conjunction with these tests, a third effort was directed towards ascertaining the capabilities of the plan position indicator (PPI) display system.

1.3 REPORT ORGANIZATION

A brief description of the VTS radars is presented in Section 2. A discussion of the manner in which the tests were conducted is given in Section 3, and the test results are presented in detail in Section 4. Section 5 contains the conclusions and related recommendations based upon the results of the test.

SECTION 2

DESCRIPTION OF MATERIEL

2.1 GENERAL

This section presents a description of the VTS FPS-109 (XN-1) radars. As shown in Figure 2-1, one radar is located at YBI and another at PTB. These radars monitor the entire harbor area from a single operations center located on YBI.

2.2 SYSTEM OPERATION

The VTS radar system consists of two high-resolution, dual-channel radars (Figure 2-2). The PTB radar is installed overlooking a seaward approach to the harbor, while the YBI radar is installed at the operations center on YBI. The PTB radar provides video, bearing, and trigger information via a wideband video data link (Figure 2-3), while control and monitoring is via an ultra-high frequency (UHF) data link or telephone line.

The VTS radars are designed to detect and display large ships and numerous small boats and buoys in the harbor and its approaches under heavy sea and rain clutter conditions. In rain and sea clutter, performance is accomplished by matching antenna polarization to the expected sea clutter conditions (i.e., vertical polarization for seaward side and horizontal for harbor conditions) and combining this with the use of a fast time constant (FTC) and logarithmic receiver processing. Rain clutter is further minimized by selectable circular polarization. The normalization of radar returns from within 1200 feet of the radar to 8 nautical miles (nmi) for the YBI radar and 15 nmi for the PTB radar is accomplished by the use of antenna pattern shaping.

A central control and monitoring center is located at the display console (Figure 2-4). These consoles are capable of five radius offset presentations of radar video with electronic leading lines and cursors. The displays enable the measurement of relative position of vessels with respect to the other vessels, buoys, or channel center lines.

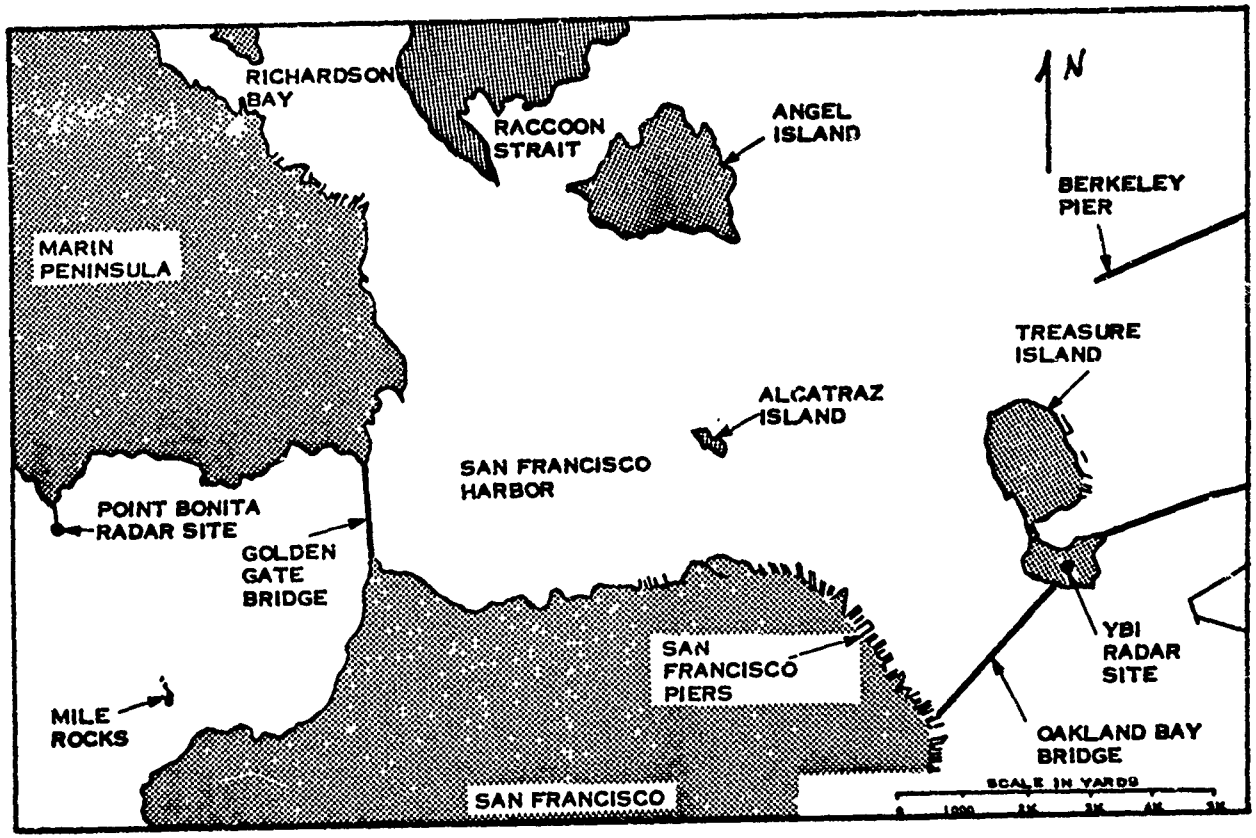

FIGURE 2-1. Location of the radar sites at Yerba Buena Island and Point Bonita.

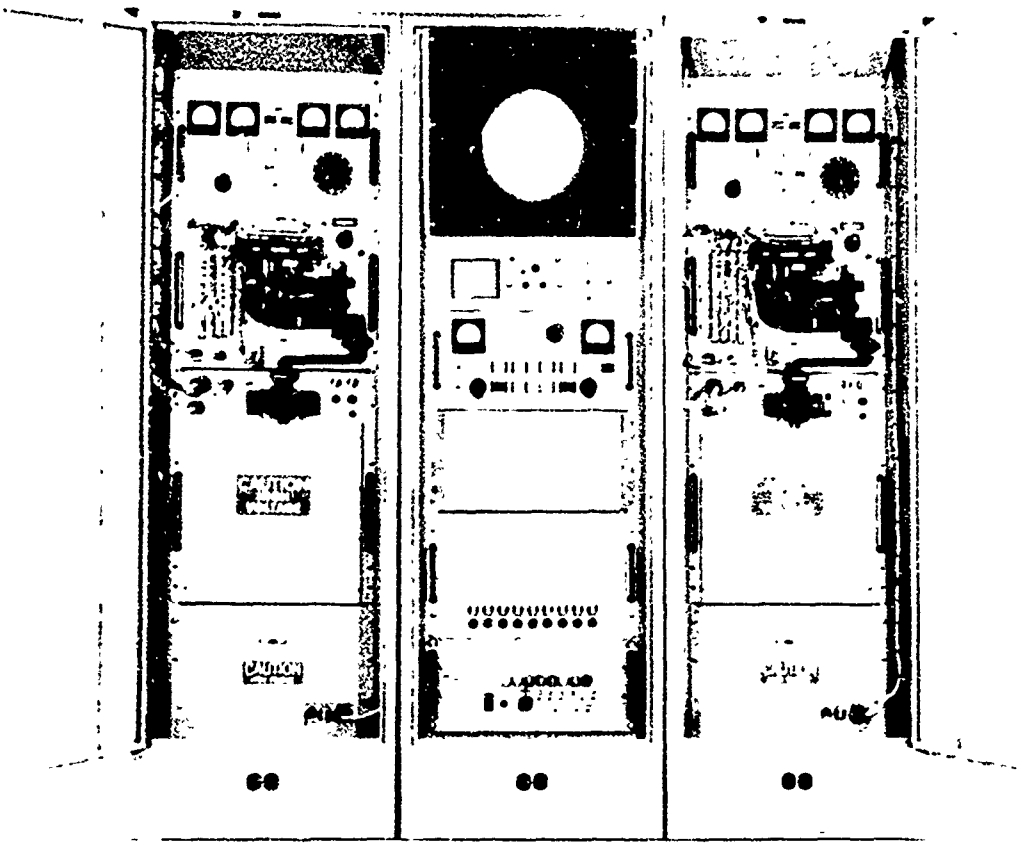

FIGURE 2-2. Dual transceivers and maintenance display of VTS radars.

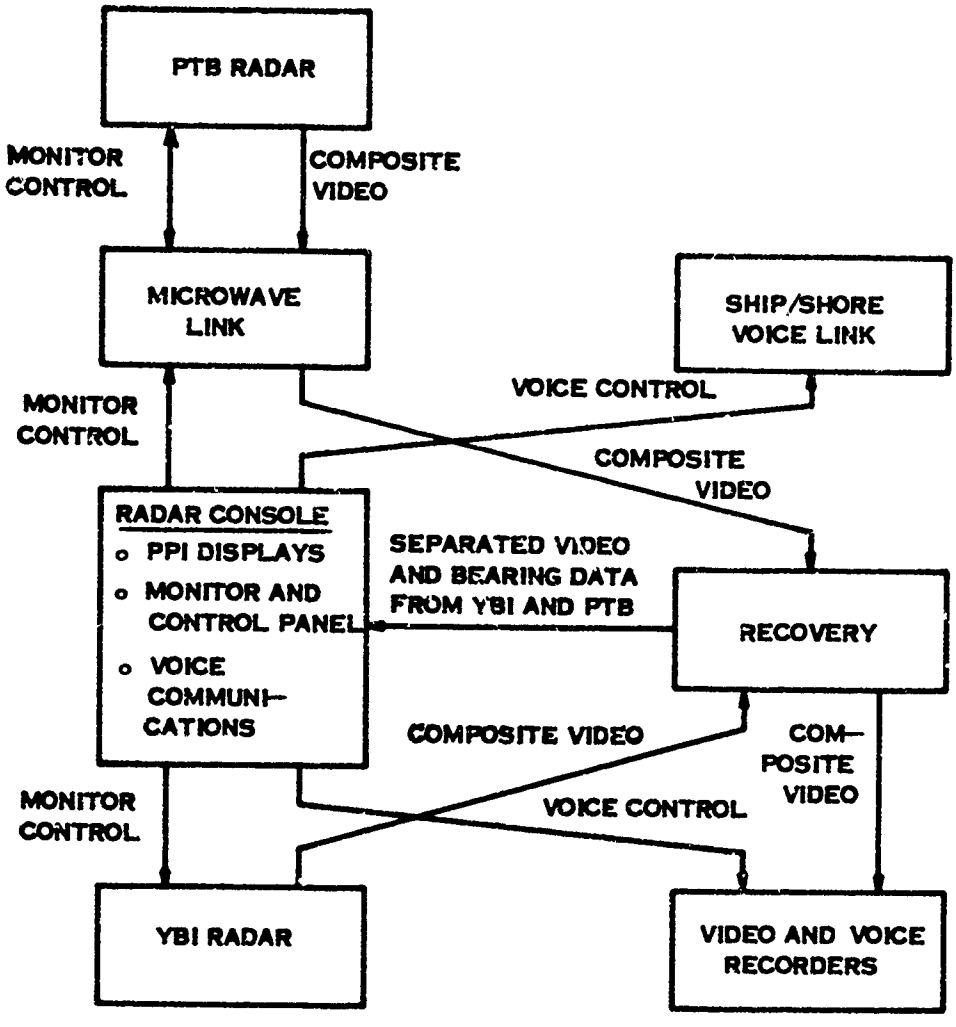

FIGURE 2-3. Block diagram of VTS manual system.

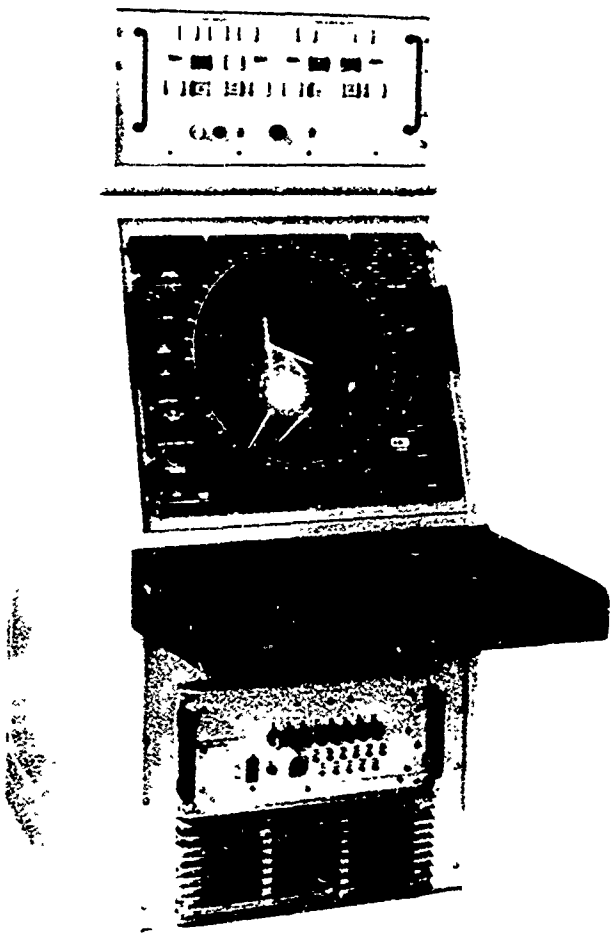

FIGURE 2-4. Display console of manual system.

The radar antenna at the YBI site is on a 90-foot tower (as shown in Figure 2-5), which is 415 feet above sea level. The radar antenna at the PTB site, which is similar to the YBI radar antenna, is on a 60-foot tower, 330 feet above sea level. These high elevations provide a commanding view of both the harbor and its seaward approaches. The antenna system at each site is composed of a high resolution antenna mounted on a pedestal, which provides continuous rotation at 20 revolutions per minute and 14-bit shaft encoder readout of instantaneous bearing angle. The antennas are parabolic cylinder reflectors with pillbox feeds, which are normally linearly polarized, but can be switched to circular to cope with heavy precipitation.

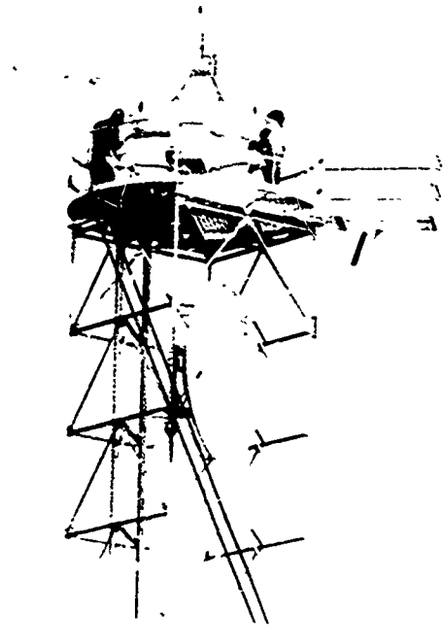

FIGURE 2-5. VTS radar antenna at YBI.

The radar transmitter uses a long-life magnetron that is conservatively rated at 50 kilowatts (kW) peak. Two pulse lengths, 50 and 200 nanoseconds, are selectable by switching in the appropriate pulse forming network. The synchronizer provides timing for the various radar functions and allows selection of a 1000, 2500, or 4000 pulses per second repetition rate. Choice of pulse length and pulse repetition frequency (prf) permit tradeoffs in resolution and range to be made by the operator, depending on the traffic problem at the moment.

The logarithmic receiver provides a dynamic range of over 80 decibels (dB) to cover the wide range of target sizes, clutter conditions, and precipitation losses.

At PTB, the radar video, triggers, and bearing data are formatted to a time-shared serial form. The composite video is then transmitted to the YBI center via microwave links, where it is separated into its constituent parts and transmitted to the PPI displays and the radar video preprocessor of the Automatic Detection and Tracking (ADT) subsystem of the VTS. The composite video is also used without change for recording on a video tape recorder for permanent records. The radar at YBI is adjacent to the ADT and PPI displays; therefore, the video and triggers are transmitted directly to those portions of the VTS. In addition, the YBI video and triggers are formatted into a serial form for the video recorder.

A separator in the recovery group at the YBI remote cabinet at the display site reconverts the composite video to parallel form in which the video pretrigger, trigger, and 14-bit parallel code are on separate lines for driving the operational displays that provide live real-time data. The live data enables the operator to advise ships of other traffic and potential hazards. The tape recorded data can be used for experimental purposes, analysis, and evaluation of the system; for training; and as a record in the event of an accident.

Any operational display can be switched to show data from either radar site. Range scales of 2, 4, 6, 8, and 16 nmi are selectable, and the display may be off-centered by up to five radii. These controls enable the operator to set up the displays in the most effective combination to show, for example, the seaward approach to the Golden Gate Bridge and the inner harbor with critical areas expanded for closer examination. Range rings are provided at one-quarter, one-half, three-quarters, and full range.

Six lead lines are set up on each display to mark traffic lanes and boundaries of interest. A cursor permits the operator to measure the angle and distance between any two objects on the display and obtain the angle and range on numerical readouts.

Maintenance PPI displays at each radar site and associated remote monitor/control panels are provided for maintenance of the radars. The remote group provides the means of monitoring and controlling the unattended equipment at the PTB site. These functions are controlled by wire lines between the display site (YBI) and the PTB site. The monitoring and control functions for the two radar sites are handled in the same manner, with identical controls and indicators on the monitor/control panels.

Remoting of the monitor and control functions for the PTB radar is accomplished by using sequential scanning encoders and decoders. The encoders are parallel-to-serial converters, which continuously scan the on/off inputs and convert these to a serial pulse train for transmission via the UHF data link. The decoders are serial-to-parallel converters, which receive and sort the serial information, in sequence, and store it

in parallel outputs that are available to drive the control relays or indicator lamps. Transmission in the opposite direction uses the same technique in reverse. The data can also be transmitted over telephone lines.

The major characteristics of the FPS-109 radars of the VTS are listed in Table 2-1.

TABLE 2-1. Parameters of VTS radars.

Parameter	Description
Peak Power (kilowatts)	50 nominal
Frequency	X-band, 9.3 to 9.5 gigahertz
Beamwidth (degrees)	0.30
Pulse Width	
Short (nanoseconds)	50
Long (nanoseconds)	200
Range Scales (nmi)	2, 4, 6, 8, and 16
Intermediate Frequency (IF) Bandwidth (megahertz)	22 (narrow pulse); 10 (wide pulse)
PRF (pulses per second)	1000, 2500, and 4000
Antenna Scan Rate (revolutions per minute)	20.6
Polarization	Vertical or circular (PTB); horizontal or circular (YBI)
PPI	16-inch operator; 12-inch maintenance; P7 phosphor

SECTION 3

CONDUCT OF THE TEST

3.1 GENERAL

The tests of the VTS manual radar system were conducted from 2 March through 30 April 1973 in the San Francisco Bay area. These tests were made in accordance with the Vessel Traffic System Manual Radar Test Plan [reference (b)]. Target services for the tests were provided by the San Francisco U. S. Coast Guard stationed at YBI. In general, one or two 40-foot metal hull cutters were provided during the testing. The following paragraphs present brief descriptions of the individual tests that were conducted.

3.2 OPERATIONAL PARAMETERS

3.2.1 Antenna Beam Pattern Measurements

This test was conducted to measure the antenna patterns including the first and second sidelobes and beamwidth. The values obtained in this test were used to correlate and substantiate the range and angle results obtained in the Comparison Test, reference (a), and to formulate the basic antenna characteristics to be used in interpreting and analyzing tracking performance. In addition, these tests enabled a comparison of the measured values with those of the design specification.

The test was accomplished by installing a low power transmitter on Treasure Island for near field beam patterns and on Pier 45 for far field beam patterns and allowing the VTS radar located at YBI to receive the transmitted signal in a line-of-sight. The modulated transmitted signal was received at the output of a bidirectional coupler in the radar receiver line. The antenna beam parameters were measured by plotting the received power as a function of radar bearing angle by slowly motor-servoing the VTS radar antenna. With the automatic antenna pattern inserted, the azimuth antenna patterns were plotted for the radar with horizontal polarization. The elevation patterns were derived from a series of azimuth cuts taken at each 2-degree negative depression angle from 0 to -20 degrees below the horizon.

3.2.2 Radiated Power Measurements

This test was conducted for the VTS radars as a correlation check on the specified antenna gain of 41.3 dB, the transmitter power output, and the measured line losses.

A standard gain horn and a crystal detector were set up on Pier 45 in the San Francisco Harbor. A signal was received from the YBI and the PTB radars. This received signal was detected and displayed on an oscilloscope. A signal generator calibrated the oscilloscope such that the peak receive power of each radar was available. These measured values were then compared with the calculated expected power.

3.2.3 Transmitter and Receiver Parameters

These tests were conducted to ensure that the transmitters and receivers of the VTS radars were operating within their design specifications after the radars were installed at PTB and YBI.

3.2.3.1 Pulse Characteristics. The transmitted pulse of the magnetron was detected at the output of the 40-dB cross guide coupler, and the pulse width was measured between the 10- and 90-percent levels for both the narrow pulse (50 nanoseconds) and the wide pulse (200 nanoseconds). Similarly, the received pulse width was monitored at the video output. To accomplish this test, a special target generator was designed and fabricated. The generator has the capability of generating either one or two targets that can be placed anywhere in range and closed to a range equivalent to 50 nanoseconds.

3.2.3.2 Receiver Noise Figure. The noise figure of transceivers 1 and 2 for both YBI and PTB radars was measured with standard commercial noise measuring equipment.

3.2.3.3 Receiver Bandwidth Measurement. A pulsed microwave signal was coupled into the radar receiver, and the microwave frequency was centered at the peak of the intermediate frequency (A-scope video) on an oscilloscope. A calibrated X-band attenuator was then placed in series with the signal generator, and as the microwave frequency was varied, attenuation was removed to maintain a constant video reference.

3.2.3.4 Receiver Transfer Function. During the test where data from the receiver was required for analytical data reduction, the radar receivers were calibrated prior to test operations. This was accomplished by inserting a calibrated microwave source with the narrow pulse width at the input of the radar receivers. The minimum discernible signal (MDS) was measured and compared with the system specification. A plot was then made of the radar receiver output versus the microwave signal input to the receiver.

3.2.4 Measurement of PPI Characteristics

Tests were made to determine the basic performance characteristics of the PPI displays of the VTS radars. Measurements were made of the sweep linearity, uniformity of the sweep as a function of bearing angle, and the accuracy of the range rings and movable range cursor.

3.2.4.1 Range Cursor Accuracy. The accuracy of the range rings and the range cursor were measured by means of an external target simulator. The test target pulse was brought into coincidence with a selected range ring, and the pulse time delay from main trigger was measured on a test oscilloscope. A comparison was also made with the range indicated by the movable range cursor. Pulse pairs could also be generated by the test generator with a variable time spacing between pulses. Range measurements between pulse pairs with the variable range cursor were compared to the time between pulses as measured on the test oscilloscope.

3.2.4.2 PPI Display Distortion. Tests were made to determine the presence of distortion in the PPI display that would be evidenced by scalloping or a noncircular display. A test target generator was used to place range rings at selected ranges as a test of deflection uniformity. Polaroid photographs were made to document the performance.

3.2.5 Microwave Data Link and UHF Control Link Tests

These tests were conducted to determine the sensitivity of the control and composite video microwave links between PTB and YBI. The target detection and tracking capabilities of the radars were evaluated as a function of signal attenuation in the microwave link. Consideration was given to the effect of disruptions, malfunctions, and failures of the PTB radar control functions on the normal detection and tracking operations of the radar system.

3.2.5.1 Microwave Data Link. To accomplish this test, a calibrated attenuator was inserted into the microwave receiver link at YBI. As the attenuation was increased in the link, the performance was monitored on the PPI display. Both the video display and bearing sweep stability were measured as a function of the attenuation.

3.2.5.2 UHF Control Link. During this test, the UHF link was disabled and a calibrated attenuator inserted in the L-band receivers. A measurement was then made of the amount of attenuation that could be sustained by the link prior to loss of data.

3.3 PERFORMANCE MEASUREMENTS

3.3.1 YBI Radar Antenna Elevation Coverage

This test was conducted to determine the elevation coverage of the antenna of the YBI VTS radar with linear polarization. A 40-foot cutter was vectored on radial courses to and from YBI, and the target return was plotted as a function of range for linear polarization. The level of the return signal was set comparable to -85 dBm (decibels referenced to 1 milliwatt) with a calibrated attenuator in the radar receiver. As the range of the cutter increased, attenuation was removed to maintain a signal whose amplitude was -85 dBm. A received power plot was made of the radar return of the cutter as a function of range.

3.3.2 Detection Range

This test was conducted to measure the capabilities of the YBI and the PTB radars in detecting targets in both clear and clutter environments. The radar cross section of various test targets was cataloged, and these targets were tracked by the radars in clear and clutter environments. When targets of specified cross section were not available, the maximum detection range of the radars was adjusted to reflect the difference in cross section of the available targets. At YBI, a 40-foot cutter was vectored on radial courses to and from YBI to determine the maximum detection range of the radar operating with linear and circular antenna polarization. Since it was not possible for a target of known cross section (such as the 40-foot cutter) to traverse beyond the Golden Gate Bridge, target tracking data for the PTB radar was obtained from data collected from channel buoys whose range product was adjusted to the range of the radar specification.

3.3.3 Angle Resolution

This test was conducted to determine the angle resolution capabilities of the YBI radar using linear and circular antenna polarization while the radar tracked targets at extended ranges. The two 40-foot cutters were vectored to ranges of 6300; 9600; 12,000; and 15,800 yards. At each range, the cutters separated in opposite directions perpendicular to YBI to a fixed distance as measured by a shot line. The cutters then followed an inbound course at the fixed separation distance. When the two cutters became resolved into two distinct target blips on the PPI display, the range and the known separation distance were recorded. The ratio of the separation distance to the range provided a direct measure of angle resolution.

3.3.4 Range Resolution

This test was conducted to determine the range resolution capabilities of the YBI radar using narrow pulse width transmissions and also to determine the range resolution of the PPI display. To accomplish this test, a microwave signal generator was coupled to the radar via a bidirectional coupler. This signal from the generator was modulated by the two-target video generator that was capable of varying the range of either or both targets. At a given range and range scale on the PPI display, the two targets were merged in time (range). This time was then expanded until two targets were discernible on the PPI, and a polaroid photograph was made of the composite video of the simulated targets. The time difference of these two targets was then converted to range. The procedure was repeated at each range scale of the PPI, enabling a determination of both the radar and the PPI resolutions.

3.3.5 Sensitivity Time Control Performance

While the PTB and YBI radars were operating in a clutter environment, a series of polaroid photographs were made at various STC levels and range scales to determine the STC effect on the attenuation of the close-in clutter levels.

3.3.6 Fast Time Constant Performance

The FTC feature of the PPI displays was tested in various conditions of sea clutter for both the YBI and PTB radars. Sample poloroid photographs were made to document the effect of the use of the FTC.

3.3.7 Test Target Calibration

This test was conducted to measure the radar cross section of various test targets with both the YBI and the PTB radars. Using a microwave signal generator, the radars were calibrated from the minimum discernible signal (MDS) to -45 dBm in steps of 5 dB. At each step, polaroid photographs were made of the A-scope presentation, and a plot was made of the received power versus the A-scope voltage. With the radars calibrated, the power received from the test buoys was measured. Expanded range polaroid photographs were also made of the buoys on the A-scope (on the same vertical scale that the radar was calibrated). Utilizing the radar range equation, the radar cross section of the cutters and the buoys was then calculated.

3.3.8 Radar Test Points and Test Equipment

During the test period, the availability of test points in the radars and the availability of suitable testing equipment were examined from an operational standpoint.

SECTION 4

RESULTS OF THE TEST

4.1 GENERAL

The results of the manual radar system test, presented in this section, are separated into the operational parameters and the performance capabilities of the VTS radars. The operational parameters provide a better insight into the radar system and enable a determination of the degree to which the radars operate within their design specifications. These parameters will also be used to provide the basis for the generation of a specification for future manual VTS installations. The performance capabilities of the radars, combined with the results obtained during the Comparison Test [reference (a)], similarly provide a better understanding of the capabilities and the limitations of the radars during normal and adverse conditions. These results will also be considered in the preparation of a specification for future manual VTS installations.

4.2 OPERATIONAL PARAMETERS

The operational parameters discussed in the following paragraphs include characteristics of the radar antennas, radiated power measurements, transmitter and receiver parameters, and PPI and control link characteristics.

4.2.1 Antenna Beam Pattern Measurements

The antenna beam pattern of the VTS radar was designed to maximize the probability of detection of targets within the coverage area of the radars and to obtain the best angular resolution possible within the constraints of reasonable size and complexity. The azimuthal beamwidth is specified to be 0.3 degree between the 3-dB power points for one-way transmission, with a modified cosecant-squared elevation pattern that is designed to give equal size targets at 1200 feet and 8.0 nmi and received signal strengths that are not less than those levels for the same target size at ranges between the specified limits for the YBI antenna. A similar specification applies to the PTB antenna except that the elevation coverage limits are 1200 feet and 15.0 nmi.

Antenna pattern measurements were made by the Airborne Instrument Laboratories (AIL) at their antenna test range to demonstrate the attained

performance. Also, measurements of at least one antenna was deemed advisable after installation at YBI and PTB to determine if the installation or environment had caused any adverse affects on the performance. The VTS radar installation at YBI was selected as being the one most easily measured. Therefore, AIL was tasked by the Coast Guard at the request of APL/JHU to make antenna pattern measurements at the YBI site. The results of the AIL efforts are presented in detail in reference (c). These tests were witnessed by representatives from APL/JHU and the Coast Guard. A representative selection of the graphical results has been excerpted from the AIL report for use in the following discussion.

The antenna drive motor was removed and a smaller motor drive installed to permit a controlled slow scan of the antenna, and a synchro set was installed to provide positioning data for the tests. A calibrated logarithmic response receiver was coupled to the bidirectional coupler in the antenna transmission line to receive the transmission from a small modulated transmitter placed at Pier 45 for far field measurements (a range of 5300 yards) and at a building on Treasure Island (TI) for near field measurements (a range of 1000 yards). As the antenna scanned in azimith, the logarithmic output of the receiver was recorded on a graphic recorder (the chart drive of which was servoed to the angular position of the antenna so that a plot of antenna response versus antenna angular position was made). Zero degrees on the chart was adjusted to correspond as nearly as possible to the maximum received power. During these tests, the radar transmitter was turned off.

Azimuth pattern measurements were made at elevation angles ranging from 0 to -20 degrees at 2-degree intervals for both the near and far field conditions. This was accomplished by adjustment of the elevation angle of the antenna on its pedestal such that the line-of-sight from antenna to target transmitter was at the desired elevation angle relative to the antenna for each azimuth pattern measurement.

Figure 4-1 is a copy of the graphic recorder output showing the received power as a function of azimuth angle at 0-degree elevation angle for the far field condition. The azimuth scale has been expanded to cover a region of ± 5 degrees about boresight in order to show the main beam azimuthal beam pattern in greater detail. It should be noted that the -3 dB points on the received power curve correspond to a beamwidth of 0.277 degrees which is smaller than the specified 0.3 degree 3-dB beamwidth. Within the ± 5-degree region about boresight, the sidelobes are all at least -30 dB below the main beam.

Figure 4-2 is a copy of the graphic recorder output showing the received power as a function of azimuth angle again at 0-degree elevation angle; however, the azimuth scale in this case covers ± 180 degrees of azimuth from the boresight position. The response scaling has also been modified to permit better delineation of the sidelobe pattern far from the beam axis. To attain this, the test receiver gain has been raised,

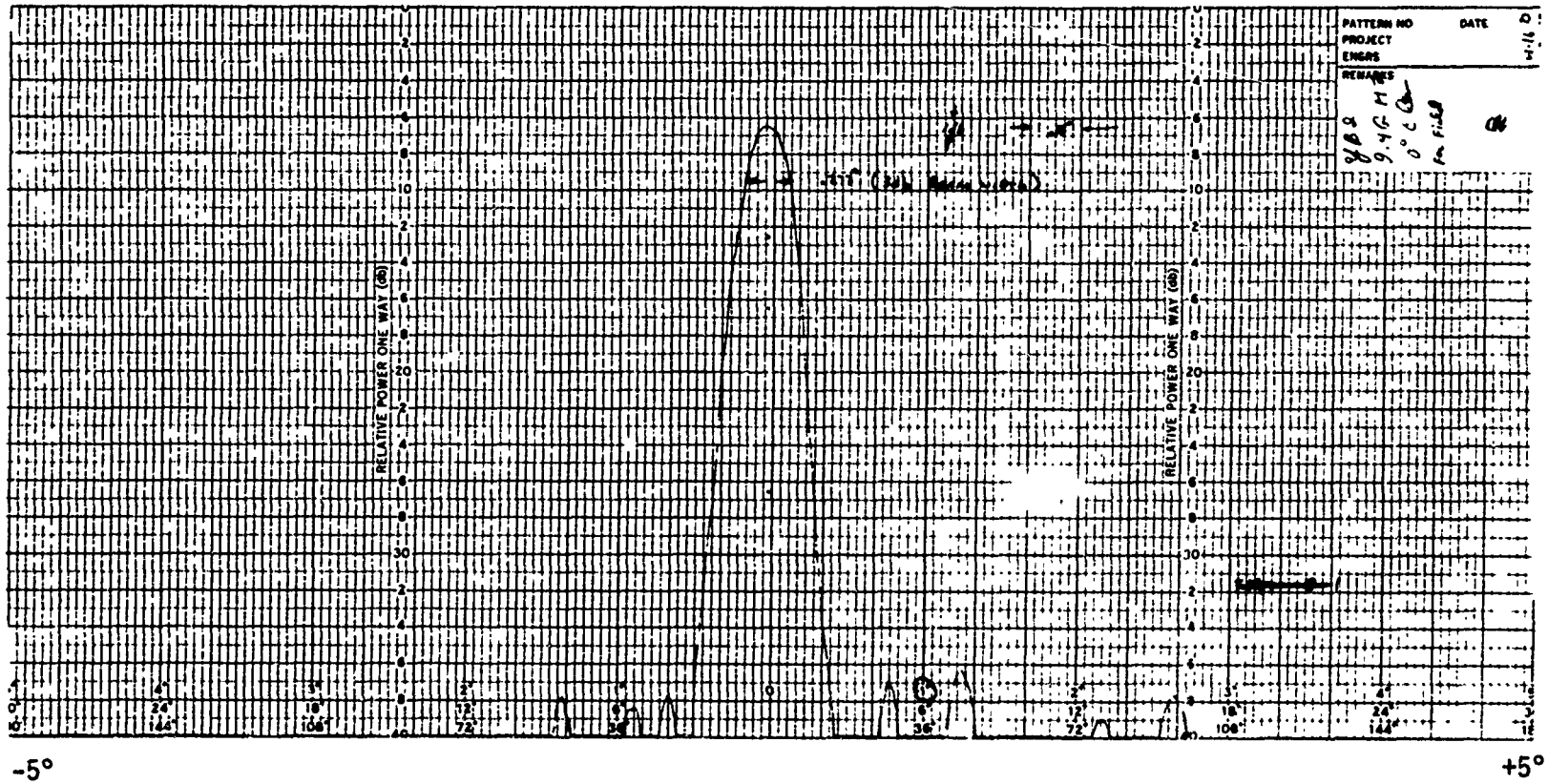

FIGURE 4-1. Far field azimuth beam pattern (±5 degrees) for horizontal polarization at 0-degree elevation angle.

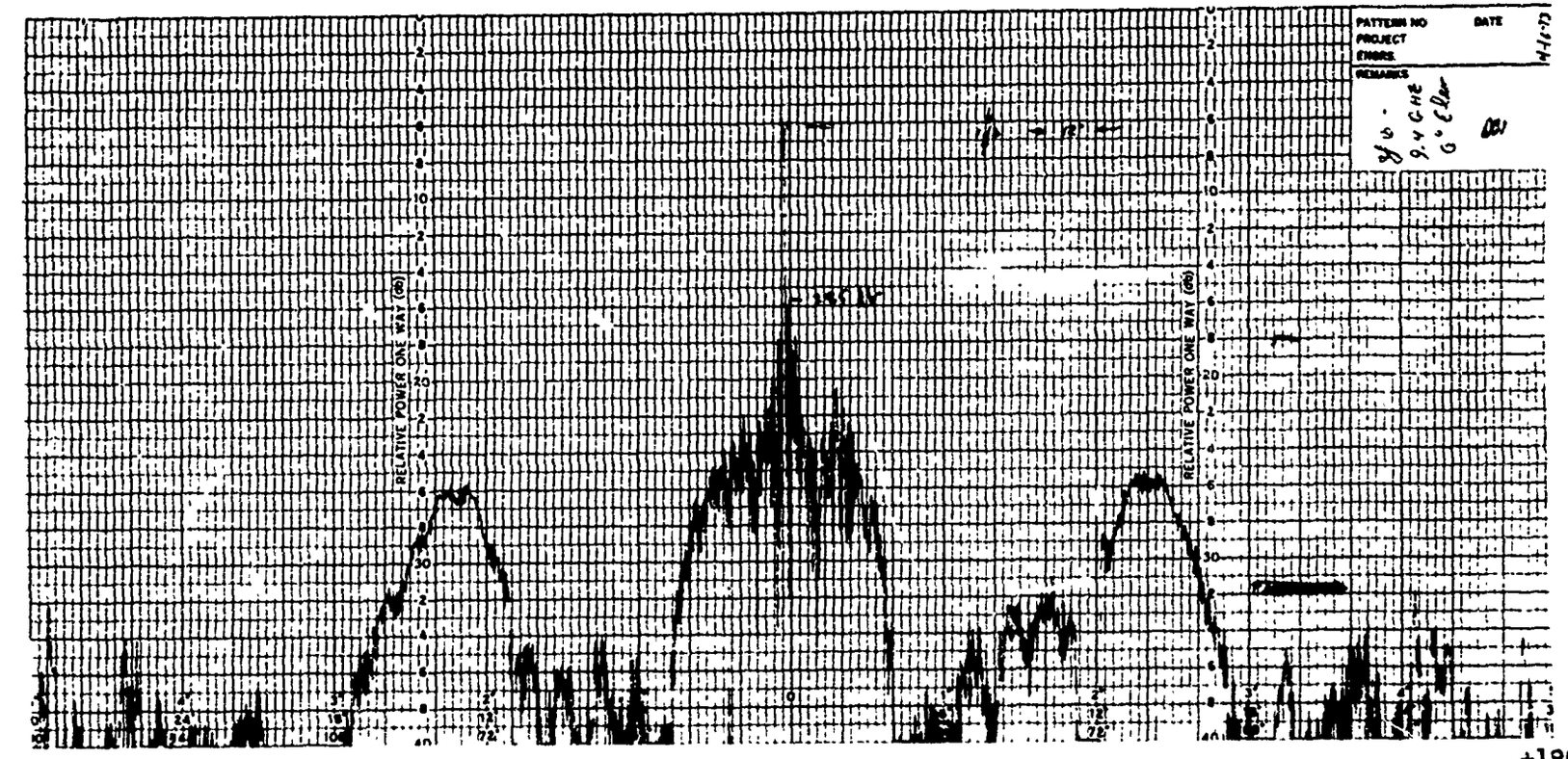

-180° +180°

FIGURE 4-2. Far field azimuth beam pattern (±180 degrees) for horizontal polarization at 0-degree elevation angle.

which has the effect of bringing the boresight beam response into the saturation region of the receiver and the logarithmic response no longer holds for the main beam. The plot has therefore been normalized to the first sidelobe response of Figure 4-1 (i.e., the first sidelobe is -30.5 dB down from the main beam response, and this is noted in Figure 4-2 at the first sidelobe response point).

By inspection of Figure 4-2, it can be seen that all sidelobes beyond the ±5-degree region are greater than -30.5 dB below the main beam throughout the ±180-degree region. The broad response regions in the vicinity of ±90 degrees are not actually sidelobes, but rather are spill-over from the feed horn of the antenna. Both are greater than 40 dB down from the main beam response and should have negligible effect on the performance.

It is apparent from Figures 4-1 and 4-2 that the observed 3-dB beamwidth of 0.277 degree is better than the specified 0.3 degree and that the low sidelobe and spill-over radiation levels observed indicate excellent antenna performance characteristics.

Figure 4-3 is a graphical recording of the far field pattern at an elevation angle of -8 degrees, covering a ±14-degree region about the boresight. It should be noted that the first sidelobe is 21.5 dB below the main lobe, which is itself 19 dB down from the peak response of the main lobe at 0-degree elevation angle. The main lobe response shown in Figure 4-4 has been annotated to show that it is 19 dB below the main lobe response at 0-degree elevation. The antenna pattern at an elevation angle of -8 degrees corresponds to the pattern which applies for targets at ranges of approximately 800 to 1000 yards for the YBI VTS radar. It is assumed that the antenna depression angle is set at 0 degrees.

Figure 4-4 also is an azimuth pattern response in the far field for a -8 degree elevation angle, but the response is shown for ±180 degrees about the boresight. It should be noted that all the sidelobes are below the level of the first sidelobe, which is 21.5 dB below the main lobe. The apparent large sidelobe at approximately ±90 degrees is, as in Figure 4-2, the spill-over from the horn feed. The spill-over energy is somewhat higher than the sidelobe energy that is 20 dB down from the main lobe at -8 degrees elevation angle. It should be noted, however, that if the spill-over is referenced to the main beam at 0 degree elevation angle, it is 39 dB below the main lobe (which is essentially the level of the feed horn spill-over observed at 0 degree elevation in Figure 4-2).

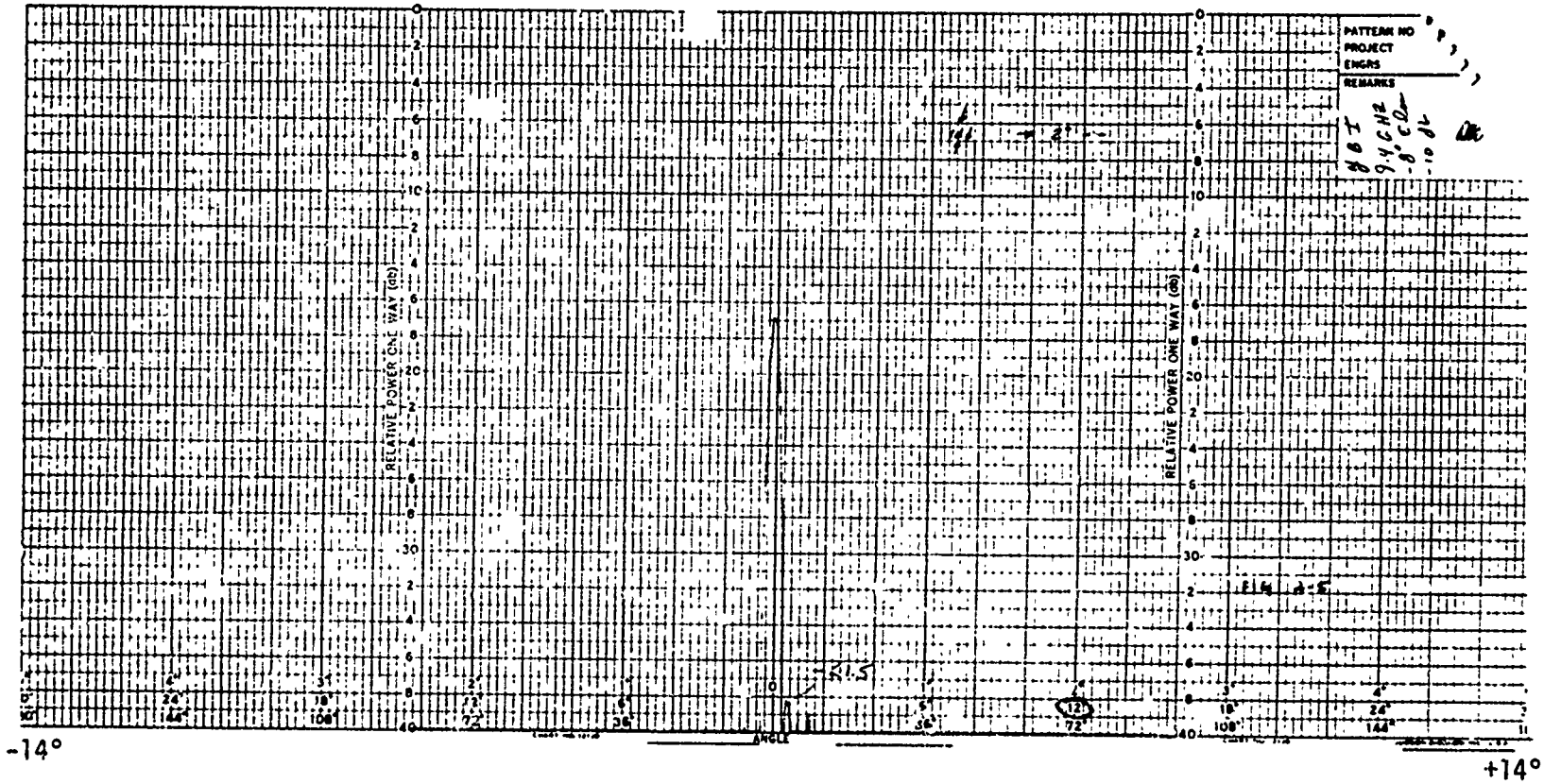

FIGURE 4-3. Far field azimuth beam pattern (±14 degrees) for horizontal polarization at -8-degree elevation angle.

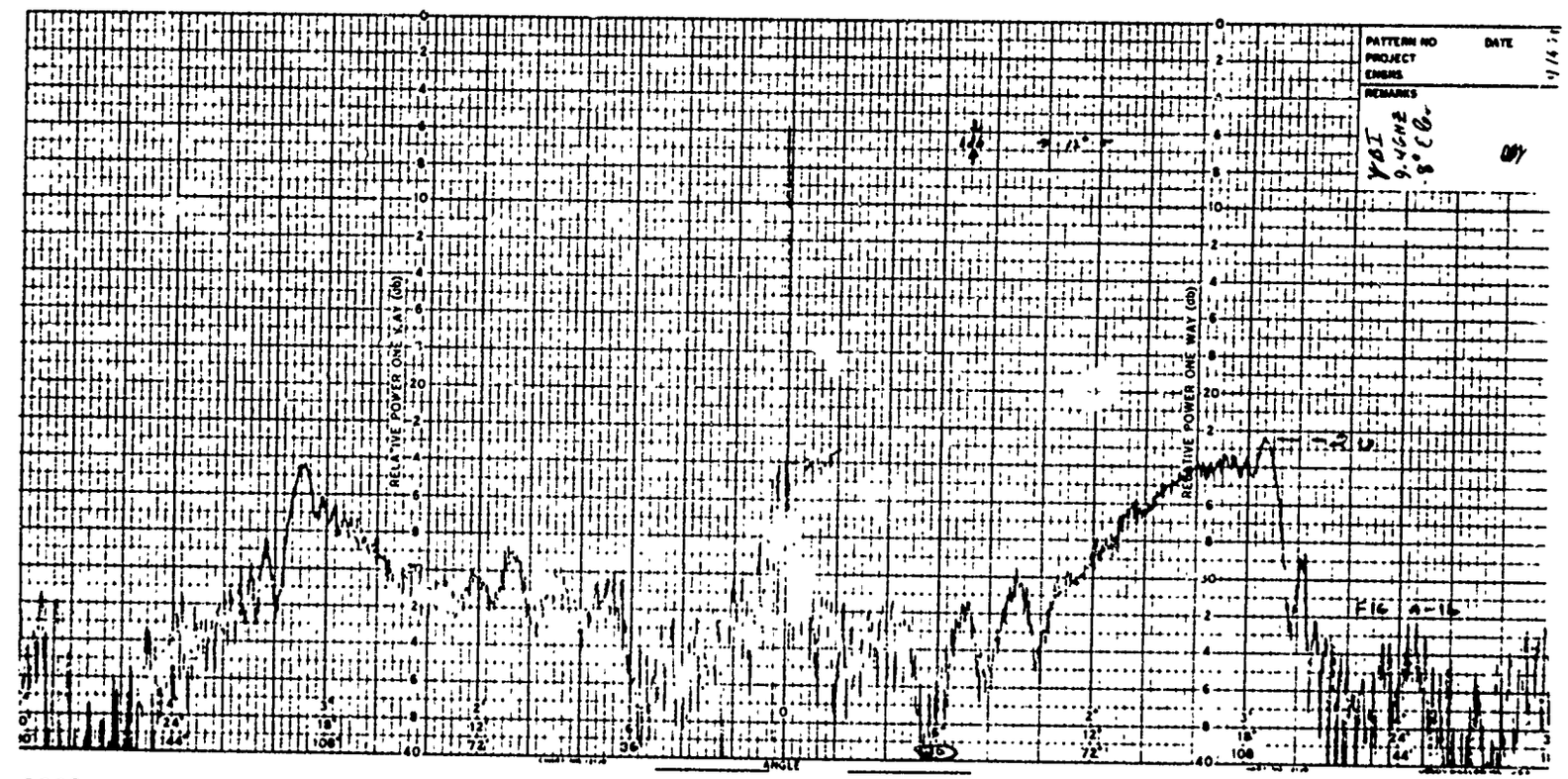

-180° +180°

FIGURE 4-4. Far field azimuth beam pattern (±180 degrees) for horizontal polarization at -8-degree elevation angle.

Figure 4-5 shows the far field azimuthal pattern for an elevation angle of -14 degrees, covering a region of ±14 degrees about boresight. It should be noted that the sidelobe level is higher for this case and that the sidelobe has almost the appearance of a pedestal at a level of 15.7 dB below the main lobe. The main lobe is, in this case, 18.2 dB below the level of the main lobe at 0 degree elevation. The primary reason for selecting this pattern for examination is that a -14 degree elevation angle corresponds to ranges from the YBI VTS radar of approximately 500 to 600 yards, which is the observed minimum tracking range for the radar reported in reference (a).

The higher sidelobe level is not considered too serious since the local shadowing at YBI prevents usable tracking at such short ranges. Figure 4-6 is similar to Figure 4-5, except the response is plotted for a ±180-degree region about boresight. The major spurious responses are the feed horn spill-over regions at approximately ±90 degrees from the boresight. The spill-over is approximately 16.2 dB below the main lobe at -14 degrees and approximately 34.4 dB below the main beam response at 0 degree elevation angle. The relatively high sidelobe response, caused by the sidelobes and spill-over, will probably result in increased close-in clutter; however, this region is in the minimum tracking range region and problems will probably not be incurred.

Several near field patterns were also made, and representative samples are shown in Figures 4-7 through 4-12. The test transmitter was installed on TI at a range of approximately 1000 yards. Because of the nearness of the target transmitter, it was not possible to obtain patterns at 0 degree elevation angle since the minimum was -3 degrees.

Figures 4-7 and 4-8 are antenna beam patterns at -3 degree elevation angle. Figure 4-7 is for a ±14 degree region about boresight, and Figure 4-8 is for a ±180 degree region about boresight. A comparison of Figure 4-7 with Figure 4-1 (taken at 0 degree elevation angle) indicates that the near field pattern is not as clean as the far field pattern and that the first sidelobe indications are only 14.5 dB down from the main lobe. In Figure 4-8, the spurious response and the sidelobe level beyond the region covered in Figure 4-7 are all at least 34 dB below the main lobe (which is comparable with the results shown in Figure 4-2 where the feed horn spill-over was on the order of 40 dB down from the main lobe).

Figure 4-9 is a near field pattern taken at an elevation angle of -8 degrees, showing the region within ±14 degrees of boresight. The first sidelobe is 17.5 dB below the main lobe, which should be compared with the sidelobe level of -21.5 dB measured in the far field (Figure 4-4). In Figure 4-10, the response at an elevation angle of -8 degrees is shown for a ±180 degree region about boresight. A large sidelobe is present at +44 degrees, which is 18.5 dB down from the main lobe, with the balance of

the spurious responses being at least 22 dB down from the main lobe. The significant point to be noted in Figures 4-9 and 4-10 is that the -8 degree elevation angle corresponds to coverage in the 800 to 1000 yard range from YBI and the patterns were taken at 1000 yards. These plots are therefore truly representative of the performance at that range increment. The level of the sidelobes is somewhat larger than would be desirable; however, they appear to be acceptable for the short range situation involved. To lower the sidelobe level appreciably very likely involves prohibitively costly engineering effort. It should be noted that the sidelobes relative to the main beam at 0 degree elevation are 37 dB down, which is excellent performance.

Figure 4-11 shows the azimuth response in the near field for an elevation angle of -14 degrees in a region of ±14 degrees about boresight. The sidelobe level is 16 dB down from the main lobe, which is down 19.5 dB from the main lobe at 0 degree elevation. In Figure 4-12, the azimuth pattern response is shown for the ±180 degree region about boresight. It can be seen that the sidelobe levels are at least 16 dB below the main lobe, and the spill-over is at least 24 dB below the main response. Figure 4-12 should be compared with Figure 4-6 (the azimuth response in the far field at an elevation angle of -14 degrees) where the sidelobe level and the spill-over radiation were approximately 20 dB down from the main beam and 40 dB down from the main lobe. There is an increase of 4 dB in the close-in sidelobe level for the near field case as compared with the far field case; however, there is a decrease of spill-over energy of about 4 dB. It is pertinent to point out that the near field measurements are more nearly representative of the normal operating conditions since the -14 degree elevation angle coverage is primarily concerned with close-in coverage at ranges on the order of the minimum range (i.e., 450 to 600 yards, which is operationally of insignificant interest). Nevertheless, the near field pattern for the -14 degree elevation case is relatively good even with the high sidelobe level.

Figure 4-13 is a plot of the elevation beam shape on boresight for both the far and near fields (as derived from the previously described azimuthal response curves). This curve is plotted from 0 to -20 degrees elevation. The pattern is approximately of the cosecant-squared form to provide constant power return from a fixed size target as a function of range. (The performance of the radar as a function of elevation angle coverage as determined with a 40-foot cutter will be discussed in detail in Paragraph 4.3.)

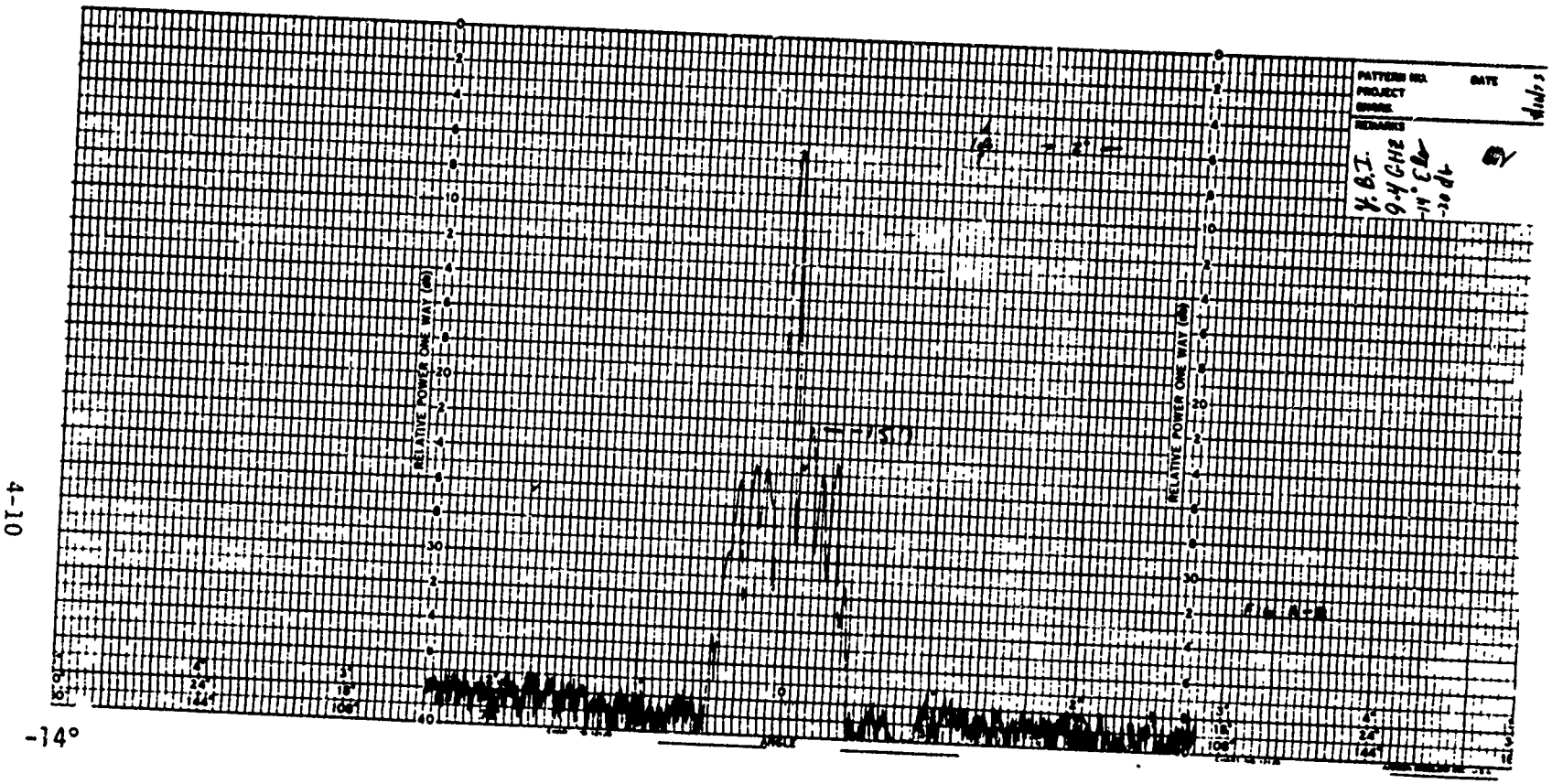

FIGURE 4-5. Far field azimuth beam pattern (±14 degrees) for horizontal polarization at -14-degree elevation angle.

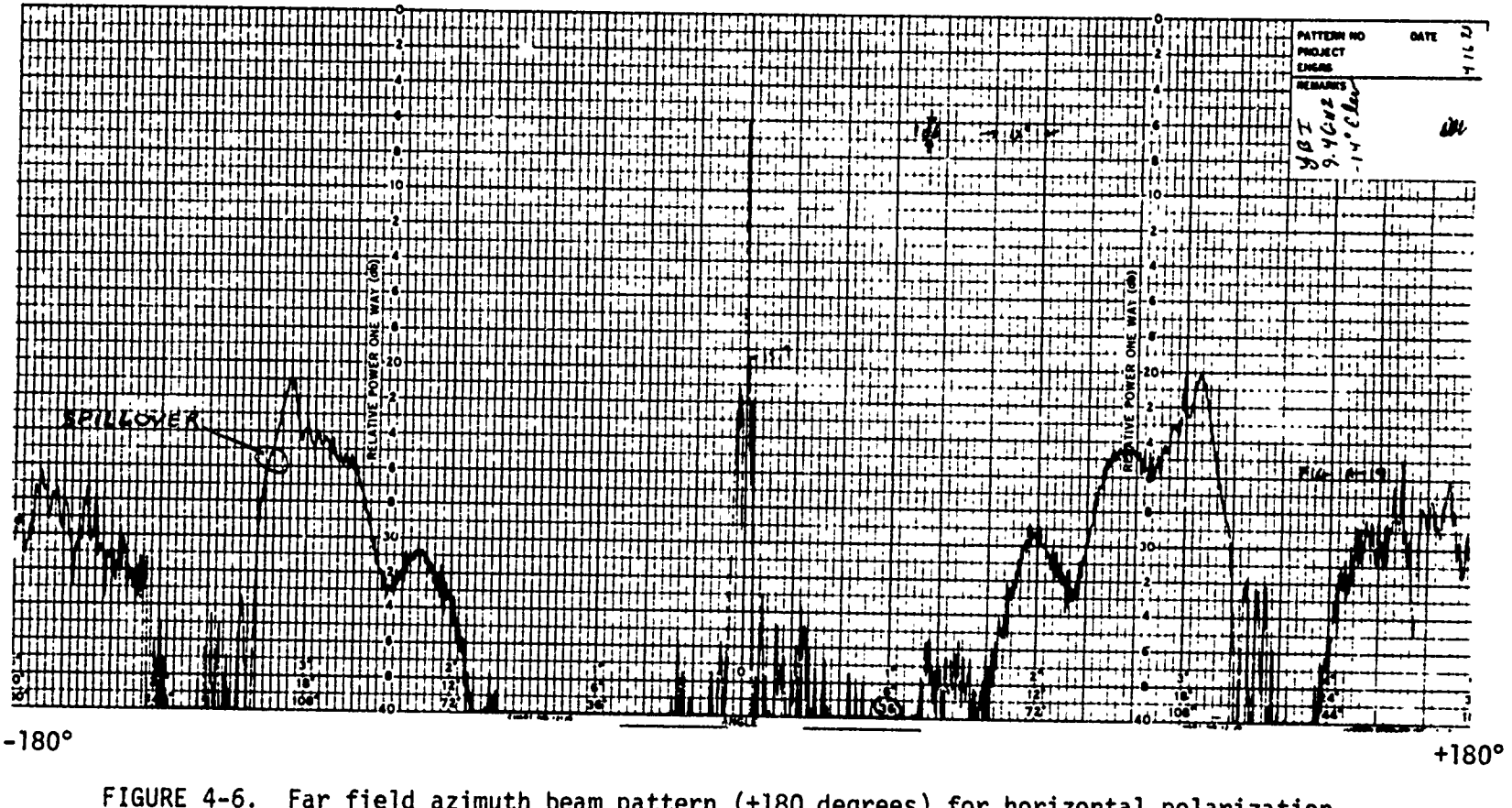

FIGURE 4-6. Far field azimuth beam pattern (±180 degrees) for horizontal polarization at -14-degree elevation angle.

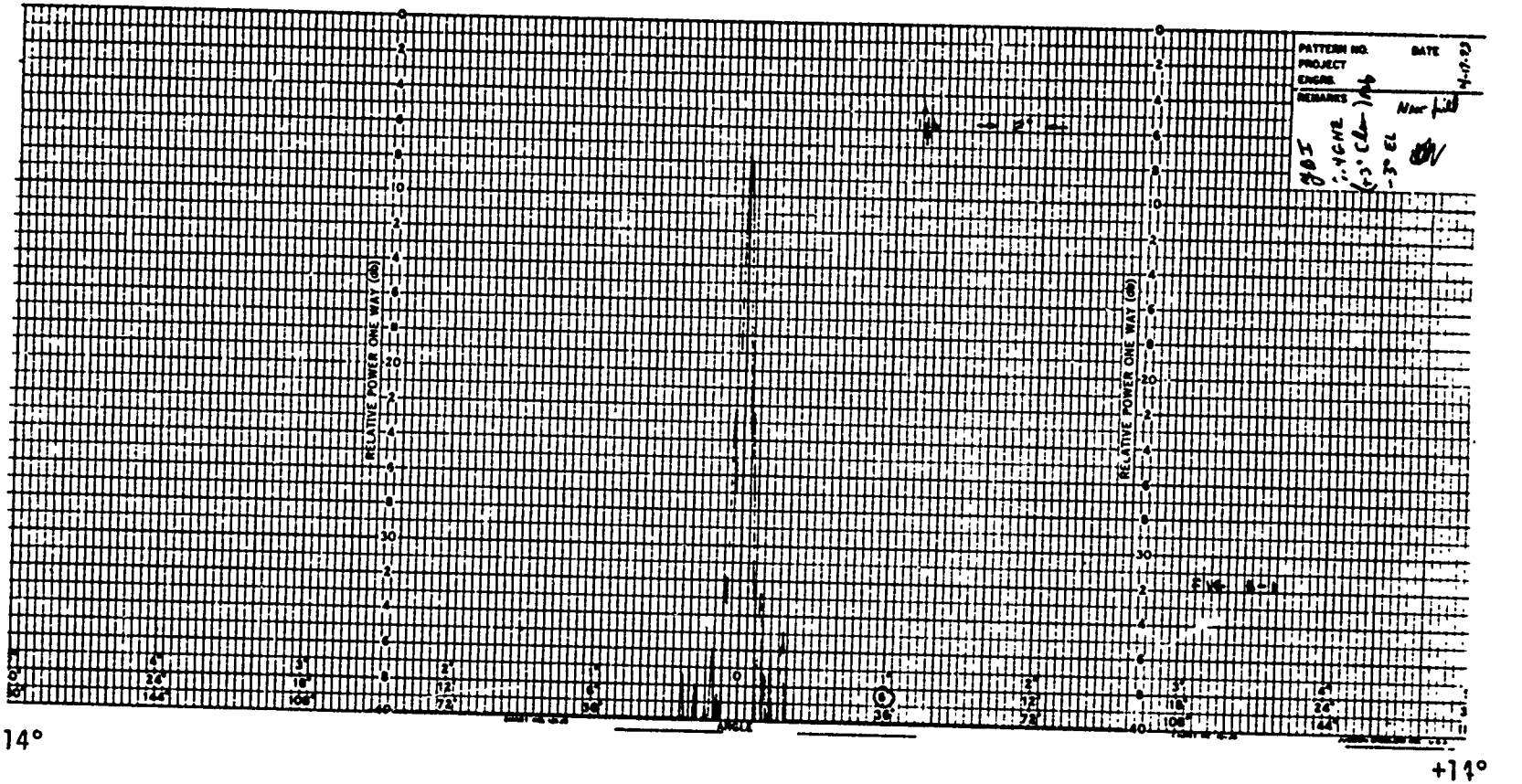

FIGURE 4-7. Near field azimuth beam pattern (±14 degrees) for horizontal polarization at -3-degree elevation angle.

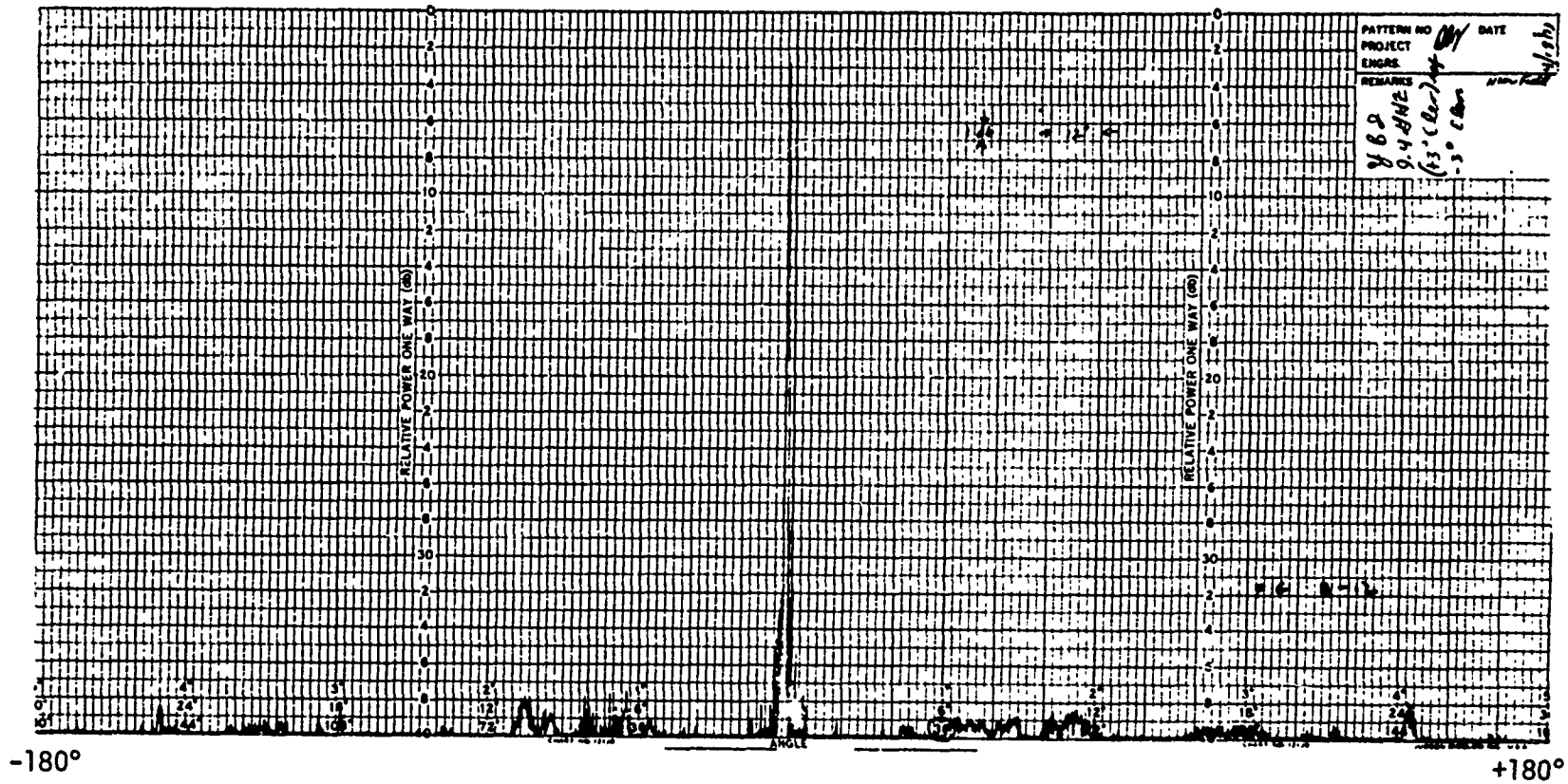

FIGURE 4-8. Near field azimuth beam pattern (±180 degrees) for horizontal polarization at -3-degree elevation angle.

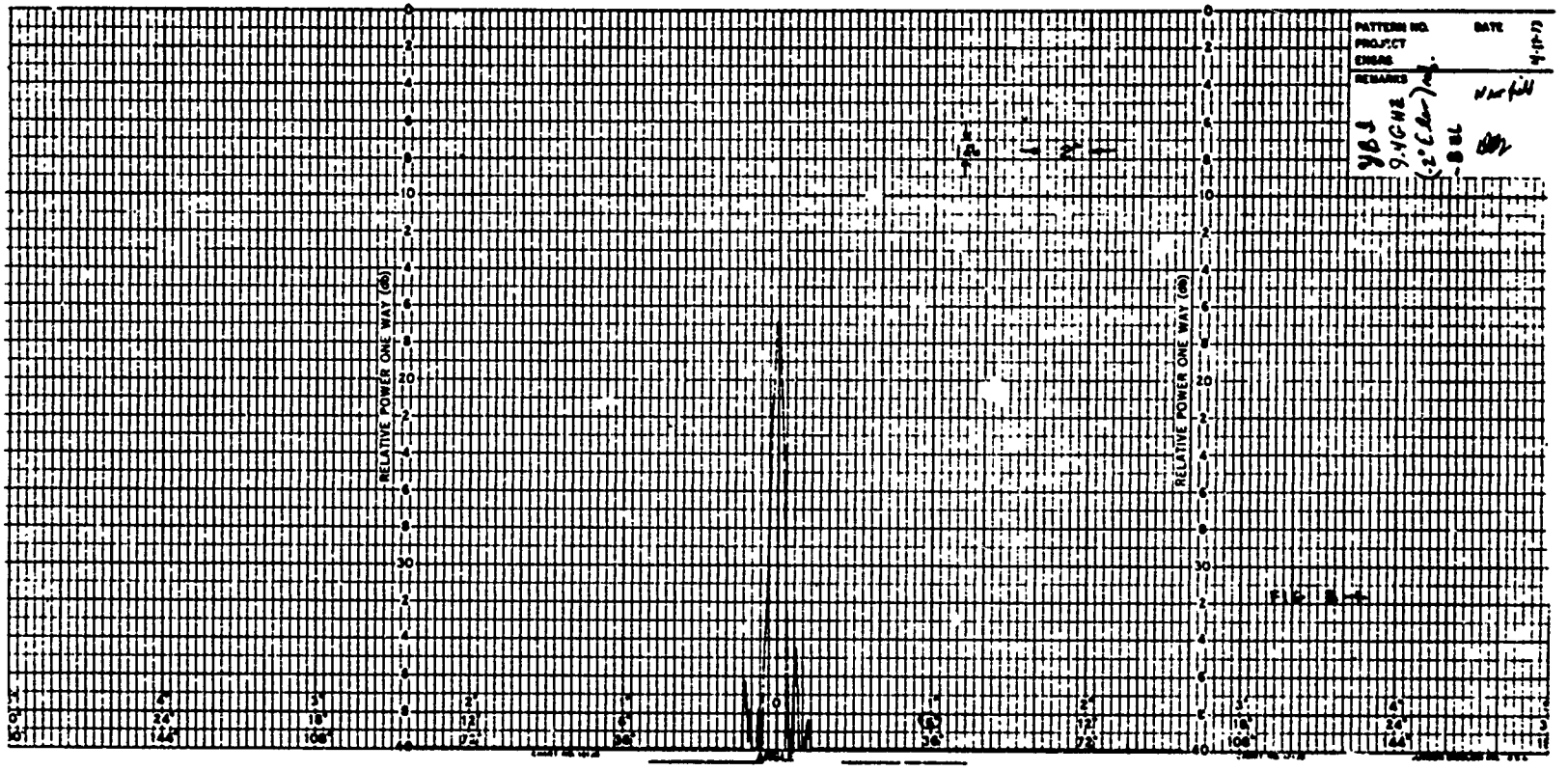

FIGURE 4-9. Near field azimuth beam pattern (±14 degrees) for horizontal polarization at -8-degree elevation angle.

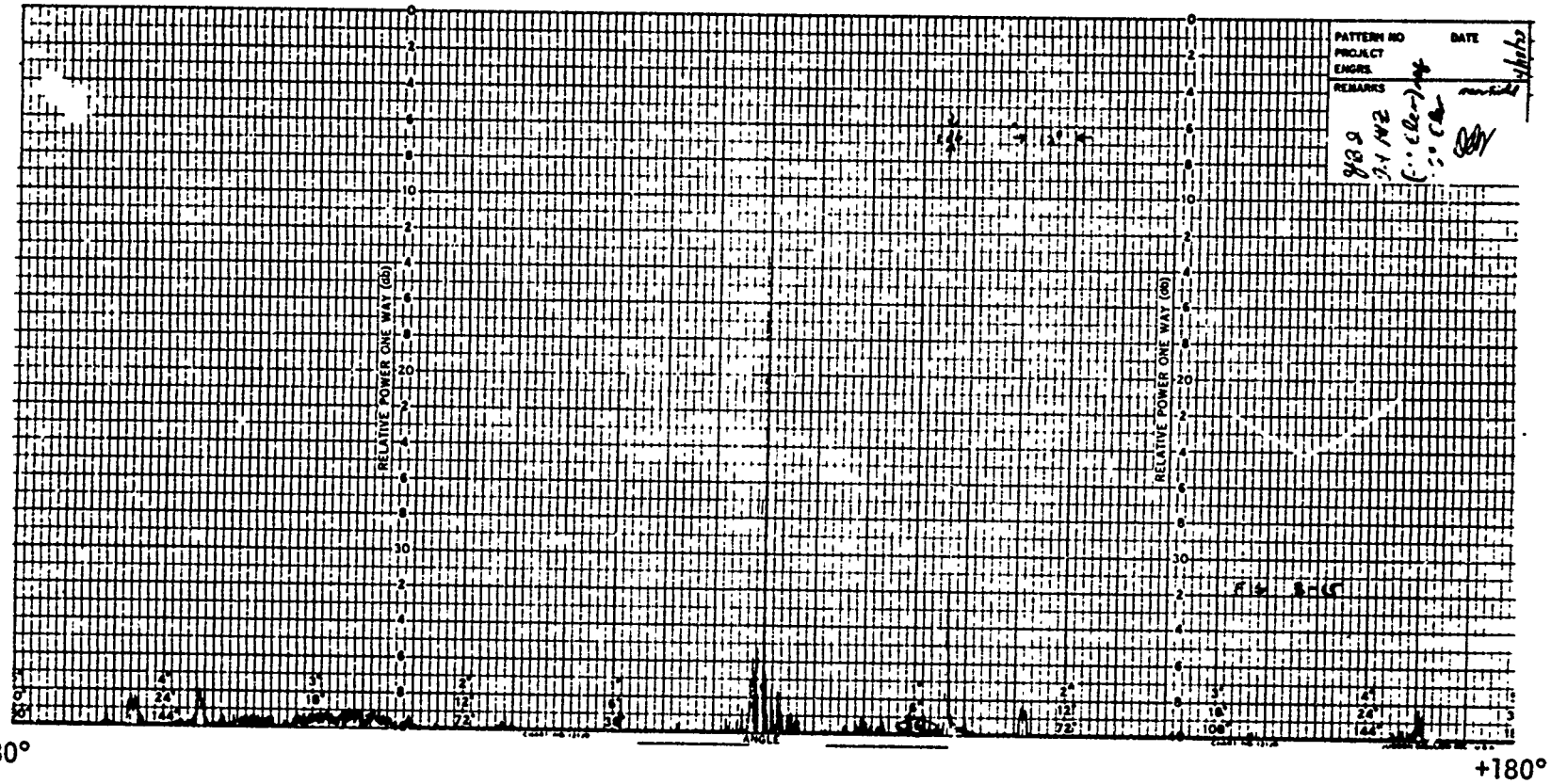

FIGURE 4-10. Near field azimuth beam pattern (±180 degrees) for horizontal polarization at -8-degree elevation angle.

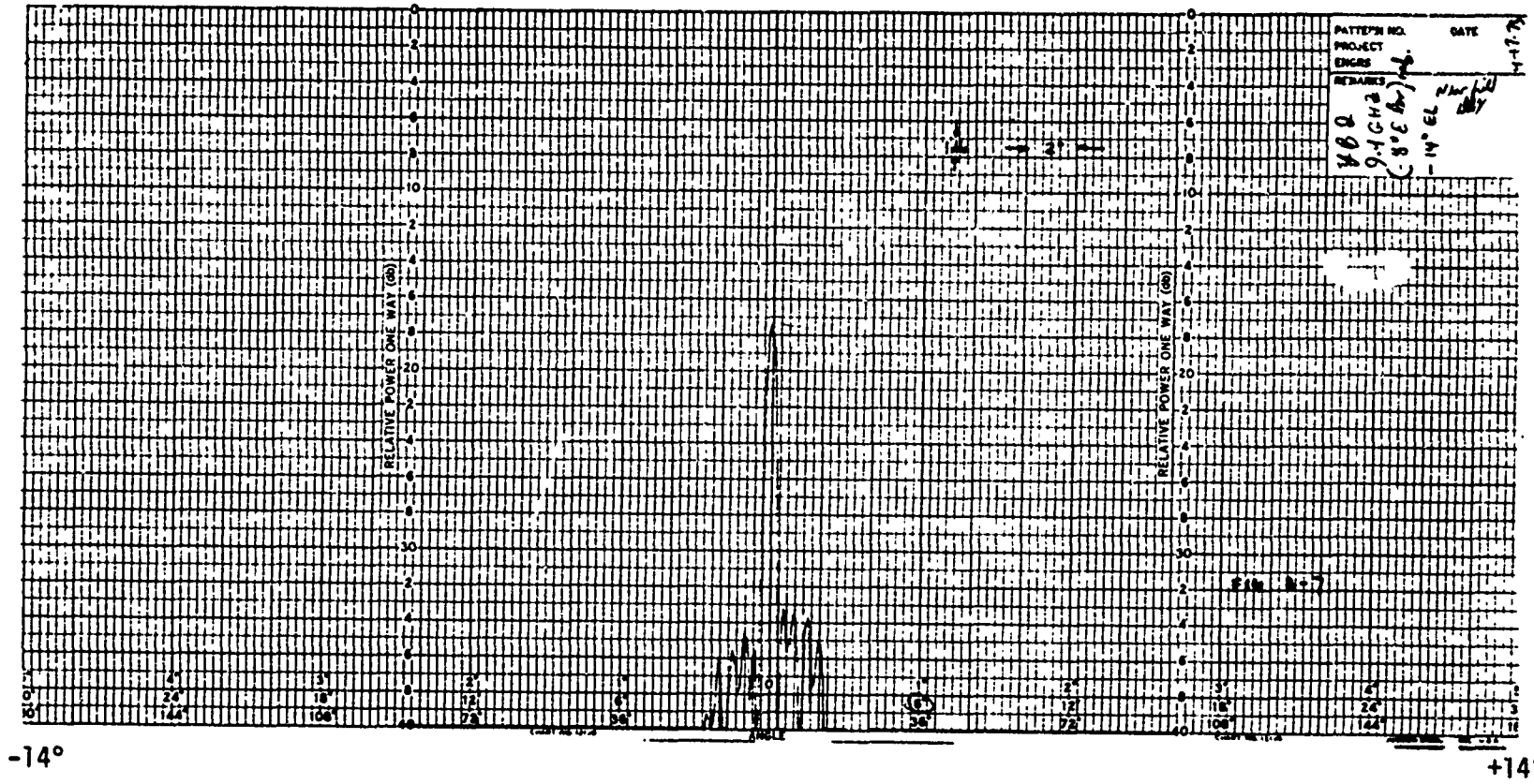

FIGURE 4-11. Near field azimuth beam pattern (±14 degrees) for horizontal polarization at -14-degree elevation angle.

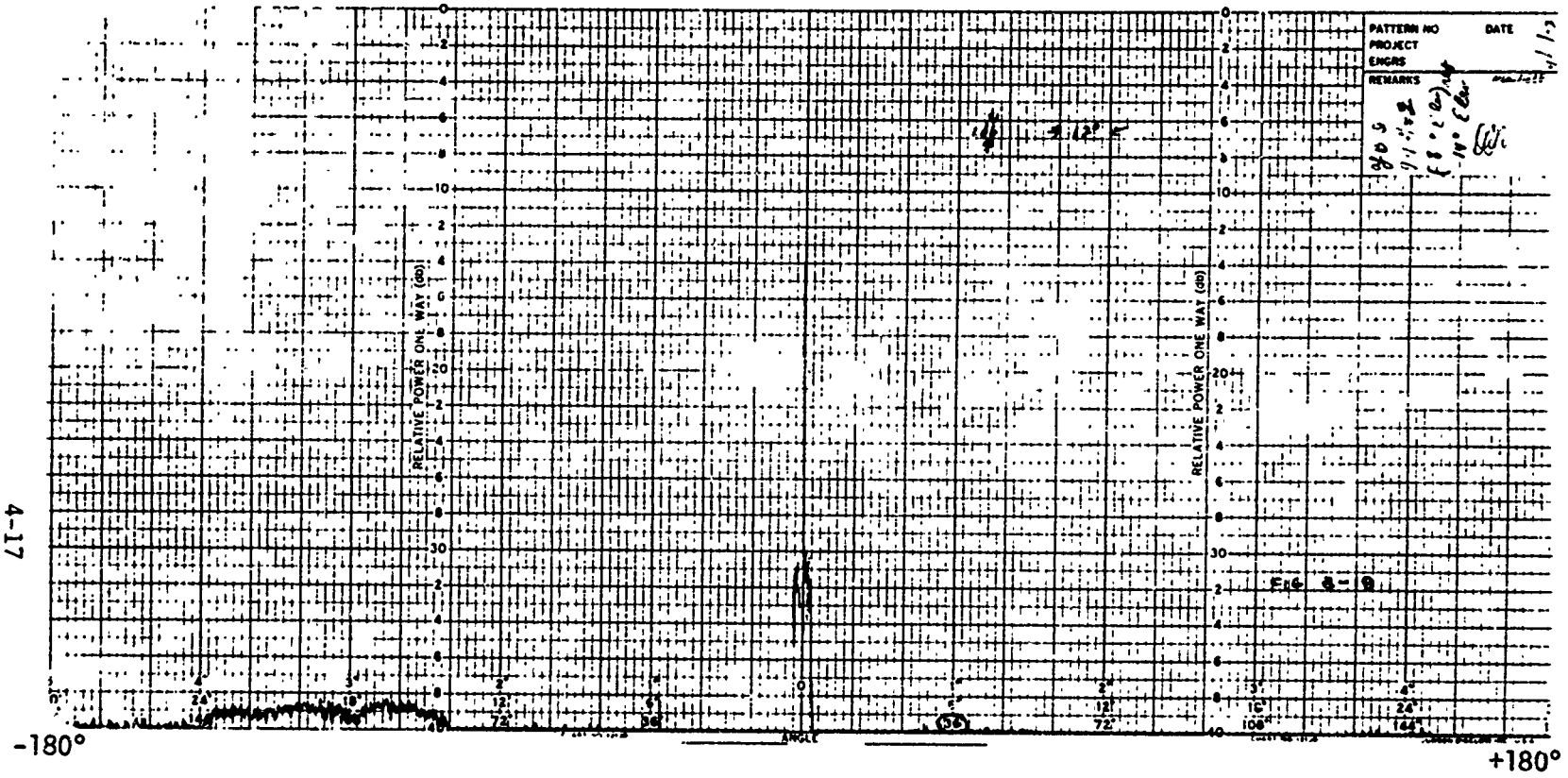

FIGURE 4-12. Near field azimuth beam pattern (±180 degrees) for horizontal polarization at -14-degree elevation angle.

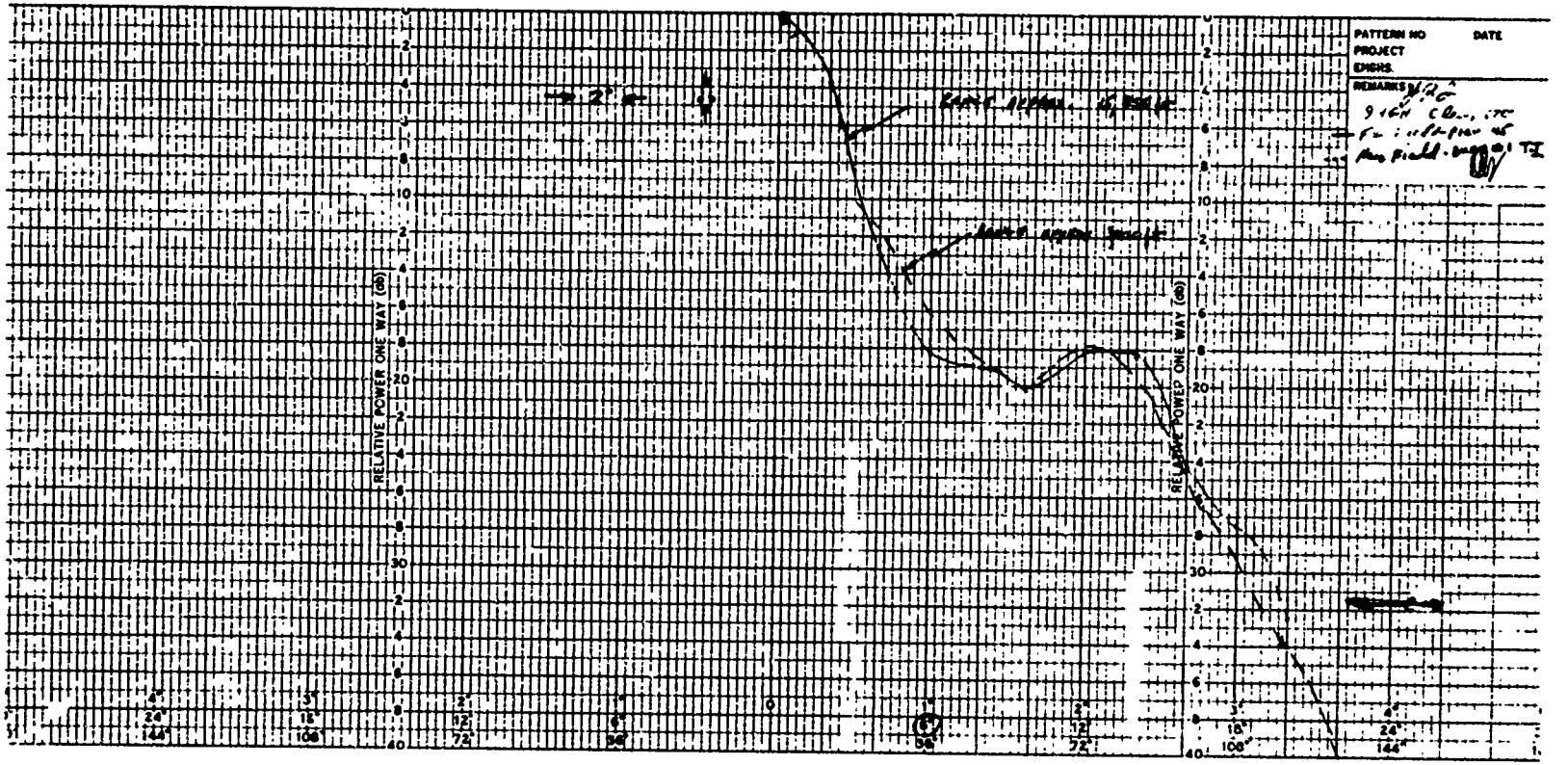

FIGURE 4-13. Far and near field elevation patterns at 0-degree azimuth.

4.2.2 Radiated Power Measurements

A measurement of the radiated power fror the VTS radars on YBI and PTB was made as a correlation check on the specified antenna gain of 41.3 dB (main lobe), transmitter output power, and measured line loss from the transmitter to the antenna.

A standard gain horn (16 dB gain) and a crystal detector were setup on Pier 45 as the receiver for the power measurement tests. The standard gain horn was removed, and the output of a calibrated test set was coupled through the horn transmission line to the detector. A pulse modulated output from the test set [with a 50-nanosecond pulse width and a pulse repetition rate (prf) of 2500 pulses per second (pps)] was applied to the detector to calibrate the receiver. The peak output of the detector was stretched in a boxcar circuit and applied to the vertical deflection input of an oscilloscope synchronized to the pulse rate. Calibration of the peak detected output in the vicinity of the expected output from the radars was then recorded.

The test set output was removed and the horn connected to the transmission line to the detector. The oscilloscope was set to sweep at a rate commensurate with the scanning frequency of the VTS radars, and the peak deflection of the stretched detected output from the particular radar under test was observed on the oscilloscope. A recheck was then made by using the test set input to the detector to obtain the same peak oscilloscope deflection amplitude, and the output of the test set was recorded. The test set output was then adjusted to account for the calibrated horn gain to obtain the incident power of the detector.

No apparent height gain effects were observed during these tests. The horn antenna was moved to different locations and heights in the test vicinity, and no observable effects occurred in the computed power density. (It was necessary of course to maintain the horn antenna at the correct azimuth angle to maintain maximum output for each position tested.)

The computed detected power from the VTS radars was derived from the manufacturer's specified antenna gain of 41.3 dB (at 0 degree elevation and 0 degree relative azimuth), the known elevation angles of Pier 45 relative to YBI (1.5 degrees) and PTB (0.7 degree), and the known antenna gain variation with elevation angle as shown in Figure 4-13. In addition, the radar transmission line loss from transmitter to antenna was known from the manufacturer's tests to be 4.4 dB for each radar. Prior to each power measurement check, the power output of the online transmitter was measured at the respective radar. The detector incident power was then computed from the radar equation taking into account the range from the radar to Pier 45.

Table 4-1 presents a tabulation of the expected power density at Pier 45 and the measured power density. It is pertinent to note that each

power measurement was repeated at least three times, and the values listed in Table 4-1 are the averages of these measurements.

TABLE 4-1. Expected detected power and measured power detected at Pier 45 from online transmitters at the VTS radars located at YBI and PTB.

Radar Location	Radar Polarization	Power (dBm)	
		Computed	Measured (Average)
YBI	Linear	+1.9	+1.8
	Circular	-1.1	-1.0
PTB	Linear	-3.0	-1.0
	Circular	-6.0	-4.2

The results for YBI indicate good agreement between the computed and measured power levels. The results for the PTB measurements are not as good a correlation, but conversely the spread of 2.0 dB is acceptable for field tests.

These results show that the radiated power of the VTS radars is well within the expected tolerance.

4.2.3 Transmitter and Receiver Parameters

A series of engineering measurements of the basic operating characteristics of the radar transmitter and receiver systems were made to determine the performance of the transmitted pulse shape, the receiver pulse response characteristics, the receiver noise figure, and the receiver bandwidth.

4.2.3.1 Transmitted Pulse Characteristics. The transmitted pulse of the radars is nominally 50 nanoseconds or 200 nanoseconds in width. The measurements of the transmitted pulse were made by detecting the pulse at the output port of the cross guide coupler of both trasnmitters at YBI and the online transmitter at PTB. The detected pulse was displayed on a calibrated oscilloscope, and photographs were made to record the results.

Figure 4-14 shows a photograph of the 50-nanosecond transmitted pulse from the number 1 transceiver at YBI. The transmitted 50-nanosecond pulse from the number 2 transceiver at YBI and from the number 2 transceiver at PTB were essentially identical to that shown in Figure 4-14. From this photograph, it can be seen that the pulse has an essentially exponential rise and fall with a rise time of approximately 55 nanoseconds and a fall time of approximately 45 nanoseconds (as measured between the 10- and 90-percent pulse amplitude points). The pulse width of the 3-dB amplitude points (0.707 of peak amplitude) is 50 nanoseconds.

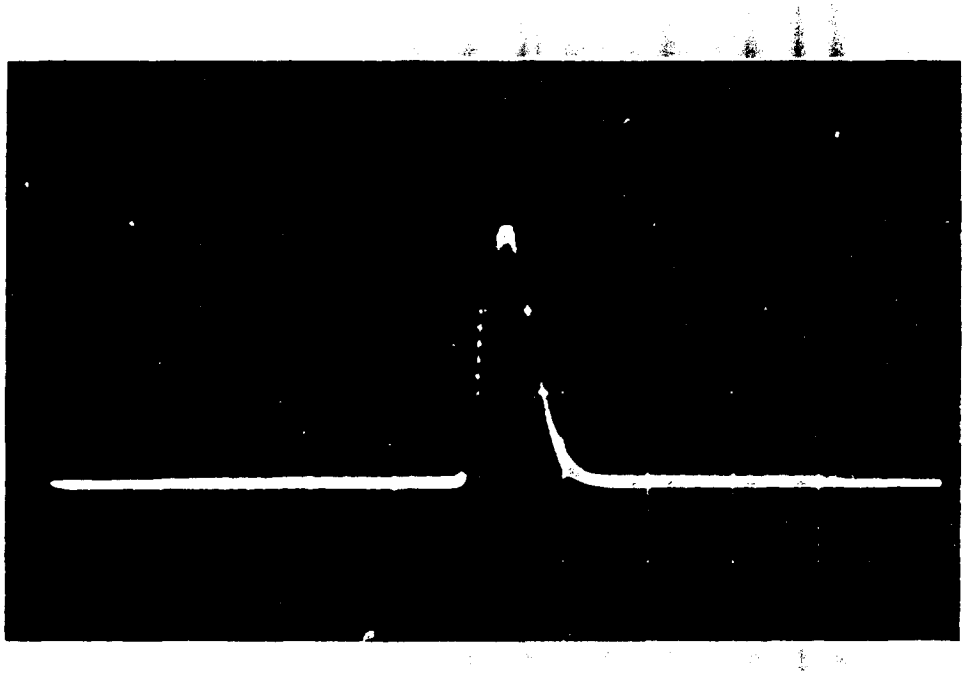

Scale = 100 nanoseconds/centimeter

FIGURE 4-14. Transmitted 50-nanosecond pulse.

Figure 4-15 presents a photograph of a representative transmitted 200-nanosecond pulse. As in Figure 4-14, the rise and fall shapes are exponential with a rise time of 45 nanoseconds and a fall time of 45 nanoseconds. The pulse width between the 3-dB points (0.707 amplitude) is approximately 190 nanoseconds.

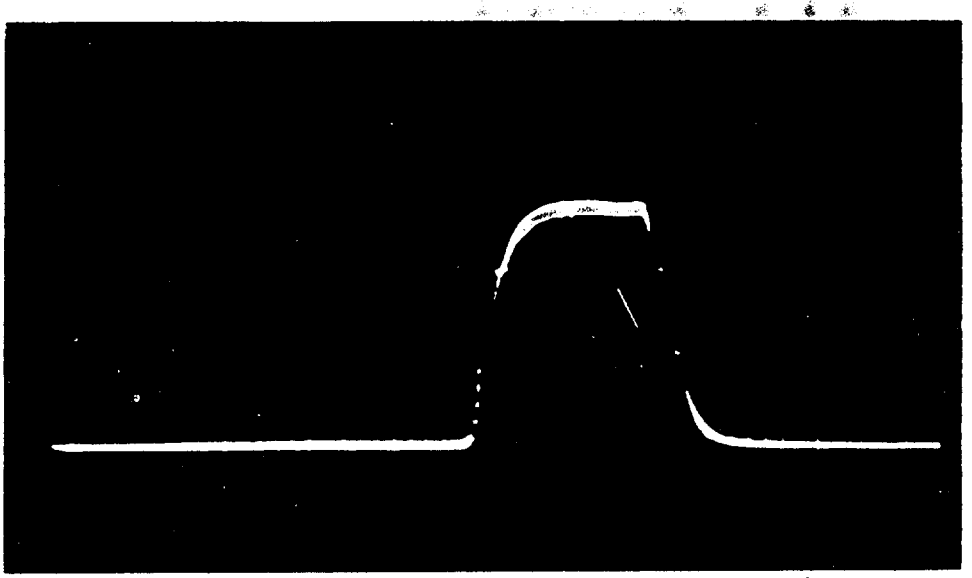

Scale = 100 nanoseconds/centimeter

FIGURE 4-15. Transmitted 200-nanosecond pulse.

4.2.3.2 Receiver Pulse Response. Ideally, the proper manner in which to obtain the response of the receiver to the transmitted pulse shape would be to pass the transmitted pulse through a nondispersive delay line and apply an attenuated sample to the receiver input; however, a suitable delay line was not available during the test and an alternate method was followed. The test set signal generator output, set to the transmitter frequency, was pulse-modulated with a Hewlett-Packard Pin Diode modulator and applied through a directional coupler to the radar receiver input.

Figure 4-16 presents a photograph of the test signal pulse as detected with a crystal diode and displayed on a 50-megahertz (MHz) Tektronix oscilloscope. The rise time of the pulse is 25 nanoseconds, and the fall time is 20 nanoseconds where it should be understood that a 10-percent tolerance would normally be applied to oscilloscope measurements made by simply scaling of the display. The pulse width is 60 nanoseconds at the 3-dB or half points. The pulse rise is essentially exponential, and the fall is exponential to the 10-percent point.

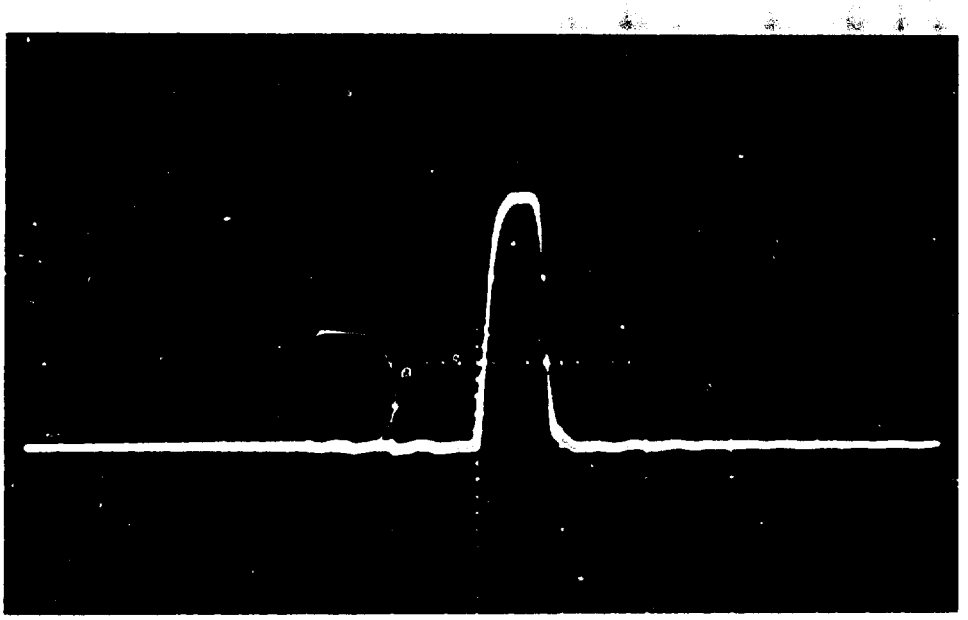

Scale = 100 nanoseconds/centimeter

FIGURE 4-16. Test signal pulse, 60 nanoseconds at 3-dB level (25 nanosecond rise; 20-nanosecond fall).

Figure 4-17 is a sample photograph of the video pulse output of the logarithmic receiver at YBI when the test pulse of Figure 4-16 was applied. The pulse response must be interpreted in terms of the logarithmic characteristics of the receiver. Scaling for the pulse is shown on the left side in terms of millivolts as observed on the oscilloscope and in terms of equivalent signal level in dBm along the right side. The scaling in terms of dBm is taken from the data on the transfer function for the YBI logarithmic receiver that is discussed in Paragraph 4.2.3.5.

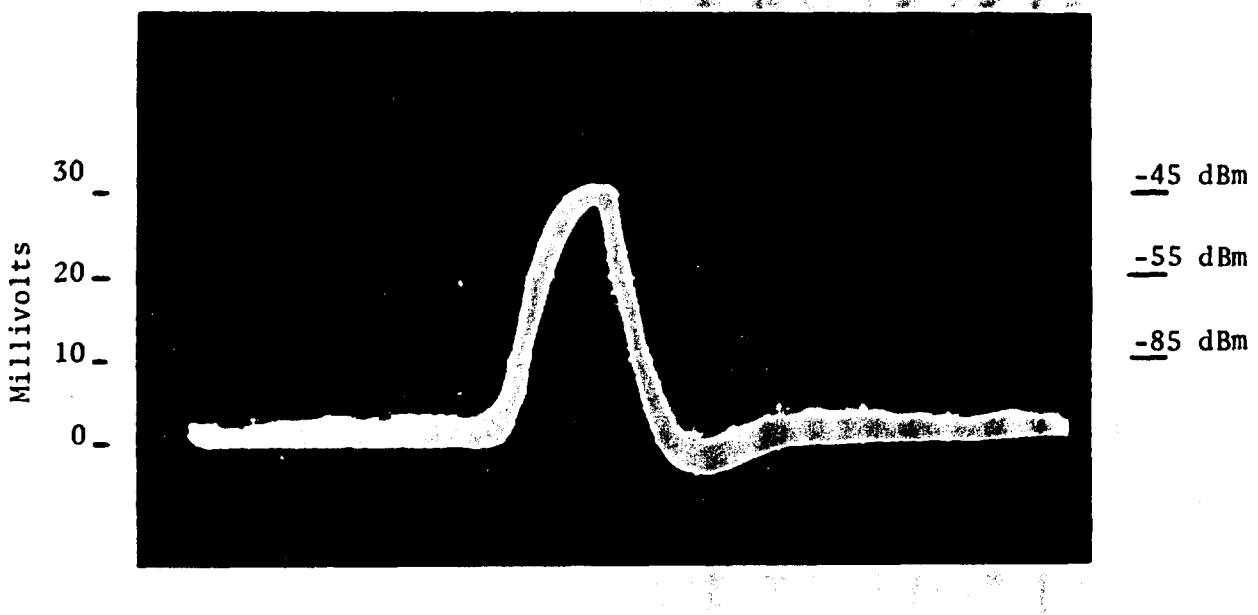

Scale = 100 nanoseconds/centimeter

FIGURE 4-17. Test pulse at receiver video output; 95 nanoseconds at 3-dB level (60-nanosecond rise and 40-nanosecond fall).

Usual pulse shape criteria are stated in terms of the pulse width at the 3-dB or 0.707 of peak amplitude level and the rise and fall times measured between the 10-percent and 90-percent peak amplitude levels. The 90-percent level corresponds to -1.0 dB from peak amplitude, and the 10-percent level corresponds to -20 dB from peak amplitude. It should be noted in Figure 4-17 in terms of the logarithmic scale that the pulse width at the -3 dB level is nearly 60 nanoseconds. The rise time is approximately 50 nanoseconds, and the fall time is 40 nanoseconds between the -1 and -20 dB points. These values compare to the input test pulse values of approximately 60 nanoseconds pulse width at the -3 dB level, a rise time fo 25 nanoseconds in

the 10- to 90-percent interval, and a fall time of 20 nanoseconds in the 90- to 10-percent interval. The rise time of the pulse is essentially limited by the effective bandwidth of the bandpass circuits in the intermediate frequency (IF) amplifier and the video amplifier; whereas, the fall time is restricted primarily by the logarithmic action.

If the pulse is examined in terms of linear processing of the test pulse, a different set of results is obtained. Inspection of Figure 4-17 will, in this case, indicate an apparent 3-dB pulse width of 95 nanoseconds, a rise time between the 10- and 90-percent levels of 65 nanoseconds, and a fall time of 55 nanoseconds. The displays and the automatic detection system will accept the pulse of Figure 4-17 as a 95-nanosecond pulse with a 65-nanosecond rise time and a 55-nanosecond fall time. The transmitted 50-nanosecond pulse will also be effectively stretched by the logarithmic amplifier in a similar fashion, and simple scaling would suggest that it will be recovered by the receiver as an 30-nanosecond equivalent linear pulse. This will effectively reduce the intrinsic range resolution of 25 feet to be expected with the 50-nanosecond pulse to approximately 40 feet.

The theoretical effect of the use of a logarithmic amplifier on the shape of a received pulse can be easily illustrated. A nominally square pulse, after passing through a bandpass amplifier, will have essentially exponential leading and trailing edges, so it can be assumed that such a pulse is to be passed through a perfect logarithmic amplifier. In Figure 4-18, a pulse is illustrated that has exponential rise and fall times and the same pulse after passing through a logarithmic amplifier.

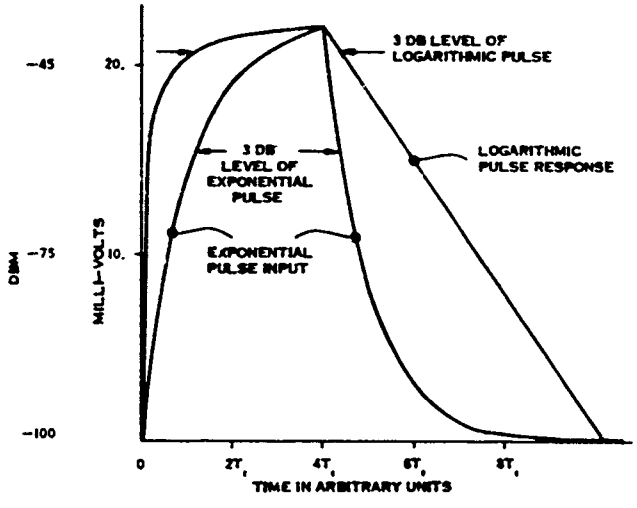

FIGURE 4-18. Comparison between pulse shape output from a true logarithmic amplifier and corresponding exponentially shaped input pulse.

Both pulses have been plotted to the same amplitude, but it should be noted that the input pulse amplitude is scaled to a linear voltage scale and the output pulse is scaled to a logarithmic scale (where the scale selected is 0.4 millivolt per decibel). The peak amplitude in this case would correspond to a -55 dBm level.

It is at once evident that the leading edge of the logarithmic pulse is apparently rising faster than the input pulse, and the trailing edge is falling much more slowly and, in fact, is falling off in a linear fashion as it should for the true exponential shape that has been assumed. The logarithmically processed pulse width is obviously greater at the -3 dB level on the logarithmic scale. The experimental pulse response results obtained with the logarithmic receiver discussed previously are at least qualitatively comparable with the theoretical results shown in Figure 4-18. The obvious conclusion can be drawn that the use of a logarithmic IF amplifier causes the received pulse to be effectively stretched by a factor of 1.5 to 2.0, the exact extent being a function of the rise and fall time characteristics of the pulse. Real pulses do not have true exponential shapes for the entire rise and fall times, and consequently deviation from the ideal shapes indicated in Figure 4-18 is to be expected.

Figure 4-19 is a sample photograph of the video pulse output of the linear IF amplifier when installed in the PTB radar transceiver and the test pulse of Figure 4-16 was applied. It should be noted that the rise time (10- to 90-percent amplitude) is approximately 60 nanoseconds; the fall time is approximately 60 nanoseconds; and the pulse width between the 3-dB points is 70 nanoseconds. The pulse output shape is nearly gaussian.

There is a small difference in the equivalent pulse width response for the linear and logarithmic receivers for the same pulse input. The logarithmic pulse has an apparent pulse width of 95 nanoseconds as contrasted with the 70-nanosecond pulse width of the linear receiver. This should result in an intrinsic range resolution performance of approximately 35 feet for the linear receiver and 48 feet for the logarithmic receiver if a 60-nanosecond pulse were transmitted. For the 50-nanosecond pulse, which is used in the radar, the range resolution should scale by simple proportion to 30 and 40 feet, respectively. The difference is not considered to be a significant factor.

Paragraph 4.3.4 presents a discussion of the tests of the observable range resolution on the PPI displays. Tests were made with both the linear and the logarithmic IF amplifiers using 60-nanosecond test pulse shapes similar to those shown in Figure 4-16. No significant difference in observable range resolution was found between the two types of amplifiers, which suggests that the large dynamic range advantages of the logarithmic amplifier have not been obtained at an excessive cost in range resolution.

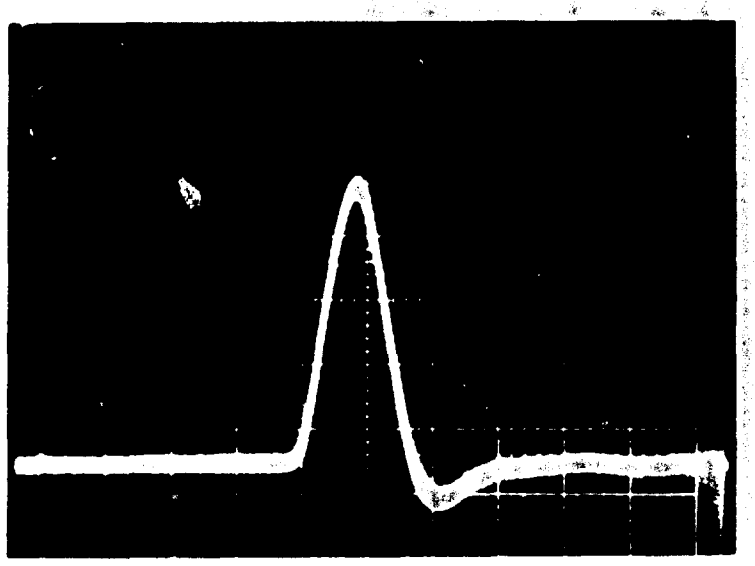

Scale = 100 nanoseconds/centimeter

FIGURE 4-19. Video pulse output of linear IF amplifier; 70 nanoseconds at 3-dB level (60-nanosecond rise and 60-nanosecond fall).

4.2.3.3 Receiver Bandwidth Measurements. The radar receivers use a logarithmic IF amplifier to attain a suitable dynamic range. The 3-dB bandwidth specified for the logarithmic IF amplifier is 22 ±2 MHz when the 50-nanosecond pulse is being transmitted and 10 ±2 MHz when the 200-nanosecond pulse is being transmitted. An IF preamplifier preceding the logarithmic amplifier has a specified 3-dB bandwidth of not less than 30 MHz and not greater than 40 MHz. The bandwidth of the total cascaded receiver network is expected to be approximately 18.6 ±2 MHz and 9.6 ±1.9 MHz for the narrow and wide pulse transmissions, respectively.

A linear IF amplifier was also procured for the purposes of making comparative performance tests with the logarithmic IF amplifier. The nominal 3-dB bandwidth specifications for the linear IF amplifier are 48 MHz independent of transmitted pulse width. The bandwidth of the cascaded receiver networks is expected to be approximately 28 MHz.

The 3-dB bandwidth of the RVP and display video amplifiers was not measured during these tests but was measured by the manufacturer and found to be 10 MHz. The effective video bandwidth of the logarithmic receiver network chain is one-half the IF bandwidth or 9.3 ±1 MHz. The overall video bandwidth of the receiver for the short pulse transmission mode is then 6.9 ±0.5 MHz. The corresponding approximate rise time or fall time for an input square pulse would be 50 nanoseconds, which is approximately the value found in the pulse response tests (Paragraph 4.2.3.2). Similarly, the overall video bandwidth of the linear receiver and video amplifier is approximately 8.1 ±0.4 MHz with a corresponding approximate pulse rise time of 45 nanoseconds for a square input pulse.

The overall IF bandwidth of a radar receiver is normally selected to maximize the detection performance of the radar. Experiment and theory have indicated that the optimum IF bandwidth is obtained when the product of the 3-dB IF bandwidth and the transmitted pulse width are on the order of 0.8 to 1.2. A value as low as 0.5 or as high as 3.0 degrades performance by approximately 2.0 dB. The bandwidth by pulse width product for the VTS radars is seen to be a nominal value of 0.93 for the narrow pulse transmission and 1.92 for the wide pulse transmission. Narrower bandwidth than the optimum for detection will also tend to result in excessive pulse stretching, which degrades range resolution performance. Wider than the optimum bandwidths tend to improve the pulse response fidelity, thus improving range resolution. Bandwidths of 2 to 4 times greater than the optimum are required to achieve any significant improvement in pulse response fidelity and consequently range resolution. The resultant range resolution improvement is normally not considered sufficient to compensate for the decreased detection performance.

Bandwidth measurements were made of the linear and logarithmic amplifiers at YBI and PTB. The bandwidth for the narrow pulse transmission mode was measured for the four receivers. The bandwidth for the wide pulse transmission mode was measured for one logarithmic receiver each at YBI and PTB. The bandwidth measurements were made by injecting a test pulse into the transceiver waveguide coupler at the radar operating frequency as previously described in Paragraph 4.2.3.2. The 60-nanosecond test pulse was used when measurements were made of the bandwidth of the receivers at YBI and the logarithmic receivers at PTB. A 1.5-microsecond test pulse was also used to measure the linear receiver bandwidth at PTB and the logarithmic receiver of transceiver number 2 at PTB. The video output of the receiver was observed on an oscilloscope. A signal input level of approximately -80 dBm was used at the center frequency (i.e., the frequency at which maximum response is obtained). The test generator frequency was then shifted in uniform increments away from the maximum response frequency. At each new frequency, the attenuation between the test set output and the waveguide coupler was adjusted to bring the pulse response observed on the oscilloscope to the value observed at the maximum response frequency.

The results of the bandwidth measurements are shown in Figures 4-20 through 4-24 and summarized in Table 4-2. The system bandwidth is defined as the bandwidth between the -3 dB response points in Figures 4-20 through 4-24.

TABLE 4-2. Measured receiver system bandwidths

Location	Transceiver Number	Amplifier Type	Transmitter Pulsewidth (nanoseconds)	Bandwidth (MHz)	
				Expected	Measured
YBI	1	Linear		28	16*
	2	Logarithmic	50	18.6 $\pm$2	16*
	2	Logarithmic	200	9.6 $\pm$1.9	16*
PTB	1	Logarithmic	50	18.6 $\pm$2	21*
	2	Logarithmic	50	18.6 $\pm$2	17*;17.6**
	2	Logarithmic	200	9.6 $\pm$1.9	14.2*
	2	Linear		28	18*

* 60-nanosecond test pulse
** 1.5 microsecond test pulse

It will be observed that the logarithmic receiver of transceiver number 2 at YBI has a bandwidth in the narrow pulse transmission mode that is slightly less than the expected lower bandwidth tolerance limit. The observed deviation is not considered to be significant from an operational standpoint. The logarithmic receiver in transceiver number 2 at YBI has a bandwidth for the wide pulse transmission mode that is in excess of the expected upper tolerance value, but this, again, is not believed to be a significant deviation.

The PTB logarithmic receivers in the narrow pulse mode had measured bandwidths within the expected bandwidth tolerances. It will be noted that two measurements of bandwidth were made on the logarithmic receiver of the number 2 transceiver. One was made with the 60-nanosecond test pulse, and the other with the 1.5-microsecond test pulse. A time interval of approximately 3 months intervened between the two measurements, and it should be observed that there has been no significant change in bandwidth during that interval. The number 2 transceiver logarithmic receiver bandwidth for the wide pulse transmitted mode has a bandwidth that is greater than the expected bandwidth tolerance limit, but this deviation is not as great as that observed for the logarithmic receiver of transceiver number 2 at YBI.

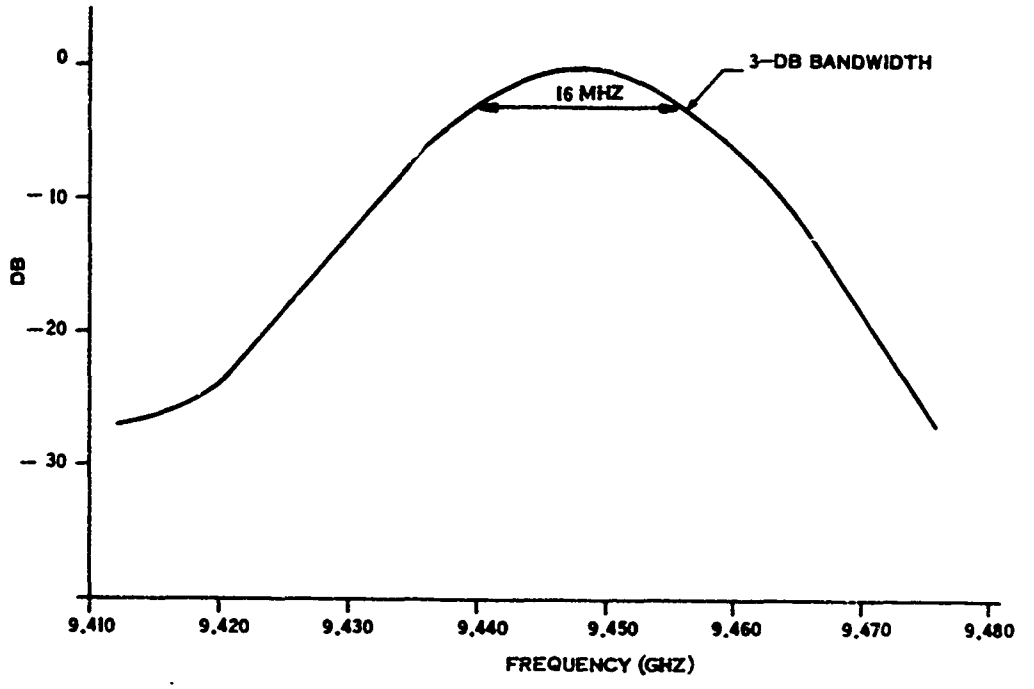

FIGURE 4-20. Frequency response of YBI transceiver number 1 (linear IF).

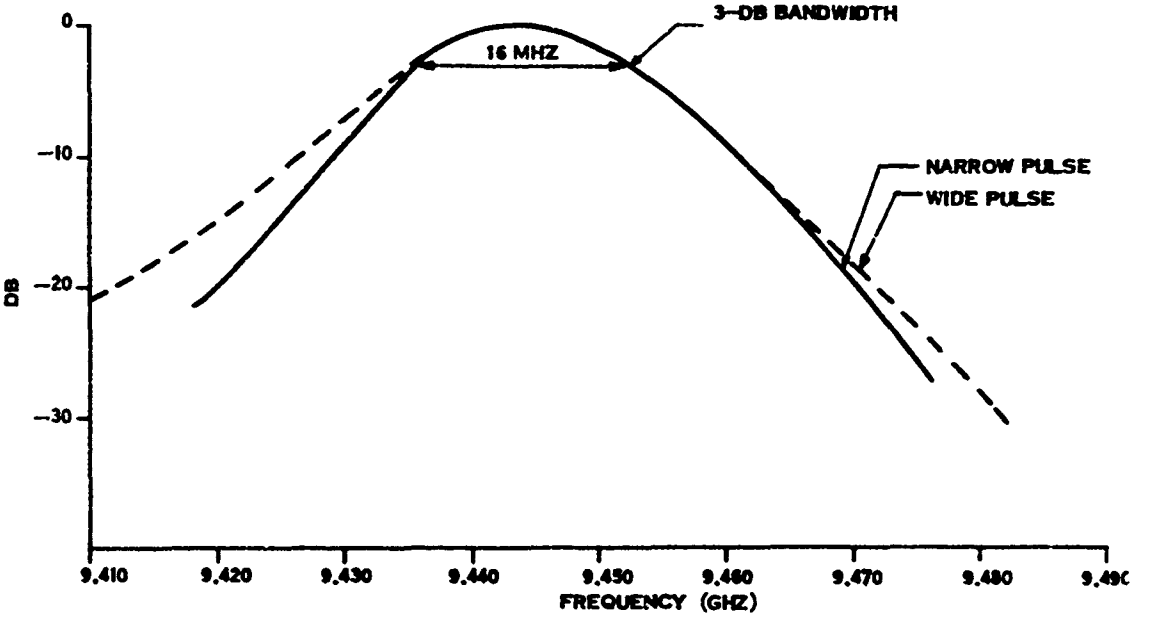

FIGURE 4-21. Frequency response of YBI transceiver number 2 (logarithmic IF, narrow and wide pulse modes).

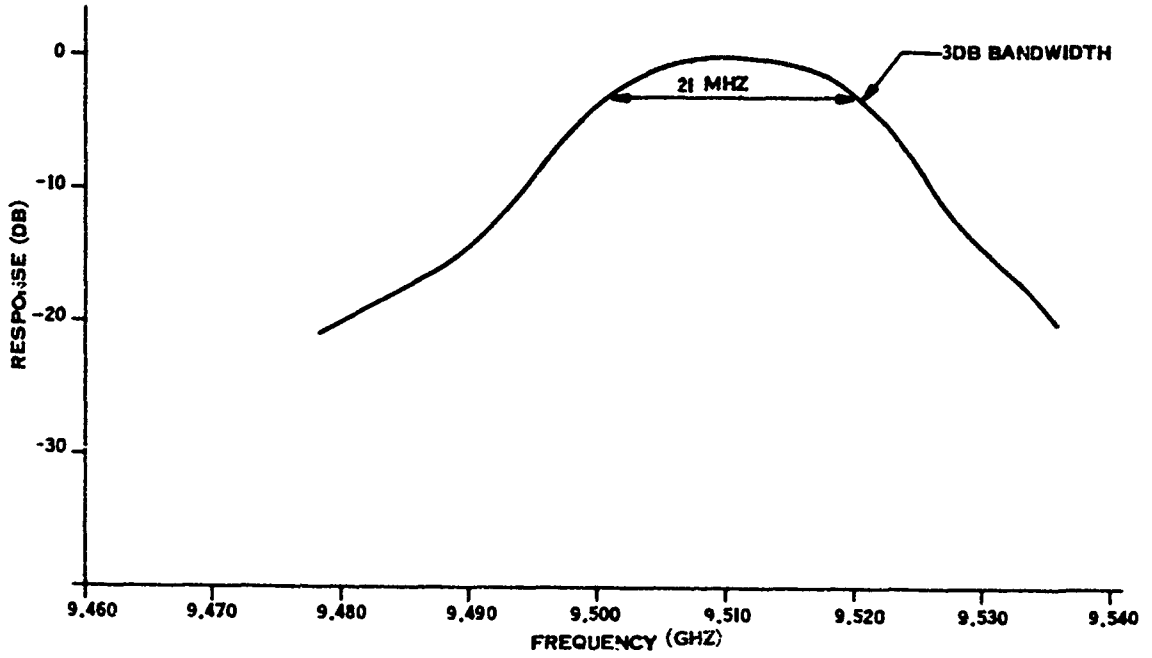

FIGURE 4-22. Frequency response of PTB transceiver number 1 (logarithmic IF, narrow pulse mode).

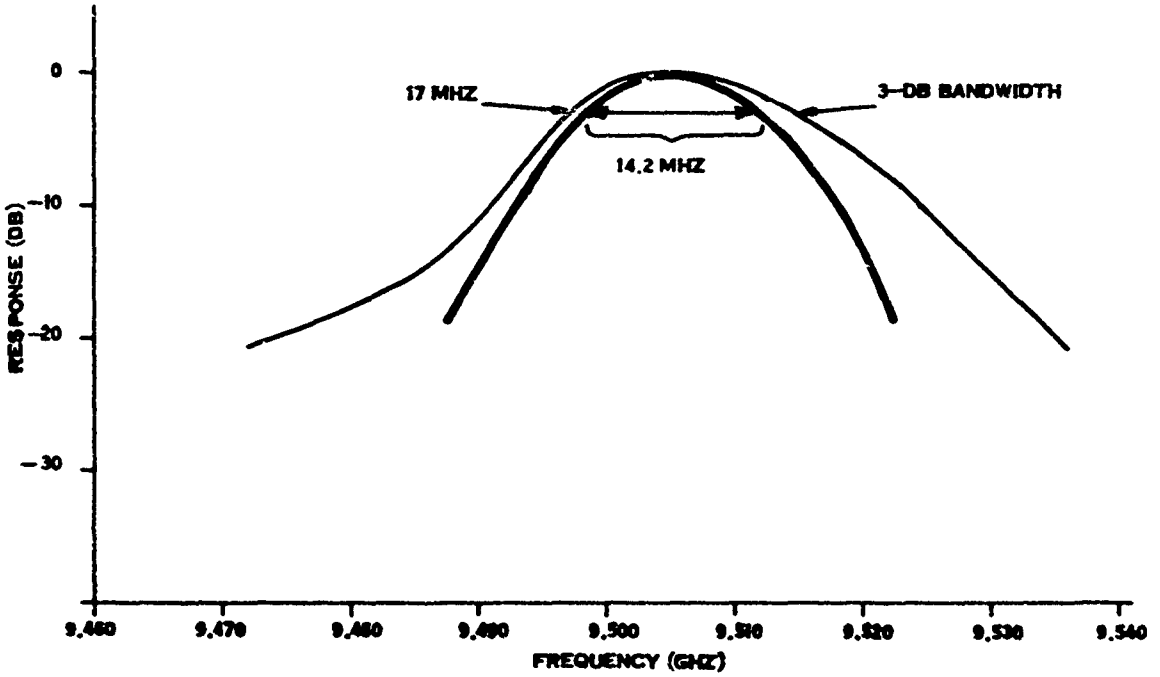

FIGURE 4-23. Frequency response of PTB transceiver number 2 (logarithmic IF, narrow and wide pulse modes).

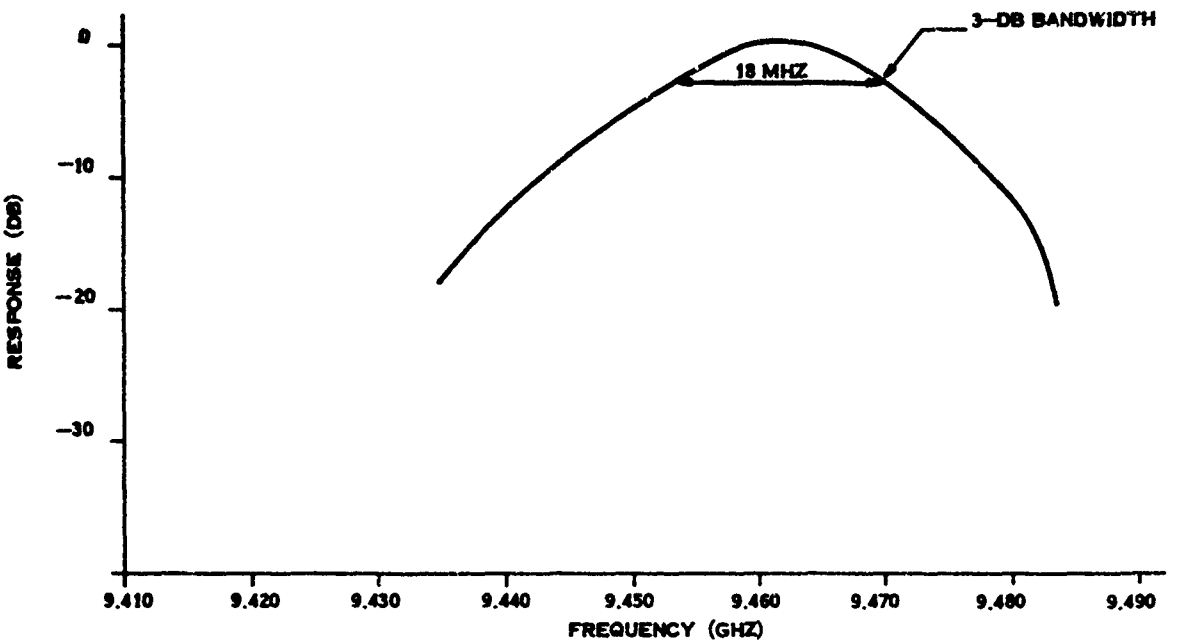

FIGURE 4-24. Frequency response of PTB transceiver number 2 (linear IF).

The linear receiver, when tested in transceiver number 2 at PTB, had a measured bandwidth of 18 MHz, and when tested in transceiver number 1 at YBI, the receiver had a measured bandwidth of 16 MHz (both measured values being considerably smaller than the expected value of approximately 28 MHz). A measurement of the preamplifier bandwidth was made on transceiver number 2 at PTB and was found to have a 3-dB bandwidth of approximately 24.0 MHz. The estimated bandwidth of the cascaded preselector amplifier and an assumed 48-MHz bandwidth linear IF amplifier would be approximately 22 MHz, which is comparable with the observed 18-MHz bandwidth. It is probable that the cut-of-tolerance preamplifier bandwidths also account for the less than expected bandwidths of the receivers of the numbers 1 and 2 transceivers at YBI (with the linear and logarithmic receivers).

The observed bandwidths are considered to be acceptable for both narrow and wide pulse transmission modes from a detectability standpoint. As pointed out previously, the detectability criterion is a pulse time by bandwidth product of approximately unity, and only small changes of detectability are observed for deviation from a value of unity.

4.2.3.4 Receiver Noise Figure. The noise figures of each receiver of the transceivers at PTB and YBI were measured for the narrow pulse transmission mode (i.e., the side intermediate frequency bandwidth condition). A Hewlett-Packard Noise Figure Meter and Argon 15.2-dB noise source were used to make these measurements. The results are presented in Table 4-3.

TABLE 4-3. Measured receiver noise.

Location	Transceiver Number	Specified Noise Figure (dB)	Measured Noise Figure (dB)
YBI	1	6.0	6.8
	2	6.0	7.5
PTB	1	6.0	9.0
	2	6.0	8.9

The noise figures measured for the receivers at YBI are 1.8 and 2.5 dB higher than the manufacturer's specification, and the PTB receivers have measured noise figures that are 2.9 and 3.0 dB higher than specified. These discrepancies are not considered to be serious problems in view of the normal uncertainties associated with measurement of receiver noise factors. In any case, the excess noise figure noted should not result in any adverse operational effects on the detectability performance of the radars since the detectability performance in the VTS service will normally be limited by sea clutter rather than receiver noise.

4.2.3.5 Receiver Transfer Function. The receiver intermediate amplifiers of the radars have logarithmic transfer functions (i.e., the output pulse amplitude is proportional to the logarithm of the input amplitude over the major portion of the total dynamic range of the receiver). This characteristic is used to prevent the "blooming" of strong targets on the display and the suppression of small targets by the limited dynamic range of the PPI phosphor, which would occur if a strictly linear intermediate frequency amplifier were used and the PPI intensity adjusted for minimum saturation by the strong targets.

Tests were made to measure the logarithmic intermediate frequency amplifier transfer characteristics of the receivers at PTB and the one logarithmic amplifier installed at YBI. The test set signal

generator was modulated to provide the 60-nanosecond pulse form previously shown in Figure 4-16 and the output applied to the receiver input via the waveguide coupler. The receiver output video pulse was observed on the calibrated oscilloscope. Data were then recorded for the receiver input in dBm versus video pulse output in millivolts (mV).

Figure 4-25 shows a plot of the data for the receiver in the number 2 transceiver at YBI. If truly logarithmic, the transfer would be a straight line of input in dBm versus output amplitude on a linear graph. It should be noted that the graph has two essentially linear regions. From -85 to -55 dBm, the slope is nearly 2.5 dB/mV; and from -55 to -40 dBm, the slope is nearly 1.25 dB/mV. The characteristic is such that the strongest signals (those above -55 dBm) have greater compression than those below -55 dBm. The average transfer slope is approximately 1.88 dB/mV, and the maximum deviation of the measured transfer from the average slope is approximately 3 dB.

Figure 4-26 shows the amplitude transfer measured for the logarithmic receivers in the two transceivers at PTB. The number 1 receiver has a slope of 1.66 dB/mV from -80 to -70 dBm and an essentially constant slope of 2.14 dB/mV from -70 to -40 dBm input. The number 2 receiver has a transfer slope of 1.11 dB/mV from -90 to -75 dBm input and a slope of 1.90 dB/mV from -70 to -40 dBm input. The logarithmic characteristics are similar in the range from -70 to -40 dBm, which is the region for the majority of the targets of interest. The average slope for the number 1 transceiver is 2.1 dB/mV, and the maximum deviation of the measured transfer from the average straight line fit is less than 2 dB. The average slope for the number 2 transceiver is 1.65 dB/mV, and the maximum deviation of the measured transfer from the average straight line fit is approximately 2.0 dB.

The absolute gains of the PTB transceivers 1 and 2 differ by about 10 dB. This difference is probably a result of a difference in the gain setting of the mixer preamplifier of the two radars.

4.2.4 Measurement of PPI Characteristics

Figure 4-27 is a greatly reduced reproduction of a San Francsico Harbor chart. This chart includes depth soundings, restricted areas, compass rose, as well as callouts of significant landmarks. The chart is presented to provide a general orientation for locations referenced in the report and visible on the PPI presentation of the VTS. Figure 4-28 shows both the chart and a radar PPI display centered at the 8-nmi range. The addition of the callouts on the illustration are intended to aid those who are not familiar with PPI scope display interpretation. The following paragraphs present discussions of the measurements that were made relative to the VTS PPI displays.

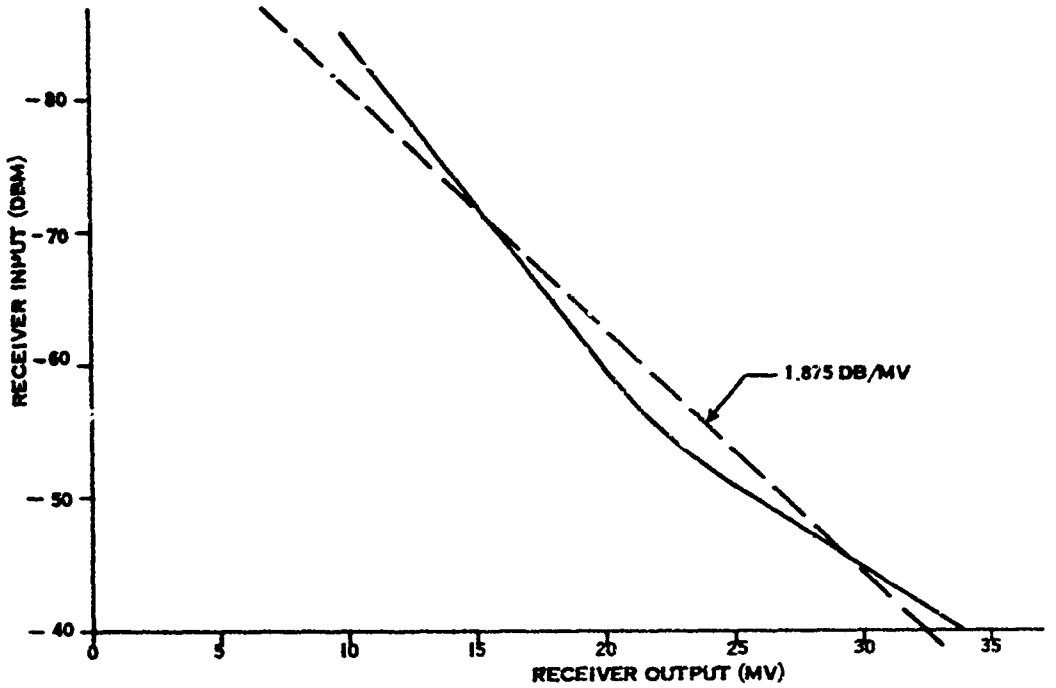

FIGURE 4-25. Calibration curve of YBI receiver number 2 output versus input.

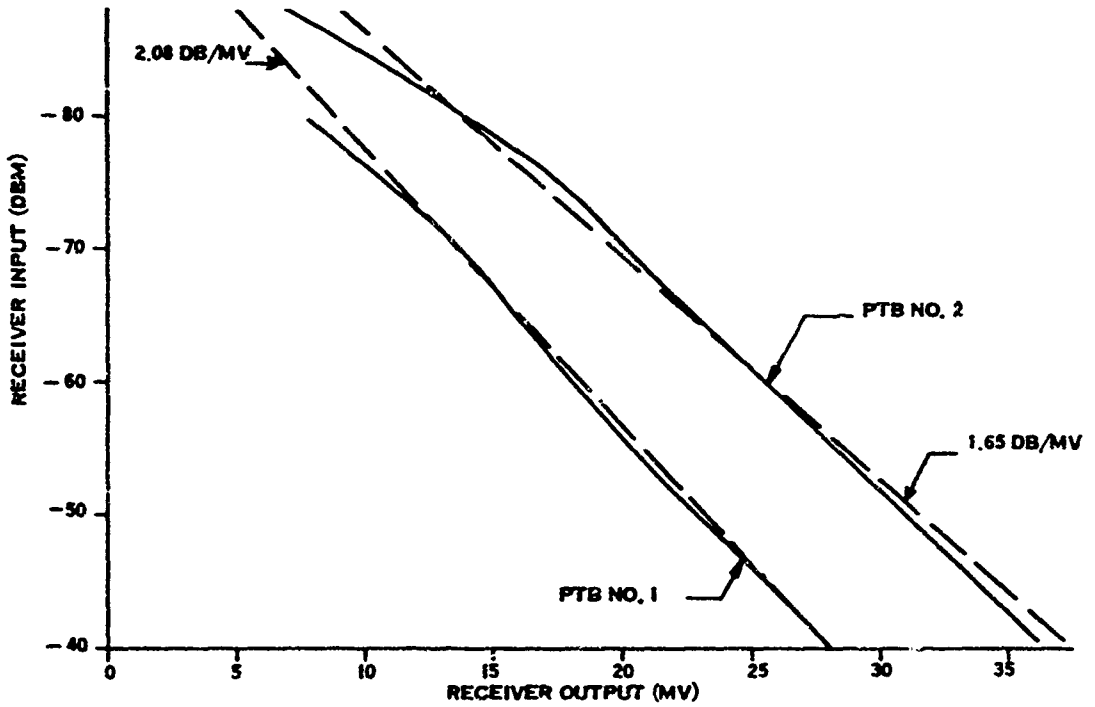

FIGURE 4-26. Calibration curves of PTB receivers numbers 1 and 2 output versus input.

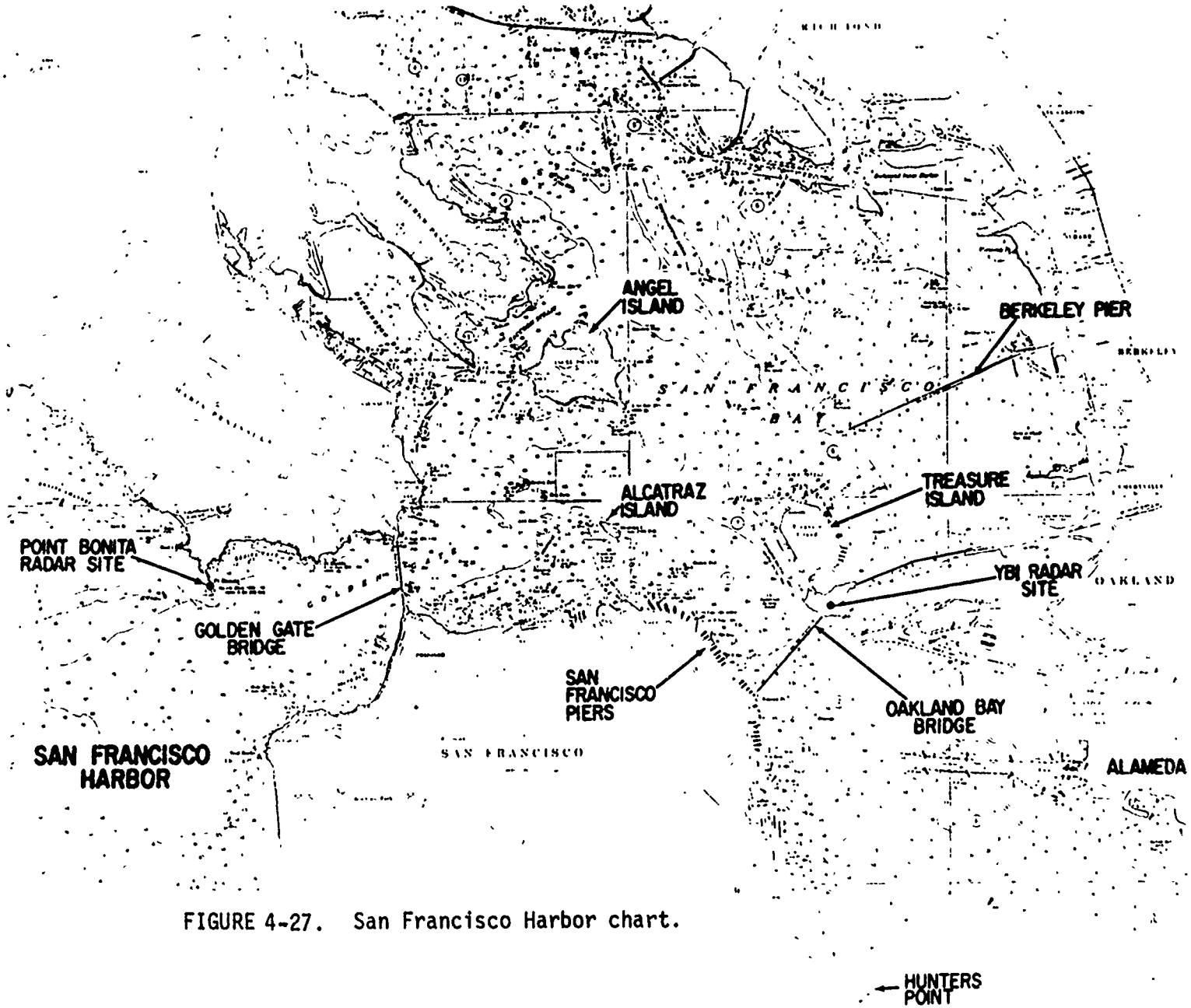

FIGURE 4-27. San Francisco Harbor chart.

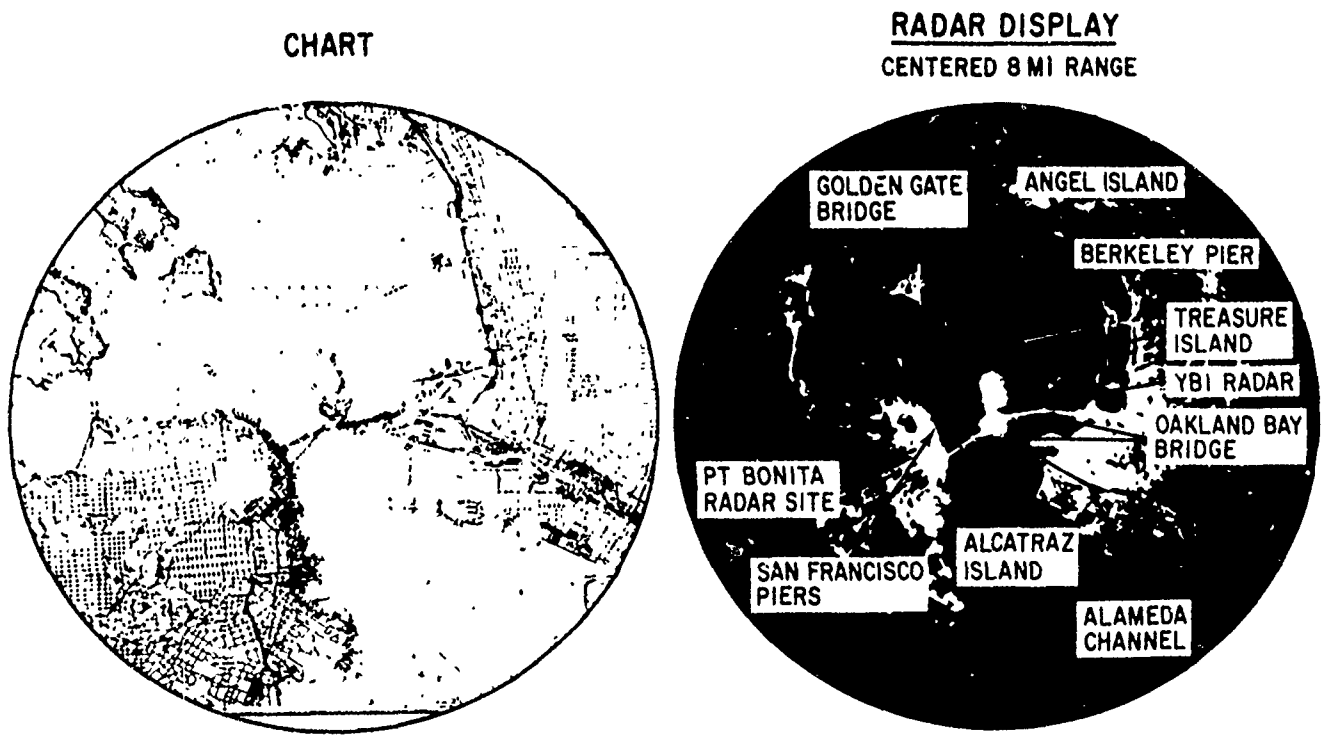

FIGURE 4-28. PPI display orientation.

The manual radar system has five PPI displays with long persistence P-7 phosphor. An orange filter is used to suppress the blue flash of the phosphor, thereby tending to enhance the presentation of the long persistence yellow phosphorescence. Range displays of 2, 4, 6, 8, and 16 nmi may be selected by the operator with either a centered display or an offset display. Provision is made for continuous control of the offset position on three preselected positions. Range rings at one-quarter, one-half, three-quarters, and full range are provided for rough estimates of range, and bearing cursors allow rough bearing estimates. Accurate range and bearing measurements can be made by means of a movable range and bearing cursor that can be positioned to measure range and bearing from the radar to a target vessel or displaced to measure range and bearing between any two selected targets. The range and bearing readouts for the cursor are in the form of a Veeder-Root type counter for bearing and a light-emitting diode type readout for range.

Additional operator assistance features of the PPI displays include sensitivity time control (STC) with three different control characteristics for use in ameliorating the effects of sea clutter saturation on sig- detection capability. A fast time constant (FTC) circuit is also provided for clutter rejection and can be used in conjunction with the STC or in lieu of the STC to provide optimum detection capability.

The many operating options available to the operator enhance the effectiveness of the system in tracking targets under most environmental conditions. The operator can optimize the display for almost any environmental condition or tracking situation to obtain proper vessel traffic monitoring and control.

A number of tests were made to determine the basic quality of the displays including the linearity of the sweep, the absence of sweep nonlinearity resulting in display distortion, and the accuracy of the variable cursor and the range rings. Tests were also made to ascertain the overall radar system performance, which directly involved the PPI displa, · (Paragraph 4.3). The following paragraphs present the results of the PPI display measurements.

4.2.4.1 Range Cursor Accuracy. The PPI displays have range rings at intervals of one-quarter, one-half, three-quarters, and full range of the range scale in use; e g., on the 2-nmi scale, range rings are at 0.5, 1, 1.5, and 2.0 nmi. These rings may be used for estimating the range of a target. For more precise measurement, a movable cursor can be set to a selected bearing and the length of the cursor adjusted to coincide with the range from the display center to the target or between any two targets. Two types of tests were made on the accuracy of the range rings and the cursor. In the first type of test, the two-target test generator was used to place two simulated targets at a known spacing apart as shown on a calibrated oscilloscope. The measured time difference converted to range was compared to the cursor measurement of range. The standard

deviation of the difference was approximately 70 yards for this method. The primary difficulty of this method is in measuring accurately the time differences between the pulses on the oscilloscope for any appreciable range difference, and most of the indicated error should probably be assigned to this cause.

A second type of test was made in which the range cursor was used to measure the distance from the display center to each range ring on the various range scales. The results of this test indicated a standard deviation of less than 40 yards for all scales and range rings. This test is more in the nature of a correlation test than an absolute test, but the previous tests with the two-target generator indicated that the standard deviation of the error of the range rings was on the order of 70 yards. It is probable that the major portion of this error is caused by the uncertainty of measuring time intervals on the oscilloscope used in the test.

4.2.4.2 PPI Display Distortion. The PPI displays were qualitatively examined for the presence of nonuniform sweep amplitudes as a function of azimuth that would result in scalloping and noncircular displays. A simple test of sweep linearity was made by inserting a non-angle-gated test pulse at the receiver input and examining the resultant circular display on the PPI. The circle diameter was then examined for signs of ellipticity and nonuniformity of sweep. Figure 4-29 shows the PPI display with the video off and range rings only displayed. It should be noted that there is no obvious display distortion. The focus was found to be uniformly good over the entire display

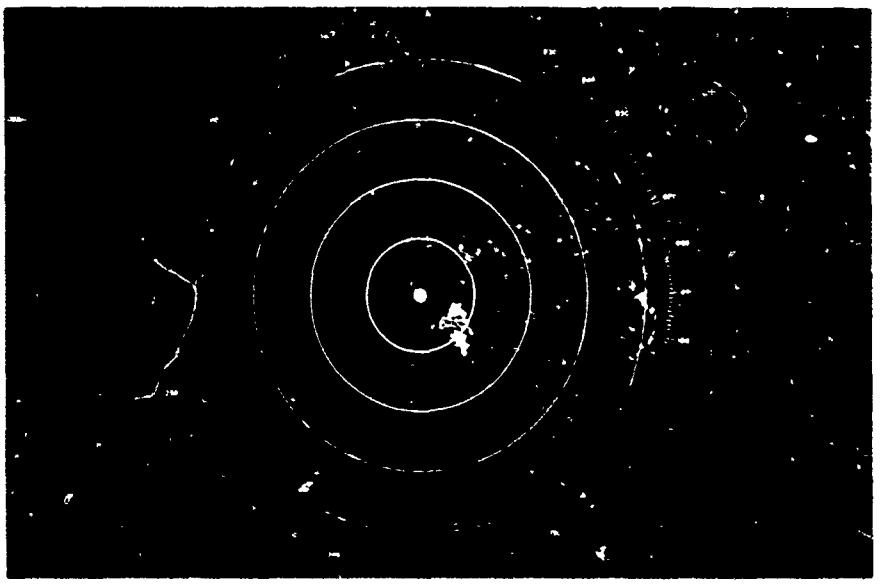

6-mai range scale; ringe rings at 1.5-nmi intervals

FIGURE 4-29. PPI display showing no distortion of range rings.

area for any range scale. The PPI display quality is considered to be uniformly excellent.

4.2.5 Microwave Data Link and UHF Control Link Tests

Several tests were made to determine the capability and the limitations of the control links in the VTS installations. The following paragraphs present the results of these tests.

4.2.5.1 Microwave Data Link. The PTB radar data is formatted into a composite video transmission that combines the received echo signals with triggers and antenna bearing information that is transmitted to YBI via a broadband microwave link. At YBI, the composite signal is reformatted to parallel form for the PPI displays. A simple test was made on the microwave link to determine the "fade margin".

An attenuator was installed in the antenna to receiver transmission line at YBI. The attenuation at the receiver input was then increased in 2-dB steps and the system performance observed on the PPI displays and radar video processor of the automatic detection and tracking system. The PPI displays exhibited some bearing data information degradation at an attenuation of 36 dB. When the attenuation reached 38 dB, the displays exhibited distinct spoking, indicating a severe loss of bearing data and small target video. The radar video processor of the automatic detection and tracking system exhibited deteriorated performance with an attenuation of 33 dB. Therefore, the microwave link has a fade margin of at least 30 dB.

4.2.5.2 UHF Control Link. The UHF control link is used to monitor and control the PTB radar from the YBI control console. A simple test of the link from PTB to YBI was made to determine the fade margin. This test was accomplished by installing an attenuator in the receiver input of the main receiver and the standby receiver. The system is arranged such that when the automatic gain control (AGC) voltage of the main (or number 1 receiver) drops below a preset value, the receiver function is switched to the number 2 (or standby) receiver. Nominally, the switchover takes place for a 15-dB change of signal level.

It was found that the main receiver requires an input signal attenuation of 45 dB before the control link operation faulted. An attenuation of 23 dB of the input signal to the auxiliary receiver caused control link failure. Therefore, these tests indicate that the UHF control link from PTB to YBI has a fade margin of at least 23 dB.

4.3 PERFORMANCE MEASUREMENTS

The performance of the manual VTS under various conditions was measured by conducting tests in which the radar tracked 40-foot cutters that were directed to follow courses that would exercise the various operational features of the system. These tests were made to determine the usable range and angle resolution, the maximum detection range, and the usefulness of circular polarization and STC in suppressing rain and sea clutter. An attempt was also made to catalog the echoing area of certain buoys so that these could be used in later performance assessments of the radar system. The following paragraphs present the results of the performance measurement tests.

4.3.1 YBI Radar Antenna Elevation Coverage

The antennas of the VTS radars were designed to have as nearly as possible cosecant-squared beam patterns in the elevation plane. This feature is intended to provide an essentially constant reflected signal power input to the radar receiver independent of range for any target whose equivalent echoing cross section is independent of range. The relationship between antenna gain required and range for a constant target reflecting cross section can be derived from the radar equation. This equation, in the simplest form, is:

$$P_r = \frac{P_t G_t^2 \lambda^2 \sigma}{(4\pi)^3 R_s^4} \qquad (1)$$

where:

P_r = Receiver input power

P_t = Transmitter output power

G_t = Radar antenna gain

σ = Echoing area of target

R_s = Slant range to target

The radar geometry is illustrated in Figure 4-30, where the radar is at a height, h, above the sea level and the targets are all at sea level. If the ratio of $\frac{P_r}{P_t}$ is to be constant, the only variable available for manipulation is G_t. Thus if equation (1) is rearranged, the following is obtained:

$$G_t^2 = K R_s^4 \qquad (2)$$

where:

$$K = \frac{(4\pi)^3}{\lambda^2 \sigma} \cdot \frac{P_r}{P_t}$$

From the geometry of Figure 4-30, it can be seen that:

$$R_s = h \csc E \qquad (3)$$

and substituting equation (3) into equation (2):

$$G_t^2 = K h^4 \csc^4 E \qquad (4)$$

or:

$$G_t = K' h^2 \csc^2 E \qquad (5)$$

Because of the physical constraints, any real antenna will have a maximum gain, G_{to}. The expression must therefore be normalized to the maximum of the real antenna.

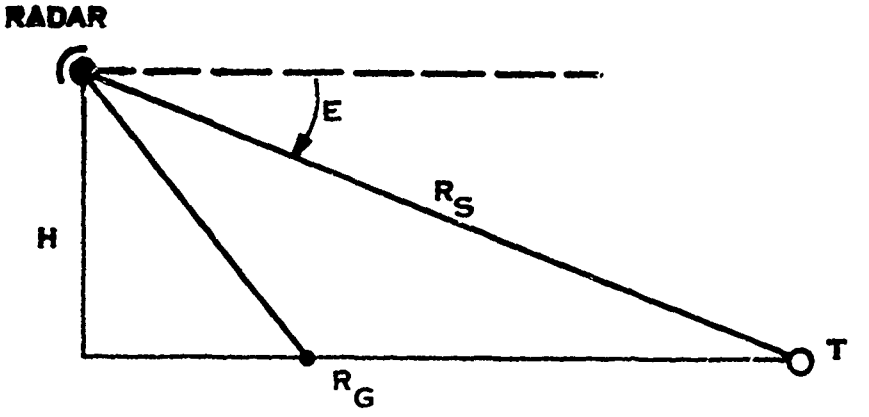

FIGURE 4-30. Geometry of the elevation plane beam coverage.

The relative gain expression then becomes:

$$\frac{G_t(E)}{G_t(E_o)} = \frac{\csc^2 E}{\csc^2 E_o} \qquad (6)$$

where:

$G_t(E_o)$ = Gain of antenna at the reference elevation angle E_o corresponding to a range, Rgm

E_o = Reference angle

$G_t(E)$ = Gain at angle E relative to reference

The expression in equation (6) can be recast in terms of Rg, the ground range and h, the radar height above sea level as shown in the following equation:

$$\frac{G_t(E)}{G_t(E_o)} = \frac{(Rg^2 + h^2)}{(Rgm^2 + h^2)} \cong \frac{Rg^2}{Rgm^2} \qquad (7)$$

where:

Rgm = Ground range corresponding to E_o and h; that is, $Rgm = h \cdot \cot E_o$

By proper selection of the beam shaping and the value E_o, the desired $\csc^2$ characteristic may be approached within a few dB. The YBI and PTB radar antennas are designed to give close approximation of the $\csc^2$ pattern in range intervals from 400 yards to 8 nmi for the YBI radar and to 15 nmi for the PTB radar. The radar specification requires that the elevation beamwidth of the YBI antenna be designed so that equal received signal strengths are obtained in the main lobe for equal size targets located at 1200 feet and 8 nmi and that signal strength for the same size target at ranges between the limits shall not be less than those levels. The same design specification applies to the PTB antenna except that the limits are 1200 feet and 15 nmi. The antenna pattern measurements were discussed previously in Paragraph 4.2.1. In addition to these measurements, a second type of test was conducted to determine the constancy of the receiver input power from a fixed size target as a function of range. A 40-foot cutter was vectored from YBI on radial courses so that the stern aspect or the bow

aspect would be presented throughout a given event. The receiver input power was measured at intervals of 200 yards throughout the given event. It had been determined in previous tests [reference (a)] that the 40-foot cutter had an apparent mean equivalent echoing area of 4 square meters for the stern aspect, 2 to 4 square meters for the beam aspect, and less than 1 square meter for the bow aspect. The measured equivalent cross sections have been observed to be quite consistent from day-to-day. The equivalent cross sections were computed from the radar equation with the known quantities being the radiated power, the received power, and the measured antenna gain. The received power was measured as described in Paragraph 4.2.3. A calibrated pulsed signal was injected into the receiver input through the transmission line directional coupler. The injected signal was adjusted to match the amplitude of the received signal and averaged over several antenna scans.

The results of the tests of the antenna cosecant-squared function are illustrated in Figure 4-31 in the curve labeled A. The signal level into the receiver as a function of range has been normalized to the signal power received at 4000 yards and is not the true value of signal power into the receiver. It should be noted that the receiver input power is not constant as a function of range and, in fact, a decrease on the order of 10 dB at 1400 yards relative to the value at 3000 yards is indicated.

The results of the test can be easily explained. Curve 2 of Figure 4-31 is the measured elevation pattern of the antenna squared and normalized to a range of 4000 yards corresponding to a 2-degree depression angle ($E = -2°$) from the maximum gain point of the antenna at zero degrees. The antenna is such that the maximum gain point on the elevation pattern is at a zero-degree elevation angle. Curve 1 is a plot in dB of the R^{-4} fall-off of signal strength with range, and it also is normalized to pass through the 0-dB level at 4000 yards. Curve 3 is the difference of curves 1 and 2 and shows that the received power will, in fact, behave very much as curve A has demonstrated. From equation (2), it is apparent that the difference of G^2 and R^4 should equal zero or a constant if a true cosecant-squared pattern were attained.

Figure 4-32 presents a plot of receiver input power versus range from 5000 to 20,000 yards. A reference line is also plotted with an R^{-4} slope. From 5000 to 10,000 yards, the receiver input power is falling off slower than an R^{-4} characteristic; however, beyond 10,000 yards, the fall-off is parallel to the R^{-4} characteristic. The transition region between the cosecant-squared characteristics and a simple fall-off proportional to R^{-4} is in the 5000 to 10,000 yard region.

The antenna elevation pattern illustrated previously in Figure 4-13 is presented in Figure 4-33 with two additional computed curves. Curve A has been added to show a computed cosecant-squared characteristic normalized to -2 degrees on the measured AIL pattern. It should be

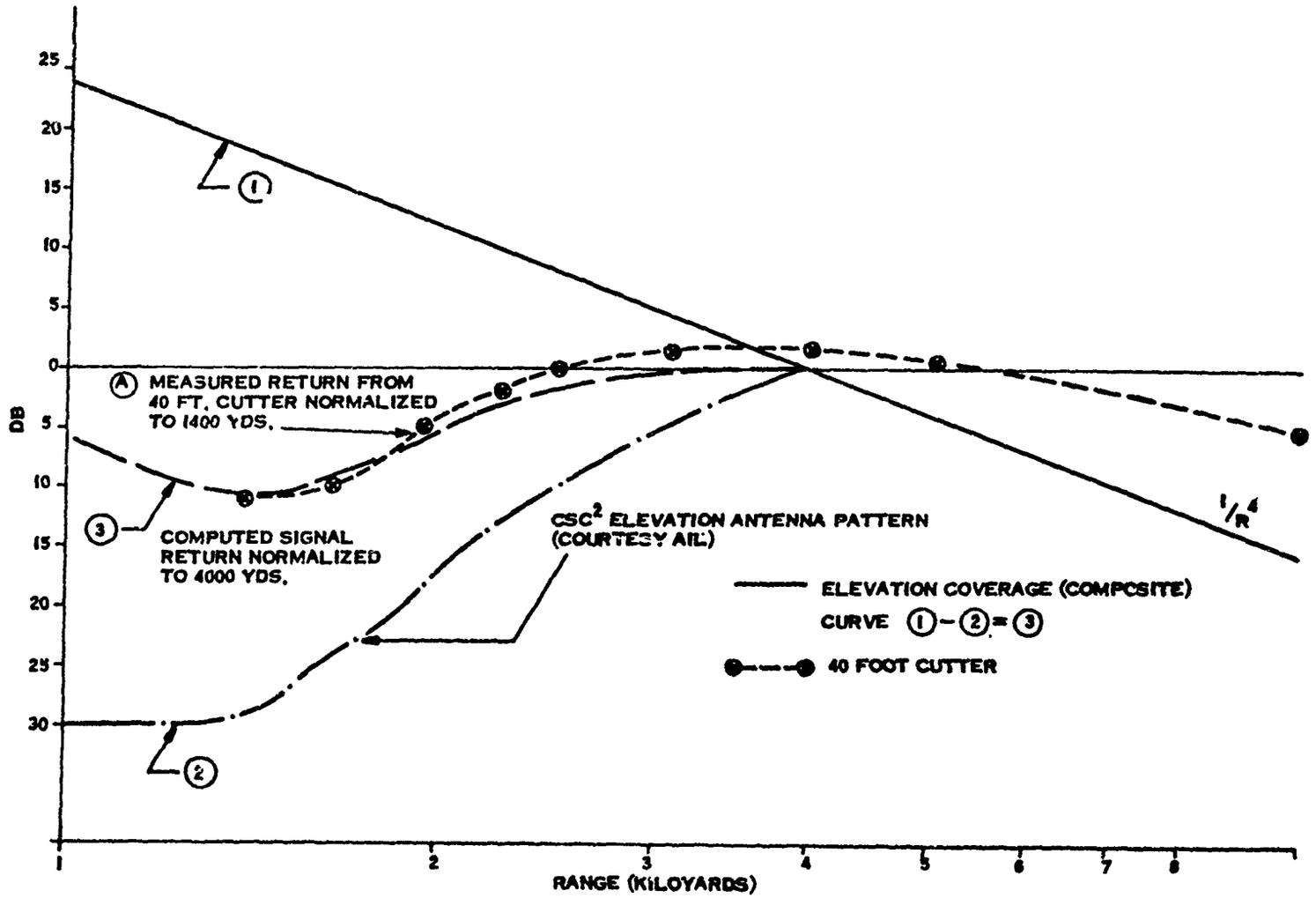

FIGURE 4-31. YBI radar coverage versus range for test of antenna cosecant-squared function.

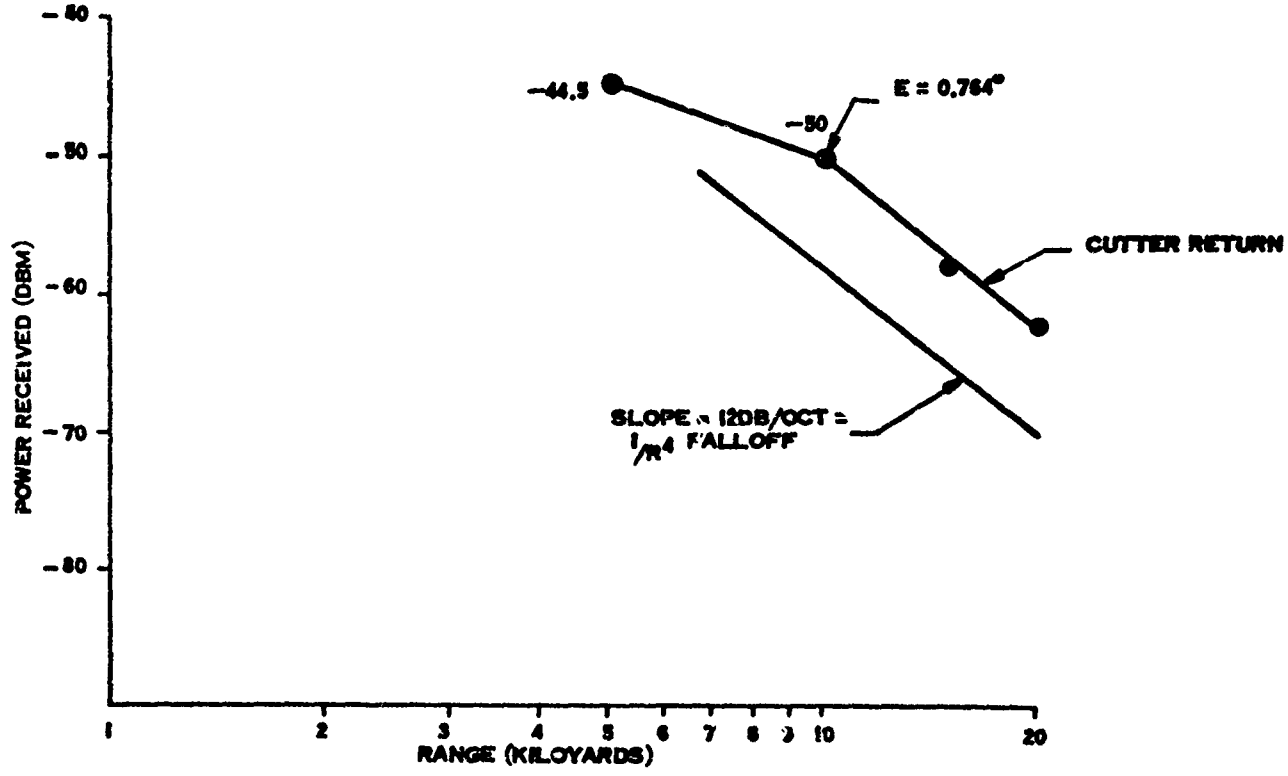

FIGURE 4-32. YBI radar elevation antenna coverage (power received from 40-foot cutter); 5000 to 20,000 yard range.

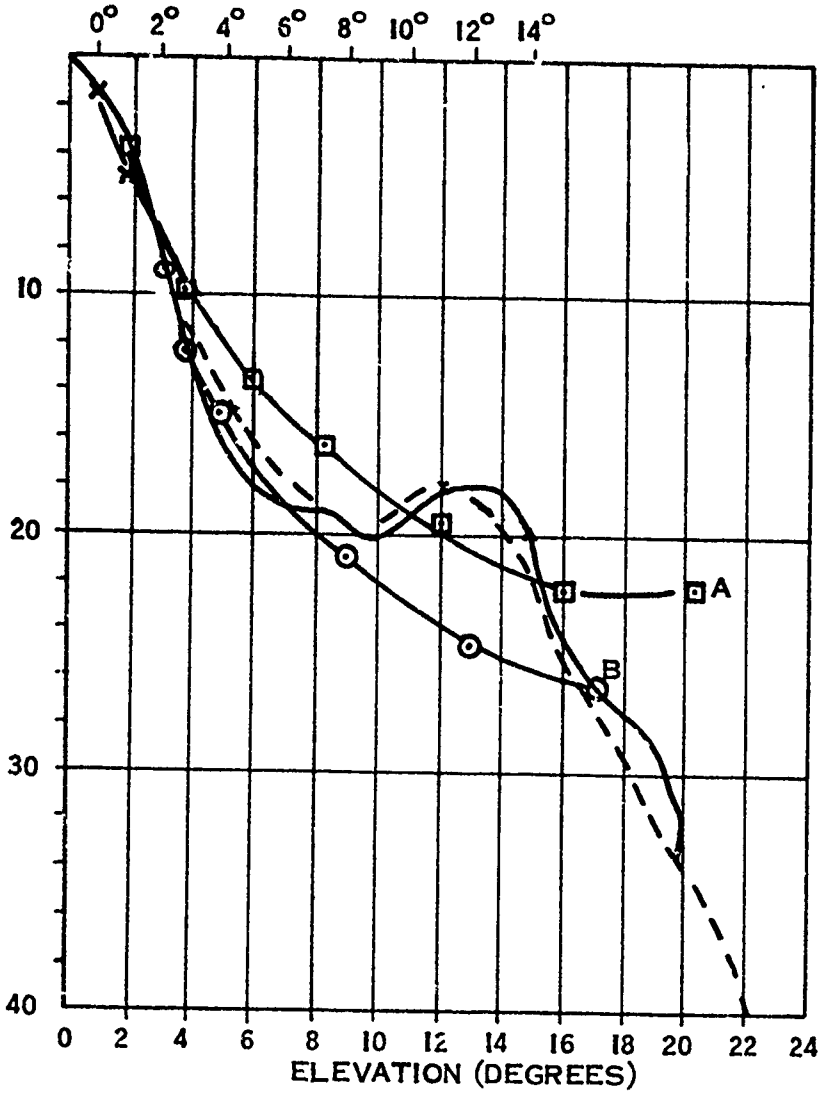

——— AIL far field pattern

– – – – AIL near field pattern

CURVE A - Computed cosecant-squared pattern normalized to -2° elevation on AIL far field pattern

CURVE B - Computed cosecant-squared pattern normalized to -3° elevation on AIL far field pattern

FIGURE 4-33. Measured antenna elevation pattern compared with computed cosecant-squared pattern.

noted that the computed curve and the measured AIL curve differ by approximately 5.5 dB at a 6-degree depression angle (on the lower scale), corresponding to 1400 yards or 11 dB for transmission and reception (which is the value indicated in Figure 4-31). It is apparent that the measured pattern does not correspond to the desired cosecant-squared pattern.

Curve B of Figure 4-33 is a cosecant-squared pattern normalized to the -3 degree point of the measured pattern (i.e., -3 degrees would correspond to a range of 4000 yards). To accomplish this match, the antenna would have to be phyiscally pointed up by 1 degree. It should be noted that the computed pattern and the measured pattern are nearly coincident in the region from -2 to -9 degress as measured on the upper scale of Figure 4-33 (which reflects the fact that the antenna would be physically moved up 1 degree). The region from -2 to -9 degrees corresponds to the range increment from 4000 to 850 yards. It is apparent that the target return power variation shown in Figure 4-31 could be substantially reduced by the simple expedient of changing the antenna elevation angle by +1 degree since in the region from -2 to -9 degrees, the computed and measured patterns show a maximum difference of 2 dB. In the region from -9 to -14 degrees (corresponding to the range increment from 850 to 500 yards), there is a substantial departure of the measured fain from the computed pattern gain, with the maximum deviation reaching +7 dB at -13 degrees. The would enhance the return from targets in this region by 14 dB over targets in the 850- to 4000-yard region and could be objectionable (although the STC in the display could be utilized to minimize the effect).

An additional objection to raising the antenna elevation by 1 degree is that the effective antenna gain for all ranges beyond approximately 1000 yards would be reduced. The effect is tabulated in Table 4-4 for selected ranges.

TABLE 4-4. Antenna gain reduction versus range for antenna tilt of +1 degree.

Range (nmi)	Elevation Angle (degrees)	Two-Way Antenna Gain Reduction (dB)
16	0.24	-2.3
8	0.48	-3.6
4	0.96	-5.8
2	1.9	-8.0
1	3.8	-7.0

The reduction in gain in the region of 1 to 4 nmi is a consequence of the flattening of the target return level in the range interval from 1000 to 4000 yards and is acceptable. The reduction in gain at the ranges beyond 4 nmi is not as acceptable because of the probable resultant detection range reduction for small targets.

A compromise adjustment of the antenna to a +0.5 degree that is a normalization to 2.5 degrees would appear to be a suitable compromise. The fit would not be as good as that of Curve B of Figure 4-33 nor as poor as that of Curve A. The magnitude of the hole shown in Figure 4-31 should be reduced to approximately 5 dB rather than 10 dB. Further, the magnitude of the increase in signal return in the region from -9 to -14 degrees would be only 10 dB relative rather than the 14 dB relative that was obtained for the +1.0 degree elevation change. The effect on maximum range capability would be smaller than that for the +1.0 degree elevation angle change. The effect of the +0.5 degree elevation angle change is tabulated in Table 4-5.

TABLE 4-5. Antenna gain reduction versus range for antenna tilt of +0.5 degree.

Range (nmi)	Elevation Angle (degrees)	Two-Way Antenna Gain Reduction (dB)
16	0.24	-1.4
8	0.48	-1.6
4	0.96	-1.8
2	1.9	-4.4
1	3.8	-3.4

The gain reductions are of the order of 1.5 dB at maximum range and should have negligible effect on system performance. The variation of signal power return in the ranges between 4000 and 1000 yards should be reduced by approximately 5.0 dB from the current value of 10 dB. (It is suggested that an antenna tilt of +0.5 degree be made at the YBI site.)

4.3.2 Detection Range

4.3.2.1 Maximum Detection Range. The specification for the radars states that they shall permit detection of a 2 square meter target at a range of 3 nmi under sea state 3 conditions. Noise-limited ranges (i.e., clear environmental conditions) for a 2 square meter target are expected to be 8

and 13 nmi for the YBI and PTB radars, respectively. Tests were previously made of the maximum detection range of the YBI radar in a clear enviornment [reference (a)] and are included in this report as being representative of the detection performance of the YBI radar.

The experimentally determined maximum detection ranges were derived by tests in which the radar tracked a 40-foot cutter that was directed in range until it was barely detectable. The proceudre followed was to observe the PPI display and to count the number of times the echo return from the cutter was visible on the PPI in a given number of antenna scans. For example, in 1 minute or 20 scans of the antenna, the echo may be displayed on 10 scans. The ratio of the number of times the echo, or "blip" is seen to the total number of opportunities is defined as the blip-scan ratio. The range at which the blip-scan ratio becomes 0.5 is commonly accepted as the mazimum detection range for a given set of conditions.

The 40-foot cutter has an apparent mean equivalent reflecting area of 4 square meters for the stern aspect and less than 1 square meter for the bow aspect. The mean equivalent reflecting cross sections were determined from the radar equation and the known parameters of the power radiated, the line losses, antenna gain, and range. The maximum detection range specifications, stated in terms of a 2 square meter echoing area, are easily converted to equivalent ranges for the 1 and 4 square meter cross sections of the 40-foot cutter and are listed in Table 4-6.

TABLE 4-6. Equivalent maximum detection ranges for targets of different cross sections.

Environment	Target Cross Section (square meters)	Specified Maximum Detection Range (nmi)	
		YBI	PTB
Clear	1.0	6.7	10.9
	2.0	8.0	13.0
	4.0	9.5	15.5
Sea State 3	1.0	2.5	2.5
	2.0	3.0	3.0
	4.0	3.6	3.6

Figure 4-34 is reproduced from reference (a) and shows the blip-scan ratio as a function of range for the YBI radar while tracking the 40-foot cutter. The environment was essentially clear in that there was only

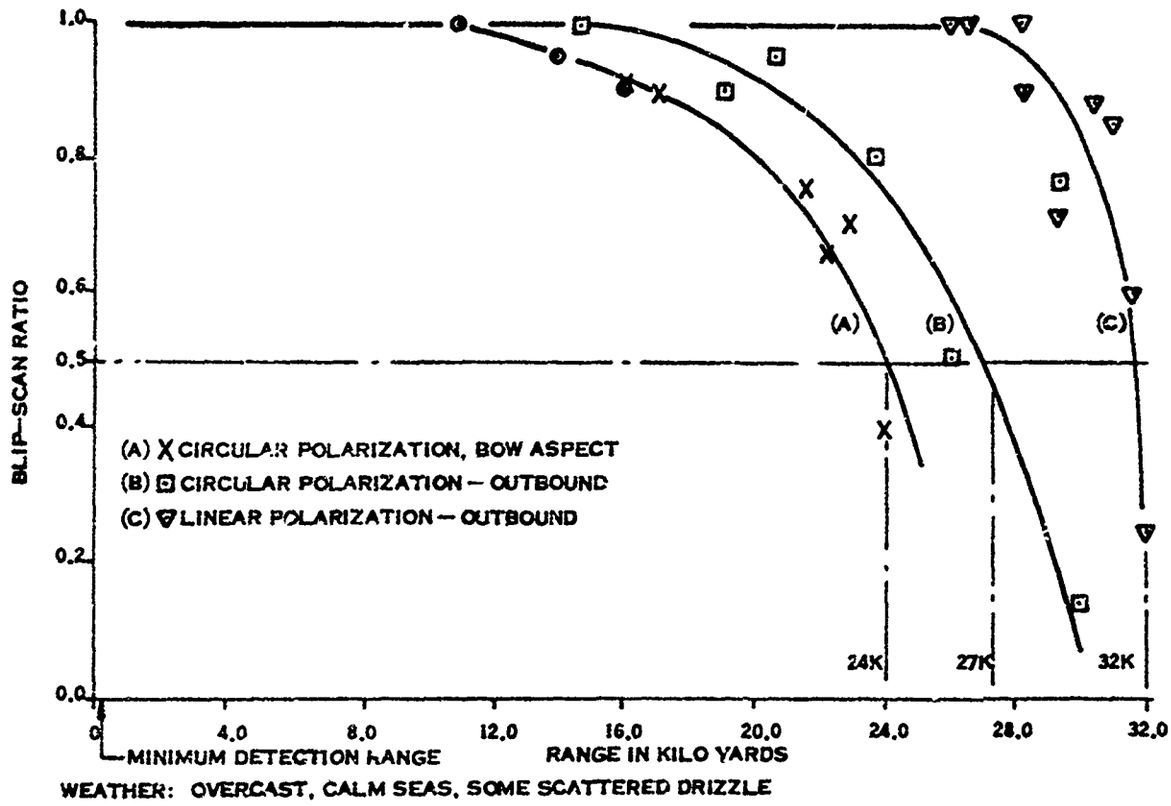

FIGURE 4-34. Blip-scan ratio as a function of range for YBI radar tracking 40-foot cutter.

scattered drizzle in the Bay. The radar was operated with narrow pulse (50 nanoseconds) and a prf of 2500 Hertz (Hz). Blip-scan ratios were measured with circular and horizontal polarization.

Curve A of Figure 4-34 is a plot of the blip-scan ratio versus range measured during a tracking event with circular polarization for the bow aspect (1.0 square meter equivalent cross section) of the cutter. It would be noted that the blip-scan ratio reached a value of 0.5 at a range of 24,000 yards or 11.8 nmi, which compares very favorably with the specified values of 6.7 nmi for the YBI radar and 10.9 nmi for the PTB radar when tracking a 1.0 square meter target.

Curve B of Figure 4-34 is a plot of the blip-scan ratio versus range measured during a tracking event with circular polarization for the stern aspect of the cutter, which has an equivalent echoing cross section of 4.0 square meters. The blip-scar ratio reached a value of 0.5 at a range of 27,000 yards or 13.3 nmi, which compares favorably with the expected value of 15.5 nmi for PTB when tracking a 4.0 square meter target.

Curve C is a plot of the blip-scan ratio versus range measured during a tracking event with linear polarization (horizontal) for the stern aspect of the cutter, which has an equivalent cross section of 4.0 square meters. It should be noted that the blip-scan ratio reached a value of 0.5 at a range of 31,500 yards or 15.5 nmi. The 15.5 nmi maximum detection range is in excess of the expected value of 9.5 nmi for the YBI radar and equal to the expected value of 15.5 nmi for the PTB radar. It should be noted that the maximum detection ranges measured are directly applicable only for the YBI radar installation and are indicative only of the maximum detection ranges to be expected for the PTB radar. Nevertheless, there is no reason to believe that the maximum detection ranges of the PTB radar would be significantly different from those measured the the YBI radar.

A number of observations were also made of the rain clutter reduction performance of the circular polarization mode of the antennas of the PTB and YBI radars. It was found that the use of circular polarization was very effective in reducing the amount and extent of the rain clutter as observed on the PPI displays. Figures 4-35 and 4-36 are sample photographs of the typical results obtained by switching from linear polarization to circular polarization at YBI. It should be observed that rain clutter extends from YBI northward over Treasure Island and eastward over the Bay Bridge in Figure 4-35 when linear polarization was used. Figure 4-36, taken a few minutes later, shows the reduction in clutter obtained by switching to circular polarization.

The reduction of rain clutter clearly makes it possible to detect targets in the rain area that could not be clearly visible when linear polarization was used. There is some reduction in maximum detection range when using circular polarization, which depends upon the reflecting characteristics of the target. In theory, a perfect square corner reflector, for example, would be invisible because it would return an echo of the opposite polarization that would be nulled by the antenna. Fortunately, perfect reflectors of this type are rare. The results of comparative tracking performance with linear and circular polarization as previously discussed indicated a maximum detection range difference of 2.2 nmi, which is a 14-percent reduction when the radar is tracking the 40-foot cutter in a clear environment. In a rain clutter situation, such as illustrated in Figure 4-35, it would probably not be possible to detect the 40-foot cutter in the rain clutter area; whereas, the use of circular polarization would provide a detection capability.

The maximum detection range tests described previously were made while using the narrow pulse transmission and the 2500-Hz prf, which is the noraml mode of operation utilized for the ADT subsystem of the VTS. A number of detection tests were also made using the narrow pulse and the 1000 and 4000 Hz rates and with the wide pulse (200 nanoseconds) and the prf's of 1000, 2500, and 4000 Hz. The performance specification for the radars

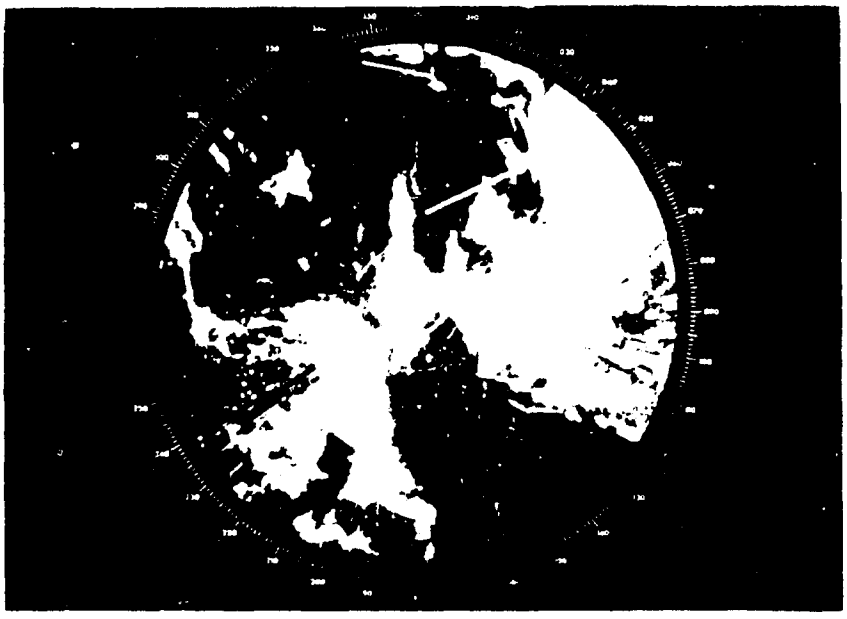

FIGURE 4-35. PPI display of VTS radar with linear antenna polarization during a rainstorm.

FIGURE 4-36. PPI display of VTS radar with circular antenna polarization during the same rainstorm.

states that the detection ranges shall be the same for all conditions of operation and for the environments specified.

Initial attempts to use the 1000-Hz rate and the long pulse transmission were unsuccessful because of a wiring error in the control circuitry at the transceiver. This was corrected and the tests were made as planned. It was found that there were no significant changes in detection performance with the alternative modes. Blip-scan measurements were made at or near the maximum detection ranges obtained with the narrow pulse and the 2500-Hz rate and were found to have essentially the same values for any of the optional combinations of pulse rate and pulse width.

It was also found that the 400-Hz rate was of little value because of the presence of second-time-around echoes in a ±15 degree sector along the 130-degree bearing line, which caused unwanted clutter on the displays. Figure 4-37 is a sample photograph of the PPI display taken while the 4000-Hz prf was in use.

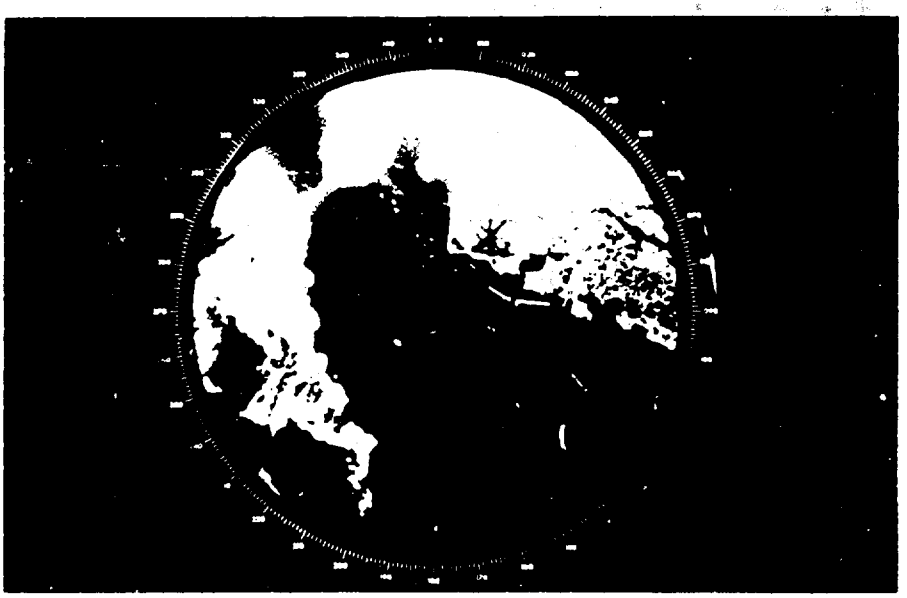

FIGURE 4-37. PPI display on 8-nmi scale showing second-time-around echoes at bearing of 130 ±15 degrees.

The second-time-around clutter return is clearly visible in the 130-degree sector. Theoretically and experimentally, an increase in repetition rate from 2500 to 4000 Hz should increase signal visibility by a factor of approximately 1.0 dB if all other factors remain constant (that is, the signal-to-noise ratio is proportional to the square root of the

number of pulses per dwell as discussed in references (d) and (e)]. This small theoretical increase of detectability is more than offset in this case by the twice-around echo clutter problem.

Conversely, going from 2500 to the 1000-Hz rate should decrease the target visibility by a factor of 2.0 dB, with all other factors being constant. A decrease of repetition rate from 2500 Hz is obviously not a desirable change even through the observed results with the FPS-109 indicated no significant difference in detectability.

The use of the wide pulse (200 nanoseconds) should, in theory, give a 40 percent greater detection range at a given repetition rate if all other factors remain constant and if the receiver bandwidth is optimized to the wider pulse as it is in the FPS-109 radar.

No attempt was made to determine this theoretical improvement because it is believed that the results obtained with the narrow pulse transmission show that the radar is adequately meeting the specified detection performance requirements. An assumption basic to the predicted detectability improvement is that the received signal is competing with receiver noise. When the radar is operated in a clutter environment, however, a different approach becomes necessary. It has been found experimentally that the best signal-to-clutter ratio is obtained by using as short a pulse as possible [references (d) and (e)] in order that the clutter patch area (beam width by pulse length) is as small as possible. This conclusion is generally supported by the results that were obtained in the series of tests of detectability reported herein.

Tests to establish the radar detection performance in sea state 3 conditions were made by blip-scan measurements on buoys of known cross section in the coverage area of the two radars during high sea state conditions. The equivalent reflecting area of a number of buoys were measured in the coverage area of each of the radars as described in Paragraph 4.3.6. Buoy number 1 at Hunters Point in the YBI coverage area is at a range of 8500 yards or 4.14 nmi and has a measured cross section of 3.6 square meters. Channel marker number 8 in the PTB radar coverage area is at a range of 7300 yards or 3.60 nmi and has a measured cross section of 1.07 square meters.

Blip-scan measurements on buoy number 1 at Hunters Point with the YBI radar and channel marker buoy number 8 with the PTB radar were made during periods when the wave height in the vicinity of the two buoys was reported to be in the 3- to 5-foot range, corresponding to a sea state 3 condition. Successive measurements of the blip-scan ratio were observed to be in the range of 0.7 to 0.9 for buoy number 1 and in the range of 0.7 to 0.9 for the channel marker number 8. The values of blip-scan ratio observed are higher than 0.5 and therefore, the buoys were not at maximum detection range.

The ranges to the buoys in both cases is greater than the required detection range in sea state 3 conditions. Table 4-6 lists the required detection range for a 4.0 square meter target as 3.6; buoy number 1, which has a cross section of 3.6 square meters, is at a range of 4.14 nmi. The required detection range on a 1.0 square meter target is 2.5 nmi, and channel marker number 8, which has a somewhat larger echoing area of 1.07 square meters, is at 3.6 nmi. The detection range capabilities of the radars in sea state 3 conditions are considered to be well within the specified values.

4.3.2.2 Horizontal Versus Vertical Antenna Polarization. The PTB antenna can be operated with vertical or circular polarization, and the YBI antenna can be operated with either horizontal or circular polarization. It has been found experimentally that in calm seas with little wind, the sea echo with horizontal polarization is considerably less than with vertical polarization. The sea echo with horizontal polarization increases with the increasing wind speed at a faster rate than the increase noted when using vertical polarization. Consequently, for rough sea conditions, there is only a small difference in sea echo magnitude for the two polarizations [reference (e)]. It has also been found experimentally that the sea clutter amplitude has a logarithmic normal distribution when short pulse transmission is used with horizontal polarization and that when short pulse transmission and vertical polarization is used, the sea clutter amplitude has a less pronounced logarithmic normal distribution. The amplitude distribution difference is such that the false alarm probability tends to be higher with horizontal than with vertical polarization for higher sea states. At low sea states, there is an obvious advantage in using horizontal polarization because of the observed lower sea clutter return.

Since the PTB radar coverage area is in a region where relatively high sea states can be expected for a high fraction of the time, the decision was made to use vertical and circular polarization of the antenna radiation. The YBI radar coverage area is in a relatively well-protected bay area where high sea states should occur less frequently; therefore, the YBI antenna polarization was selected to be horizontal and circular.

A comparative test of vertical versus horizontal polarization was made with what can be termed as only indeterminate results. A 40-foot cutter was poisitioned at a point midway between PTB and YBI and oriented such that each radar was looking at the beam aspect of the cutter, approximately 4 square meters. The nominal range from each radar was 7990 yards, which is well within the maximum detection range of the YBI radar. Blip-scan ratio measurements were made on the two radars as nearly simultaneously as possible. No discernible difference in pattern was found for the blip-scan measurements that were in the range of 0.9 to 1.0.

A more definitive test would require that the radar at each site be capable of horizontal and vertical polarization. Detection tests would then be made at each site on a long term basis with alternate vertical and

horizontal polarization under a variety of conditions to determine long term trends of the data.

4.3.2.3 Logarithmic Versus Linear IF Amplifier. The PTB and YBI radars have logarithmic receivers that were supplied in accordance with the specification requirements. In addition, one linear receiver was procured for test and evaluation purposes. A number of tests were made of the comparative detection performance capabilities of the two receiver types. Blip-scan measurements were made under relatively clear environmental conditions at and near the maximum detection ranges of the YBI radar for a 40-foot cutter (i.e., in the 25,000 to 32,000 yard region). The measurements were made alternately with the logarithmic receiver and the linear receiver to obtain data on a nearly simultaneous basis. No significant diff rence in detection performance was found under the clear environmental conditions existing during these tests. On the basis of these tests, it could be concluded that the basic performance of the two receiver types from a sensitivity standpoint is equal.

Additional tests should be made to compare the performance of the receiver types in conditions of heavy sea clutter and rain. It is particularly desirable to make such tests at the PTB location because of the greater frequency of heavy sea clutter at that site.

Current practice in radar deisgn favors the use of a logarithmic receiver because of its large dynamic range that prevents receiver saturation and limitation by large signals. It has also been found that clutter noise output of a logarithmic receiver has essentially two components, one of which varies slowly in amplitude with range that can be rejected by an FTC circuit following the receiver and another component that varies rapidly with range and whose spectral characteristics are much like white noise regardless of the clutter strength. To the extent that the slowly varying component can be rejected by an FTC circuit, a constant false alarm receiver can be achieved [reference (e)]. A linear receiver on the other hand normally has a limited dynamic range and STC circuits, and AGC must be used to control the receiver to prevent saturation and the consequent masking of targets by clutter and rain. The STC controls gain in accordance with the average expected rain or clutter over the coverage area, and deviation from the average results in less than the expected performance improvements [reference (e)].

4.3.3 Angle Resolution

The intrinsic ability of a radar system to resolve two targets in close proximity is determined by the transmitted pulse length and the antenna beamwidth. Normally, the antenna beamwidth is stated in terms of the angular spread between the one-way 3-dB points (half power) points of the antenna beam pattern. The 3-dB points correspond to a 6-dB total two-way loss between transmit and receive. The PPI will have a 10- to

20-dB linear dynamic range; therefore, the target return must drop substantially more from its maximum value at beam center than the 6-dB two-way beam pattern attenuation before it is no longer discernible on the display. For two contiguous targets, the radar "paints" a single target spot on the PPI if the two targets are not separated by more than a beamwidth in azimuth or by the range resolution increment in range.

The angle resolution tests were made by vectoring two 40-foot cutters on a radial course toward the YBI radar site. The cutters were run on parallel courses at a fixed distance apart (established by a calibrated shot line attached to the cutters) and at equal ranges from the radar. At the start of the event, the cutters were at a range such that for the separation used, they were unresolved by the radar. When the cutters reached the range at which separation was observed, the range was recorded. The technique used obviated the need to maintain instant communications with the cutters (which would have been required if the separation distance had been varied and the range fixed). The tests were conducted with the logarithmic and the linear intermediate frequency amplifiers to determine their influence, if any, on the observed resolution.

The test results are illustrated in Figure 4-38. The mean value of the observed angular resolution out to a range of 14,000 yards is indicated to be 0.35 degrees for either the logarithmic or the linear intermediate frequency amplifier. This observed resolution compares favorably with the observed 3-dB beamwidth of 0.277 degrees.

4.3.4 Range Resolution

The intrinsic range resolution of the radar is limited by the transmitted pulse width, the receiver, and the video amplifier pulse amplification fidelity, and the PPI resolution. Range resolution improves as pulse length is reduced so that intrinsic resolution of an ideal 200-nanosecond pulse (that is, a pulse with a perfectly square leading and trailing edges) is 100 feet and an ideal 50-nanosecond pulse has a 25-foot resolution. This assumes that two such pulses are displayed on an A-scope, side-by-side, and brought as close together as possible without overlapping. Normal practice in radar design is to optimize the bandwidth of the receiver from a signal-to-noise standpoint and consequently, square transmitted pulses will not be square after reception but will have essentially exponential rise and fall times. Some degradation of range resolution therefore is incurred.

The PPI resolution is basically limited by the focused spot size of the cathode-ray beam on the screen. The light intensity of a cathode-ray tube spot measured as a function of radial distance from the center normally follows a gaussian function. The spot size is arbitrarily defined to be the 50-percent light intensity diameter. A standard method of measuring spot size is the "shrinking raster" method. A television type scan pattern is displayed on the screen and the line scan focused. The raster

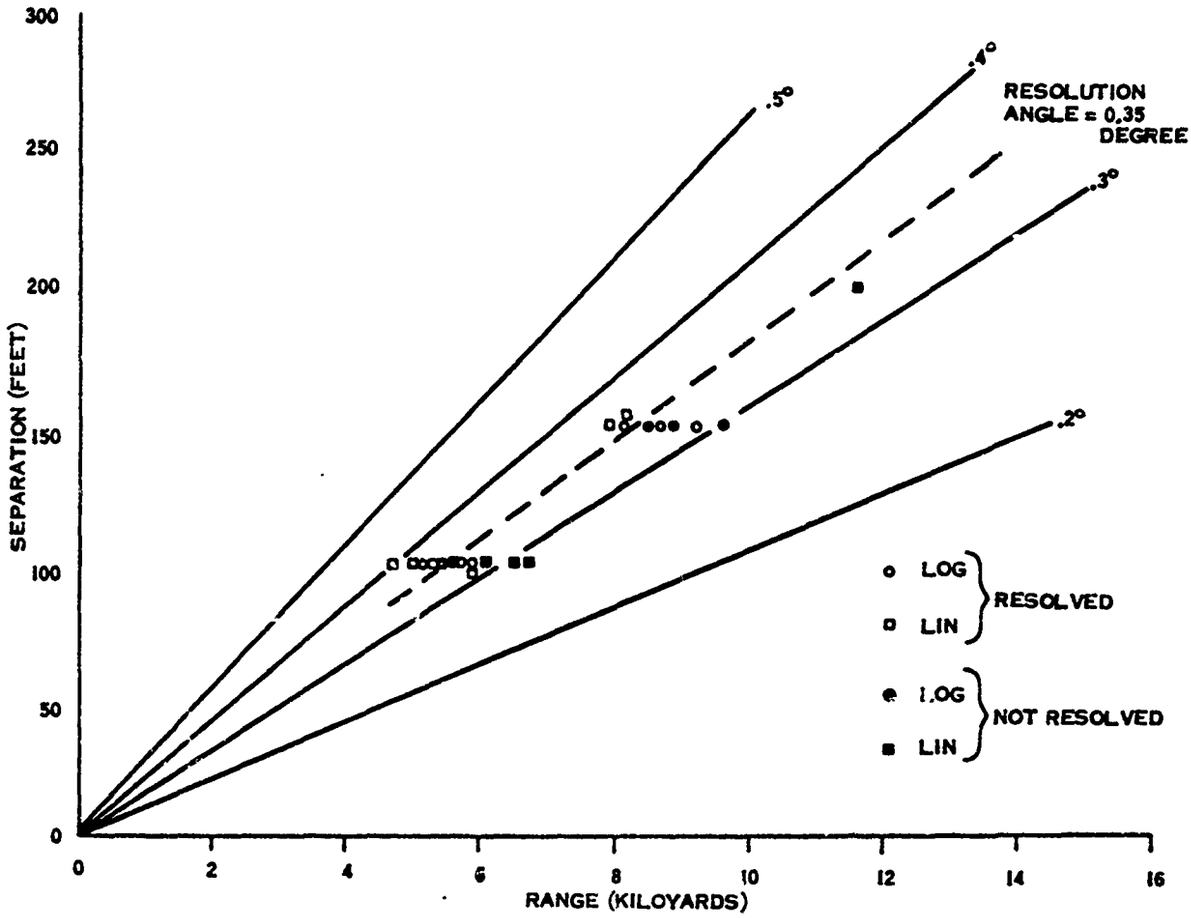

FIGURE 4-38. Angle resolution measurements at YBI.

scan perpendicular to the line scan is then decreased in amplitude until the raster lines essentially merge to a continuous bright flat field. The height of the raster divided by the number of lines is then the resolvable spot size for that tube design. The spot size determined in this manner is about 0.78 times the 50-percent amplitude measurement [reference (e)].

Reolution of the VTS PPI displays is stated to be 1000 lines for a full tube diameter, giving a spot size of 0.016 inch under ideal conditions.

It is apparent that the spot size given is an essentially undeflected spot size since the size is measured perpendicular to the sweep direction of the scan. The spot size then represents the absolute minimum size that will be displayed for an arbitrarily small pulse width used for intensity modulation of the cathode-ray tube, assuming the pulse is

at least long enough to cause a significant beam current to flow. When the pulse width is a finite fraction of the sweep length, the target blip size on the screen will be the sum of the pulse width equivalent fractional sweep length and the minimum spot diameter. The reason for this is that at the leading edge of the pulse the minimum spot size diameter will be displayed and will spread radially, both in the direction of the sweep and obviously in the opposite direction. The apparent leading edge of the target blip is thereby displaced backwards in time by a distance equal to one-half the minimum spot diameter. Similarly, the trailing edge of the pulse will be apparently extended forward by one-half of the minimum spot diameter.

For example, on the 2-nmi scale the 60-nanosecond pulse has an equivalent length of 1/406 the length of the sweep; i.e., the length of the sweep is 24,320 nanoseconds and the pulse length of 60 nanoseconds divided into sweep length is 406.

The specified PPI spot size is 1/500 of the sweep length for all range scales for a centered display. On the 2-nmi scale, the 60-nanosecond pulse has a display length in the sweep direction of (1/500 + 1/400) part of the total sweep length, equalling 1/224 part of the sweep length. The spot size perpendicular to the sweep is, of course, still 1/500 of the sweep length. The equivalent pulse length on the display is then 24,320 nanoseconds divided by 224, which equals 108 nanoseconds or 54 feet. Two adjacent pulses should, to be distinguishable, be at least 108 nanoseconds or 54 feet apart. This simplified development has neglected the fact that the intensity of the display is nearly proportional to the cube of the grid driving voltage between visual cutoff and saturation. For example, at one-half amplitude of the driving pulse, the spot intensity will be approximately one-eighth of the maximum intensity at the peak amplitude. The effect of the nonlinear drive characteristic is to sharpen the displayed target blip so that the target blip will be smaller than would be calculared by the preceding analysis.

The range resolution was tested by inserting two contiguous 60-nanosecond pulses at the receiver input by means of the bidirectional coupler installed in the waveguide. Pulse spacing and range were controlled, but the pulses were not angle gated. Consequently, the pulses were displayed as concentric rings. As the spacing between the pulses was varied, the PPI was observed. When two distinct rings were observed, the range separation of the pulses was noted. Tests were made with both the linear and the logarithmic receivers. Figure 4-39 is a set of photographs of a dual trace oscilloscope display showing the envelope of the receiver input pulse pair on the upper trace and the corresponding pulse pair at the output of the logarithmic receiver video amplifier. Figure 4-40 shows similar pulse pair inputs and outputs for the linear receiver. Each photograph corresponds to the data points listed in Table 4-7.

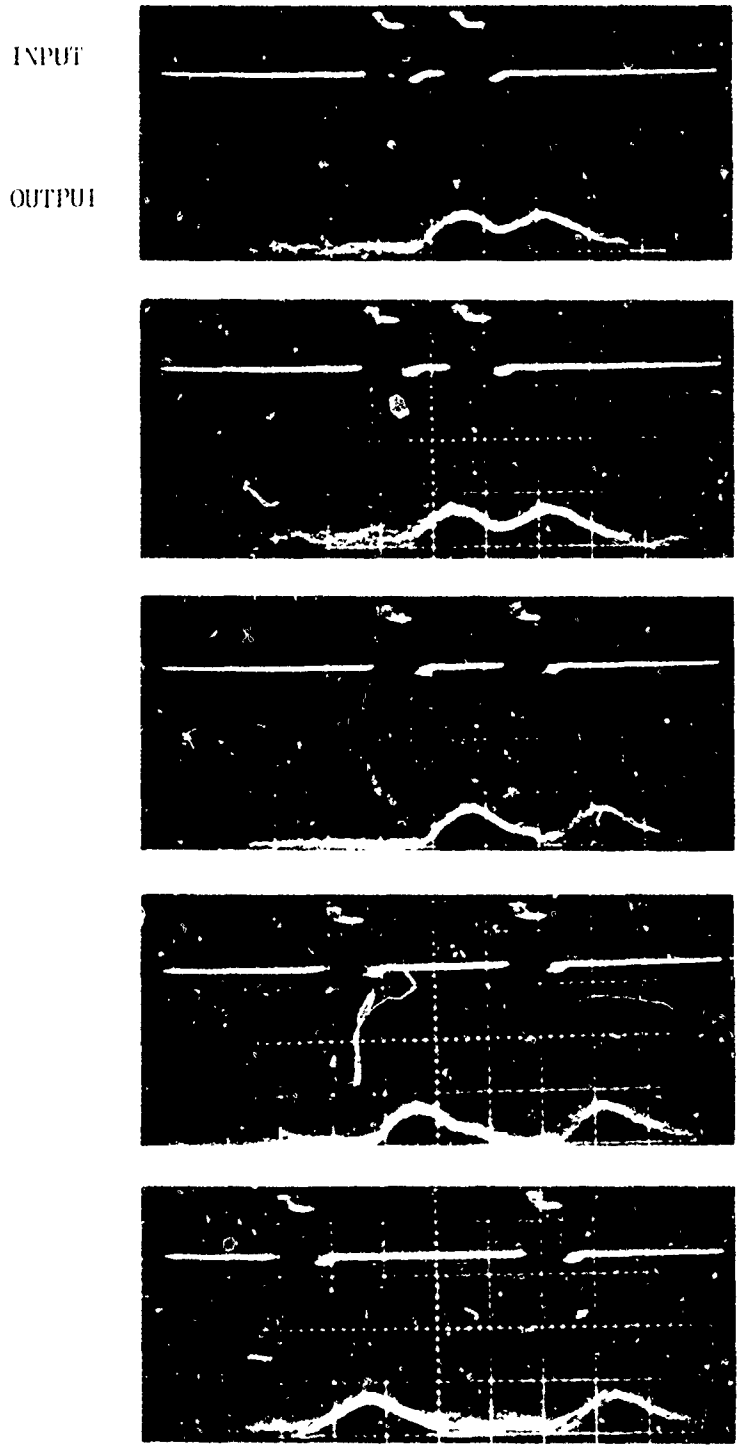

FIGURE 4-39. Input and output test pulse pair with logarithmic IF amplifier.

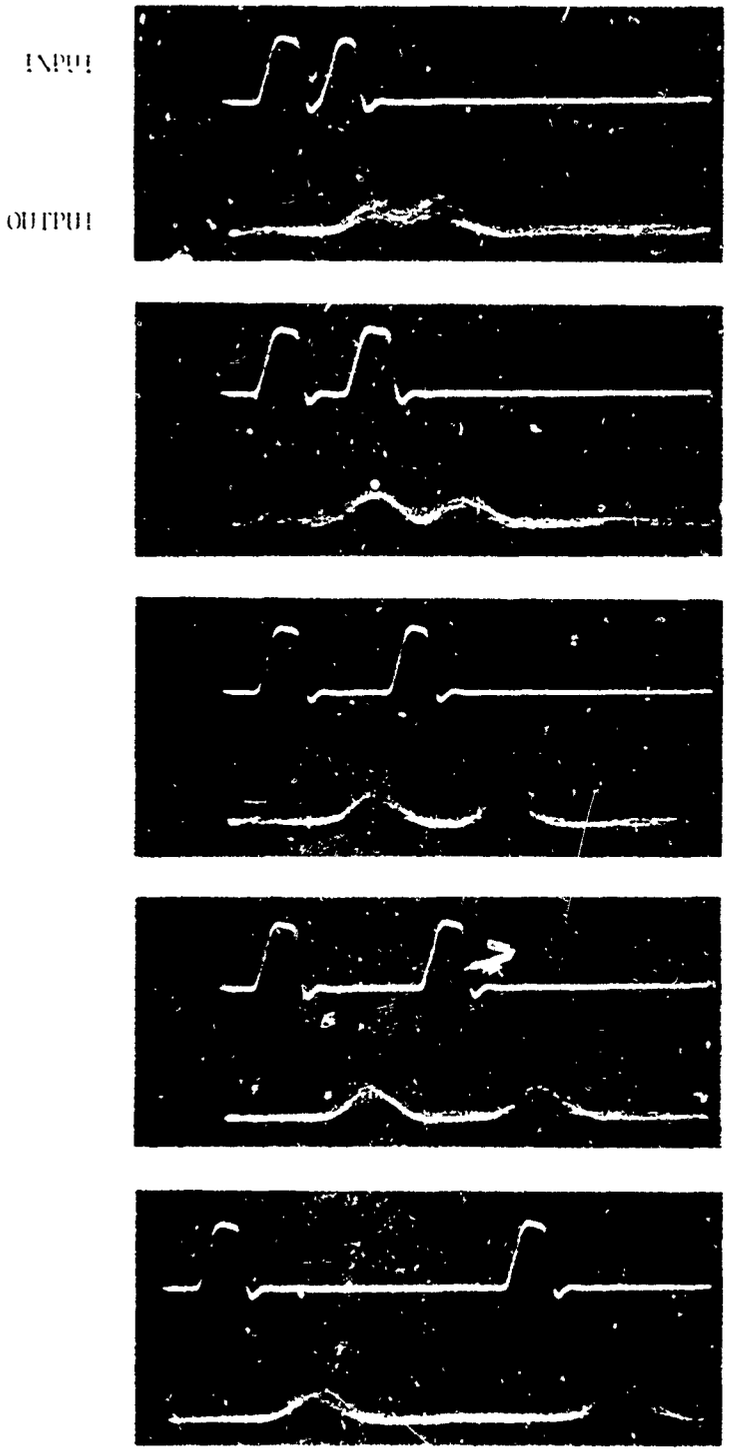

Range Scale (nmi)	Measured Resolution (feet)
2	60
4	90
6	130
8	170
10	290

FIGURE 4-40. Input and output pulses with linear IF amplifier.

TABLE 4-7. Observed range resolution versus theoretical range resolution.

Range Scale (nmi)	Observed Resolution (feet)		Theoretical Resolution (feet)	
	Logarithmic Receiver	Linear Receiver	100-nanosecond Pulse	60-nanosecond Pulse
2	80	60	75	54
4	90	90	99	79
6	130	130	123	104
8	180	170	148	123
16	230	290	245	225

The range resolution observed is tabulated in Table 4-7 in columns two and three. In column four, the theoretical resolution based on spot size and sweep rate for an assumed 100-nanosecond pulse (discussed previously) is listed for each range. Column five indicates the theoretical resolution based on the nominal spot size and sweep speed for an assumed 60-nanosecond pulse.

It should be noted that there is a fairly good correlation between column two, the logarithmic receiver results, and column four, the theoretical resolution for a 100-nanosecond pulse. Similarly, column three, the linear receiver results, and column five, the theoretical resolution for a 60-nanosecond pulse, show a fairly good correlation. As discussed in Paragraph 4.3.3.2, the logarithmic receiver pulse output with the 60-nanosecond test pulse input has an effective 95-nanosecond pulse width, and the linear receiver output pulse width is on the order of 70 nanoseconds.

It is evident that the observed range resolution is reasonably close to the computed values and that the range resolution is limited by the combination of effective pulse width and the nominal spot size of the PPI display. For the short range scales, the resolution approaches the pulse width resolution limits but is strongly influenced by the nominal spot size. For example, on the 2-nmi scale, the effect of the finite spot size is effectively double the observed displayed target blip. For longer range scales, the nominal spot size becomes the major factor in limiting the nominal target blip size and consequently the effective range resolution.

4.3.5 Sensitivity Time Control Performance

The PPI displays of the manual traffic system at YBI have sensitivity time control, which is used as an operator aid for those conditions

in which there is excessive clutter displayed on the PPI display. The clutter return from surface waves can be of such a height so as to saturate extensive regions of the display. For uniform sea state conditions in the coverage area, the clutter return can be expected to fall off approximately inversely as the range to the fourth power. The STC is designed to control the gain of the video amplifier in the PPI in a manner such that the gain is increased in an inverse relationship to the expected clutter return (i.e., as the fourth power of range).

Nominally, the control signal relationship may be approximated by voltage that decays from maximum video gain reduction to minimum gain reduction in an exponential fashion.

Figure 4-41 illustrates the three STC control voltage characteristics that are available. One of these three may be selected by means of a panel control. Position 1, or STC 1, provides a control voltage that holds the video gain at a minimum for 3.5 microseconds, equivalent to a range of 584 yards, and then decays exponentially to full video gain in 21.5 microseconds (corresponding to a range of 4175 yards). Position 2, or STC 2, holds the video gain at minimum for 7.5 microseconds, corresponding to a

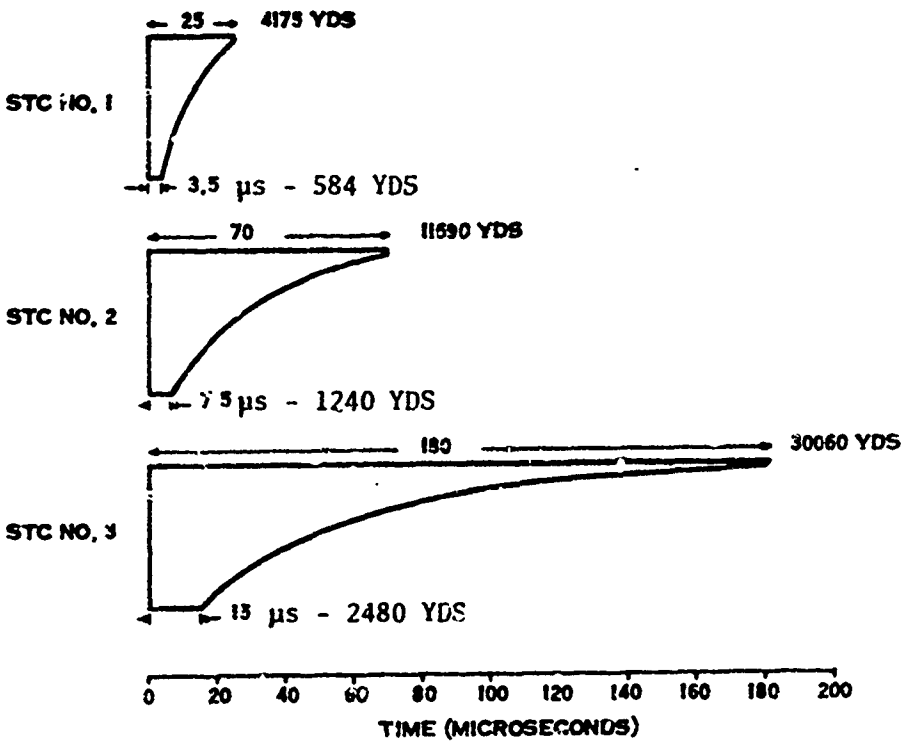

FIGURE 4-41. STC control voltage as a function of time.

range of 1240 yards, and then increases video gain exponentially during a period of 62.5 microseconds (corresponding to a range of 11,690 yards). Position 3, or STC 3, holds the video gain at a minimum for 15 microseconds (2480 yards) and then exponentially increases the video gain to normal in 165 microseconds (30,000 yards). The selection of a specific STC function position is at the discretion of the operator who will select that position providing the best PPI display performance. It should be emphasized that the use of the STC does not directly affect the detection probability, since the target echo signal must be greater than the clutter signal in amplitude or it will not be seen. Obviously, the STC will assist by providing a greater contrast between the target echo and the clutter on the display by preventing saturation by clutter return in the vicinity of the target.

Some examples of the use of the STC in providing a cleaner and more easily interpreted display are shown in Figures 4-42 through 4-47. Figures 4-42 and 4-43 are photographs of the YBI radar display on the 6-nmi range scale with and without the use of the STC. In Figure 4-42, the clutter to the north of YBI is noticeable although not too objectionable. In Figure 4-43, the STC is set to position 2, and the clutter at short range is dramatically reduced and substantially reduced at the longer range. The clutter from Treasure Island has been essentially eliminated.

Figures 4-44 and 4-45 show the effect of STC on the 16-nmi range scale. In Figure 4-44, a large portion of the near range coverage is saturated by the clutter return. In Figure 4-45, the STC has been set to position 3, and the improvement is obvious.

Figures 4-46 and 4-47 show the usefulness of STC for the PTB radar. Figure 4-46 shows the display for an 8-nmi range scale without the use of STC. In Figure 4-47, the STC has been set to position 3 with a very obvious improvement in display readability.

It should be noted that the operator had to exercise caution in manipulating the video gain because in some cases with small targets that were about the same signal strength as the clutter, the STC attenuation would simultaneously suppress the target and the clutter. Since these settings are critical, it would appear to be more functional to substitute a variable STC range setting instead of the three fixed positions that are currently available.

4.3.6 Fast Time Constant Performance

The PPI displays also have a fast time constant, FTC, display option. FTC means that the time constant of the ac coupling between one of the video amplifier stages is smaller thant that necessary to provide

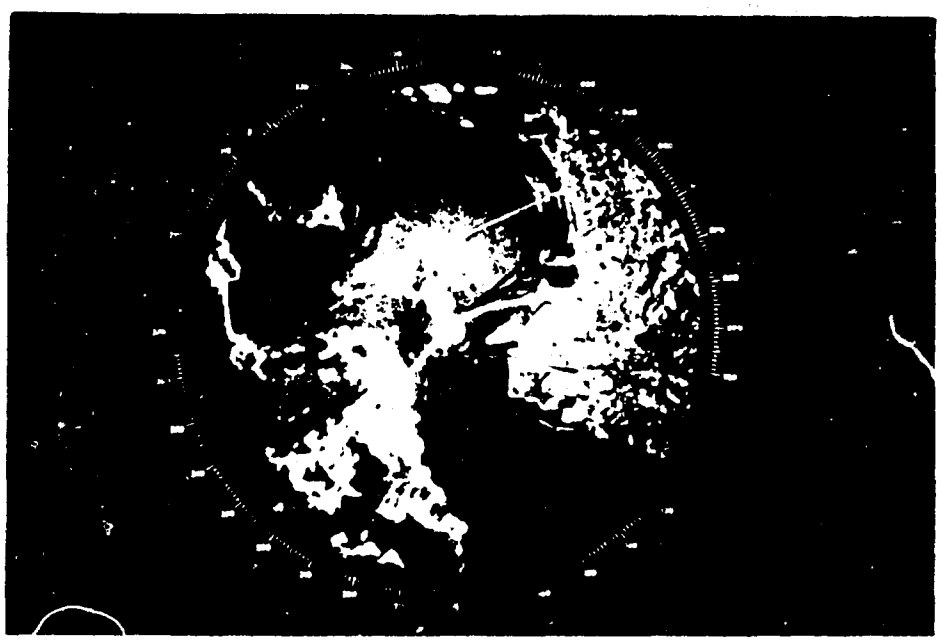

FIGURE 4-42. PPI display of YBI radar with STC off - centered 6-nmi range scale.

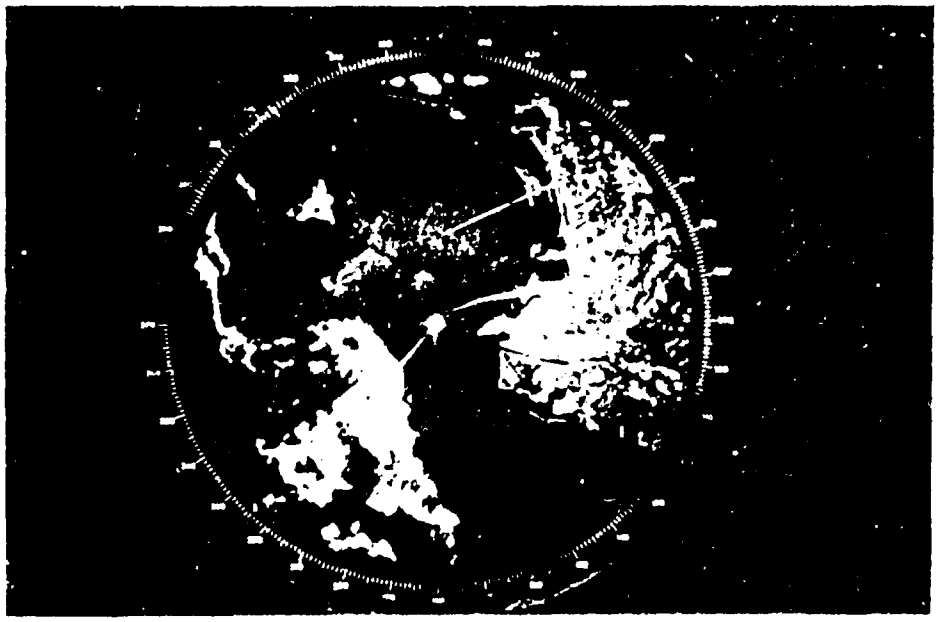

FIGURE 4-43. PPI display of YBI radar with STC set to position 2 - centered 6-nmi range scale.

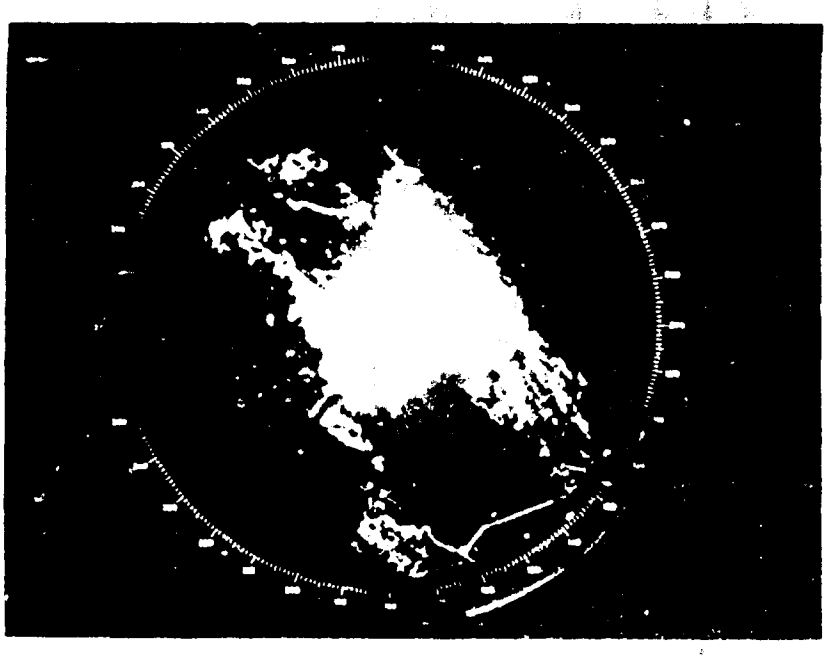

FIGURE 4-44. PPI display of YBI radar with STC off - centered 16-nmi range scale.

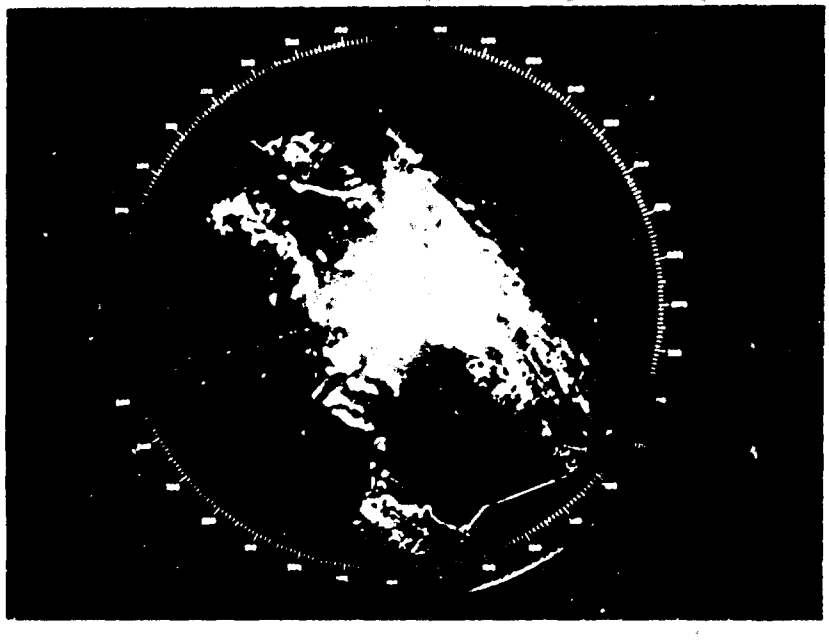

FIGURE 4-45. PPI display of YBI radar with STC set to position 3 - centered 16-nmi range scale.

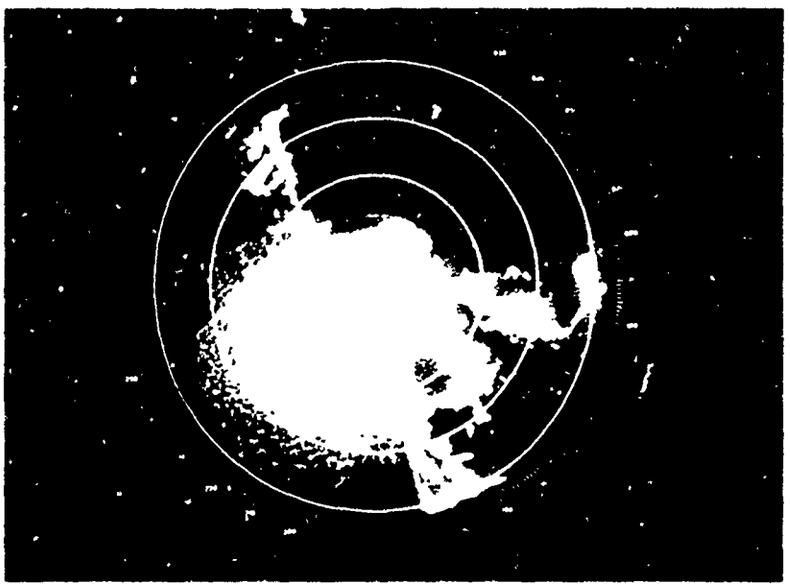

FIGURE 4-46. PPI display of PTB radar with STC off - centered 3-nmi range scale.

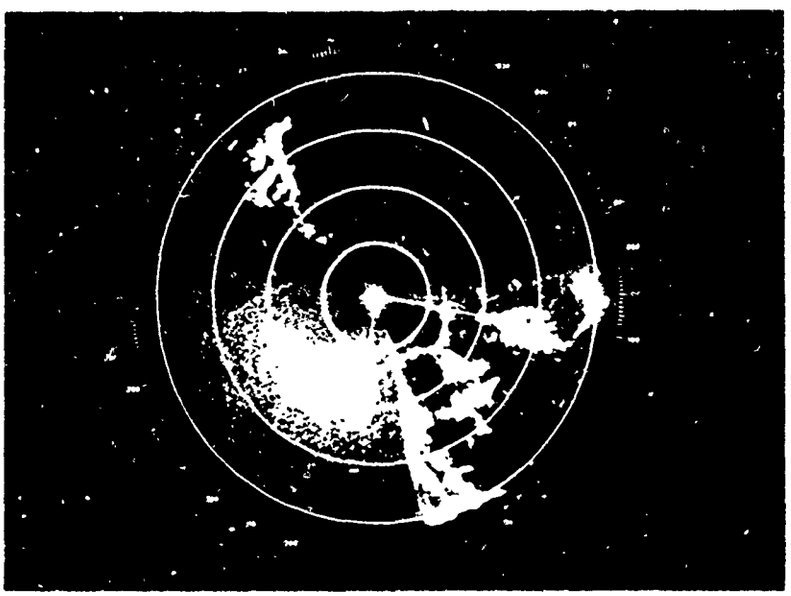

FIGURE 4-47. PPI display of PTB radar with STC set to position 3 - centered 3-nmi range scale.

adequate low frequency pulse fidelity and, in fact, the time constant is chosen to give essentially a differentiating action on the received pulse. The purpose of the differentiating action is to break up large blocks of clutter and thereby aid in the detection of targets in clutter. In order for the target to be detected, it still must have a larger signal return than the average level of the clutter, with the usual signal-to-noise ration requirements still holding. The most obvious effect of the use of FTC is a reduction of the extent of the clutter on the PPI display that is certainly an aid to the operator in distinguishing targets from the clutter.

Figures 4-48 and 4-49 are sample photographs taken during a period of heavy clutter in the YBI coverage area with and without FTC. It is pertinent to note that circular polarization of the antenna was used when these photographs were made. A comparison of Figure 4-48 with 4-49 indicates that the FTC does tend to reduce the saturating effects of the clutter on the display by breaking up the clutter into smaller randomly distributed noise-like blips. It should also be noted that the outlines or edges of the various fixed targets are displayed, whereas the balance of the target is darkened. For example, the outline of Alcatraz Island is shown in Figure 4-49; however, in Figure 4-48, the visible portion of the island is solidly painted on the display. As previously discussed in Paragraph 4.3.2, clutter rejection is maximized by the use of the shortest transmitted pulse width feasible.

4.3.7 Test Target Calibration

Daily system operability tests of the VTS radars should be made in order to provide a quantitative measure of system performance, to monitor system performance trends, and to provide a quantitative measure of the need for preventive or periodic maintenance. Normally, there will be some variation in the nominal parameters of the radar from day-to-day as noted in Table 4-8, which presents a summary of measurements made on the radar at YBI during the period from 6 February through 16 February 1973.

A comprehensive radar system test would include the measurement of the transmitter power output, the pulse width, the transmission line losses, the antenna power gain, the receiver noise figure, the receiver minimun discernible signal, and the receiver gain. Some of these factors can be measured easily at the radar site. Others such as the transmission line loss and antenna gain are difficult and entail extensive radar down time. To make such a comprehensive series of tests on a daily basis would require an inordinate amount of time and effort. A simpler, faster test that would provide an overall measure of system performance would utilize a reflector of known equivalent cross section at a known range.

The daily system operability test would then consist of a measurement of the received signal power. In addition to the reflector, a

FIGURE 4-48. PPI display of YBI radar without FTC; 4-nmi range scale; circular antenna polarization and logarithmic IF with narrow pulse transmission.

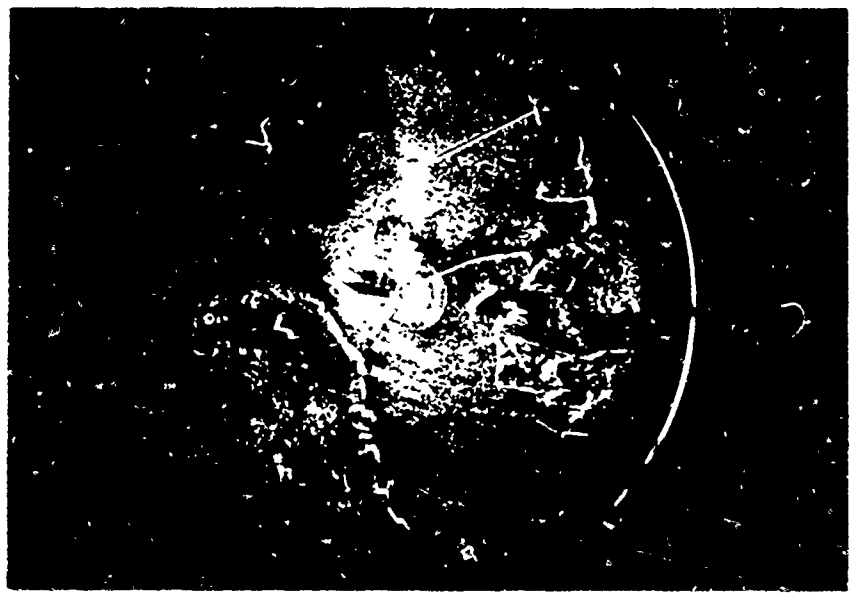

FIGURE 4-49. PPI display of YBI radar with FTC; 4-nmi range scale; circular antenna polarization and logarithmic IF with narrow pulse transmission.

TABLE 4-8. Summary of VTS radar parameter measurements at YBI.

Date (February 1973)	PRF (pps)	Pulse Width (nanoseconds)	Peak Power (dBm)	MDS (dBm)	Frequency (Megahertz)
6	4000	42	+74.6	-93	9437
	4000	205	+75.7		
	2500	42	+75.6		
	2500	205	+77		
	1000	42	+75.7		
	1000	205	+77.2		
7	4000	50	+74	-95	9438
	4000	200	+75.7		
	2500	50	+74.4		
	2500	200	+76.9		
	1000	50	+75.4		
	1000	200	+77.0		
8	4000	43	+76.1	-96	9438
	4000	200	+77.3		
	2500	43	+76.4		
	2500	200	+78.5		
	1000	43	+77.5		
	1000	200	+75.2		
9	4000	45	+76.4	-93	9438
	4000	205	+78.6		
	2500	45	+76.3		
	2500	205	+79.5		
	1000	45	+77.7		
	1000	205	+79		
12	4000	45	+75.5	-95	9438
	4000	200	+77.4		
	2500	45	+75.6		
	2500	200	+78.5		
	1000	45	+76.8		
	1000	200	+79		

TABLE 4-8 (Continued)

Date (February 1973)	PRF (pps)	Pulse Width (nanoseconds)	Peak Power (dBm)	MDS (dBm)	Frequency (Megahertz)
14	4000	50		-93	9438
	4000	200			
	2500	50			
	2500	200			
	1000	50			
	1000	200			
15	4000	45	+75.7	-93	9435
	4000	200	+77		
	2500	45	+76		
	2500	200	+78.4		
	1000	45	+77.5		
	1000	200	+77.2		
16	4000	50	+76.4	-93	9438
	4000	200	+78		
	2500	50	+76.2		
	2500	200	+79.4		
	1000	50	+78.2		
	1000	200	+79		
Mean Values	4000	46.3	+75.6	-93.9	9437.5
	4000	201	+77.2		
	2500	46.3	+75.8		
	2500	201	+78.4		
	1000	46.3	+77.1		
	1000	201	+77.8		

calibrated signal generator is required to provide a calibrated signal input to the receiver that can be compared with the target reflected signal. The standard reflector should be one that is relatively insensitive to orientation toward the radar or rigidly attached to a fixed mounting structure that has an equivalent cross section not more than one-tenth of that of the reflector.

At the present, calibrated reflectors are not installed in the coverage area of the VTS radars. A number of buoys in the coverage area of each radar were therefore selected as possible interim standard reflectors. The effective reflecting cross section of the buoys was determined in the manner described in Paragraph 4.3.2 (i.e., the reflected signal power from the buoy was compared to a calibrated pulse injected into the receiver at the radar operating frequency and the cross section computed from the radar equation using the known parameters of range, antenna gain, radiated power, and line losses).

The buoys that were calibrated for the YBI radar included the South Channel Marker #3, Buoy #1 East of Hunters Point, NAS Buoy #1, and South Channel Marker #6. These buoys are located as shown in Figure 4-50. The computed equivalent echoing areas of the buoys are tabulated in Table 4-9.

TABLE 4-9. List of calibrated buoys in the YBI radar coverage area.

Buoy Identification	Range (yards)	Received Power (dBm)	Cross Section (square meters)
South Channel Marker #3	17,300	-57.3	225
Hunters Point #1	8500	-63	3 6
NAS #1	4500	-51	7.2
South Channel Marker #6	20,500	-60	286

Note: The transmitter power output was +76.8 dBm.

The buoys calibrated for the PTB radar included Channel Marker Buoys #1, #2, #8, A, and B. The computed equivalent echoing area for each buoy is given in Table 4-10, and the location of the buoys is shown in Figure 4-51.

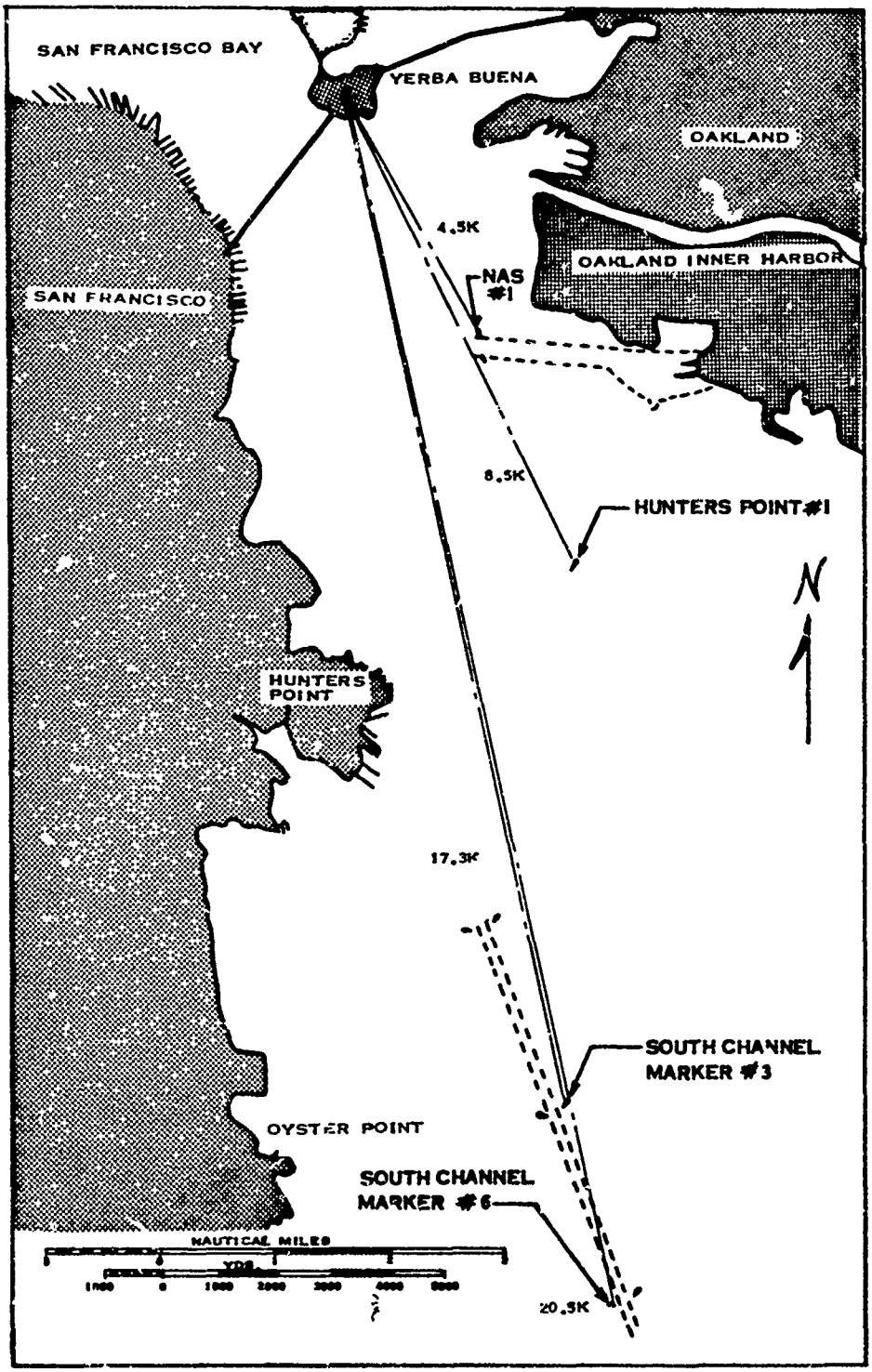

FIGURE 4-50 Location of the buoys calibrated for YBI radar.

TABLE 4-10. List of calibrated buoys in the PTB radar coverage area.

Buoy Identification	Range (yards)	Received Power (dBm)	Cross Section (square meters)
Channel Marker #1	10,200	-67	1.3
Channel Marker #2	11,300	-75	1.0
Channel Marker #8	7300	-70	1.07
Channel Marker A	23,700	-84	2.8
Channel Marker B	29,300	-85	5.0

Note: The transmitter power output was 75.5 dBm.

4.3.8 Radar Test Points and Test Equipment

During the testing of the VTS radars, it was found that the manufacturer of the radars had not provided any test points on the printed-circuit cards of the radar. This makes it a very time-consuming effort to conduct routine checks on the radar. The radar must be shut down, the board placed on a card extender, and then wait 3 to 5 minutes for the radar to cycle out before resuming work.

Therefore it is suggested that future VTS radar systems include the following minimum test features:

a. A 30-dB bidirectional coupler in the output of each transceiver to allow for daily routine power, MDS, and VSWR checks and off line tests of the standby transceiver without interference with the on line transceiver.

b. Each individual circuit card provided with readily accessible test points for all the critical functions of that card. (This will allow maintenance personnel to tell easily if that card is performing its job properly or to monitor a specific function for a short or long period of time without having to shut down the radar.)

It is also suggested that future radar systems be provided with a built-in test set to enable the maintenance personnel to perform daily routine checks on the radar. The test set shouls have at least the following minimum test features: I-band rf signal generator, pin diode modulator, power meter, frequency meter, and precision attenuator.

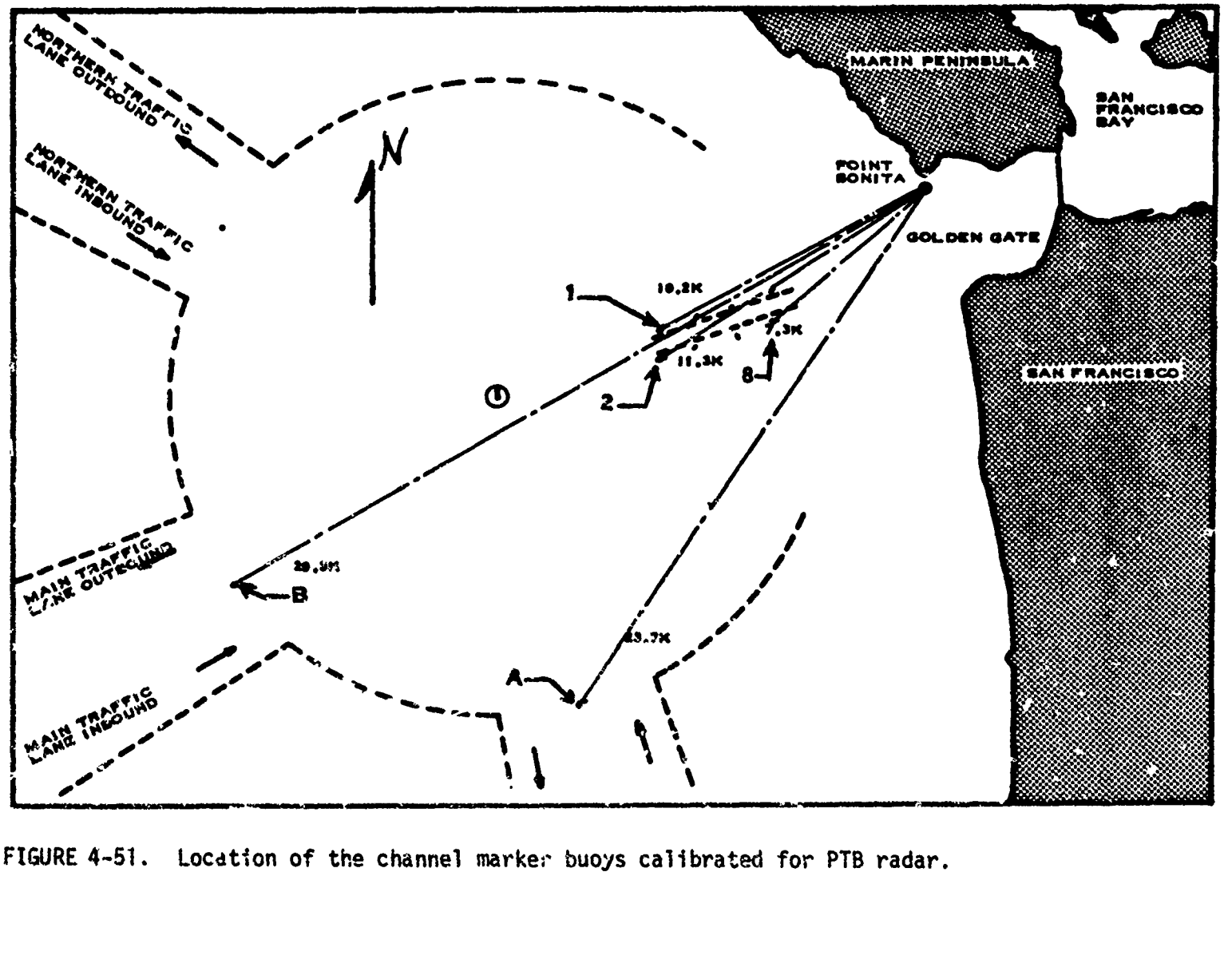

FIGURE 4-51. Location of the channel marker buoys calibrated for PTB radar.

4.3.9 Performance Characteristics Summary

A summary of the measured performance characteristics is given in Table 4-11. This table also includes, where applicable, the performance specification or expected performance level for each characteristic. It should be noted that the only items failing to meet the expected performance levels were the uniform antenna coverage requirements as a function of range from 400 yards to 8 nmi for the YBI radar, the somewhat excessive noise figure for all receivers, and the slightly less than specified IF bandwidth of one of the logarithmic receivers and of the experimental linear receiver.

TABLE 4-11. Comparison summary of the measured system parameters and the specified/expected specifications for each parameter.

Parameter	Specified/Expected	Measured
Antenna		
Azimuth beamwidth	0.3 degrees	0.277 degrees
Maximum antenna gain	40.9 dB	41.3 dB
Elevation beamshape	$\csc^2$	$\csc^2$
Sidelobe levels		
Azimuth within ±10 degrees of main lobe	Greater than 25 dB down relative to main lobe	-30.5 dB
Outside ±10 degrees of main lobe	Greater than 25 dB down relative to main lobe	Greater than -30.5 dB
Elevation	Greater than 15 dB below main lobe	Greater than 15 dB
Radiated Power (incident power at monitoring point)		
YBI		
Circular polarization	-1.1 dBm	-1.0 dBm
Linear polarization	+1.9 dBm	+1.8 dBm
PTB		
Circular polarization	-6.0 dBm	-4.2 dBm
Linear polarization	-3.0 dBm	-1.0 dBm
Transmitted Pulse	50 ±10 nanoseconds 200 ±20 nanoseconds	50 nanoseconds 190 nanoseconds
Received Pulse Response		
Linear receiver (60-nanosecond test pulse at 3-dB level)	70 nanosecond 3-dB width; 50 nanosecond rise and fall	70 nanosecond 3-dB width; 60-nanosecond rise and fall
Logarithmic receiver (60-nanosecond test pulse)	75 to 100 nanosecond 0.707 amplitude width; 50 to 60 rise and 60 to 100 nanosecond fall	95 nanosecond pulse width; 65 nanosecond rise and 50 nanosecond fall

TABLE 4-11 (Continued)

Parameter	Specified/Expected	Measured
Receiver Bandwidth Logarithmic receiver Short pulse mode	18.6 ±2 MHz	16 MHz (YBI Number 2); 21 MHz (PTB Number 1); 17.6 MHz (PTB Number 2)
Long pulse mode	9.6 ±1.9 MHz	16 MHz (YBI Number 2) 14.2 (PTB Number 2)
Linear receiver (independent of pulse width)	28	16 MHz (YBI Number 1) 18 MHz (PTB Number 2)
Receiver Noise Figure	Less than 6 dB	6.8 (YBI Number 1); 7.5 (YBI Number 2); 9.0 (PTB Number 1); 8.9 (PTB Number 2)
Logarithmic Receiver Transfer	80 dB dynamic range	Over 45 dB range
	Logarithmic transfer with ±2 dB tolerance to best fit straight line fit	±3 dB tolerance (YBI 2) ±3 dB tolerance (PTB 1) ±1 dB tolerance (PTB 2)
	Equal return at 400 yards and 8.0 nmi. Not less than return at 400 yards and 8.0 nmi for any intermediate range for fixed size target	Essentially constant return 2500 to 8000 yards; 10-dB hole at 1400 yards; falloff as R^{-4} beyond 10,000 yards
Maximum Detection Range Clear environment YBI (4 square meter target)	9.5 nmi	15.6 nmi (linear); 13.3 nmi (circular)
PTB (4 square meter target)	15.5 nmi	Not measured

TABLE 4-11 (Continued)

Parameter	Specified/Expected	Measured
Maximum Detection Range (continued)		
Sea State 3/clutter		
YBI (4 square meter target)	3.6 nmi	4.2 nmi (linear on 3.6 square meter target)
PTB (1 square meter target)	2.5 nmi	3.6 nmi (linear on 1.07 square meter target)
Angular Resolution	0.3 degrees	.35 degrees
Range Resolution		
2 nmi scale	75 feet (logarithmic) 55 feet (linear)	80 feet (logarithmic) 60 feet (linear)
4 nmi scale	100 feet (logarithmic) 80 feet (linear)	90 feet (logarithmic) 90 feet (linear)
6 nmi scale	125 feet (logarithmic) 105 feet (linear)	130 feet (logarithmic) 130 feet (linear)
8 nmi scale	150 feet (logarithmic) 125 feet (linear)	180 feet (logarithmic) 170 feet (linear)
16 nmi scale	245 feet (logarithmic) 225 feet (linear)	230 feet (logarithmic) 290 feet (linear)
Sensitivity Time Control		Appeared to aid in enhancing contrast of targets in clutter (subjective assessment of clutter rejection)
Fast Time Constant		Appeared to aid in enhancing contrast of targets in clutter (subjective assessment of clutter rejection)

SECTION 5

CONCLUSIONS AND RECOMMENDATIONS

5.1 GENERAL

This section presents the major conclusions reached as a result of the tests on the VTS manual radar system and the related recommendations.

It is difficult to capture completely the performance of the FPS-109 radar in a tabulated list of measured engineering and radar parameters. Therefore, the following discussion is presented as a qualitative commentary based upon the daily use of the radar in routine detection and tracking exercises that were conducted during teh 2-month test period.

The FPS-109 is an excellent radar for the purpose for which it was designed. It allows an operator to perform his function of target detection and tracking on a large uncluttered PPI display with ease and precision in a variety of weather and sea conditions. Targets, both large (super tankers) and small (buoys), docks, bridges, islands, and large land masses are easily isolated and identified out to 16 nmi on the PPI display. The capability of detecting and resolving these various targets stems from the basic radar design parameters of narrow pulse width and narrow beam width, coupled with the flexibility of many modes and operator features of the PPI display (such as variable range scales, PPI center offset, variable video and sweep intensity settings, FTC, and STC).

Surveillance of the total San Francsico Bay area is further enhanced by the utilization of the five individual PPI displays that are centered by the offset feature to five overlapping regions of the Bay. In this mode, high resolution range scales can be used to enhance target discrimination by utilizing the high resolution design features of the radar over the entire Bay area and not just in the immediate vicinity of the radar site. This feature was particularly helpful when tests were conducted at various ranges and bearings in the Bay.

The variable prf and the long pulse features of the radar were seldom used in the routine detection and tracking of targets. The short pulse and the 2500 prf were utilized throughout most of the test, and there were no situations that occurred that seriously demanded a change in these settings. From an experimental viewpoint, these settings were useful

to determine the effect on detection and tracking; however, in future operational systems, consideration should be given to the particular port and function of the radar before such features are included in the design.

The use of the FTC was also very helpful in detecting and tracking targets in clutter conditions. From an operator point-of-view, FTC would effectively break up large solid areas of clutter into a small dotted pattern. This effectively increased the contrast between the solid target echo and the random clutter returns that surrounded the target. It should be pointed out that the target had to be moderately larger than the clutter before the target was easily distinguished from the clutter. FTC is a useful feature, particularly when small targets are being tracked in a dense clutter area, and should be seriously considered for future marine surveillance radars.

The use of the STC was found to be another useful feature that assisted in the detection and tracking of short range targets in high clutter regions. This situation was particularly true when the target was in a tide rip region. The use of STC effectively suppressed background sea clutter when the test target return was sufficiently stronger than that of the sea clutter. By setting the STC and adjusting the radar video gain, the operator could suppress the sea clutter to the point where it disappeared from the scope while the target remained. It should be noted that the operator had to exercise caution in maniuplating the video gain because in some cases with small targets that were about the same signal strength as the clutter, the STC attenuation would simultaneously suppress the target and the clutter. Since these settings are critical, it would appear to be more functional to substitute a variable STC range setting instead of the three fixed positions that are currently instrumented.

The circular polarization design feature was particularly useful in helping to detect targets in rain squalls. On several occasions when the polarization was switched to circular, small targets that were previously obscured by the rain squall became detectable. Unfortunately, this technique was used only to detect targets in squalls at short range and in the immediate vicinity of the YBI radar; therefore, the total effect of using circular polarization at increased ranges was not cataloged. However, it is expected that since the effect of clearing up the scope in the vicinity of the rain squall was so dramatic at the shorter ranges, similar effects would be obtained at longer ranges. In future marine surveillance radars, consideration should be given to including this antenna polarization feature.

Throughout the test period, logarithmic and linear IF amplifiers were used in the radar alternately to determine if one device performed better than another. Unfortunately, no clutter or heavy rain situations occured that would enable these two receivers to be exercised to their performance limits. Therefore, an appropriate comparison could not be made. Although

both receivers provided the same good detection on small targets at long ranges, a direct quantitative comparison showed no significant differences in performance. Consideration should be given, however, to the design characteristics of the two amplifiers and their differences. The linear IF amplifier has a known dynamic range of 40 dB, which is only one-half that of the logarithmic IF amplifier. In severe rain squalls or heavy clutter situations, a large target would be obscured in the rain or clutter if the returns from the target, the rain, and the clutter simultaneously exceed the dynamic range of the linear receiver. When this situation occurs in the logarithmic receiver, the target is expected to be detected from the rain and clutter background since the target would appear as a stronger signal on the PPI display. In the design of future VTS radars, serious consideration should be given to using the logarithmic IF amplifier.

5.2 CONCLUSIONS

5.2.1 Operational Parameters

5.2.1.1 Antenna Beam Patterns. The azimuth and elevation beam patterns for horizontal polarization of the YBI antenna were found to be essentially identical to the patterns measured at the manufacturer's antenna test range. The azimuth 3-dB beamwidth was 0.277 degree, which is well within the specified 0.3 degree. The sidelobe levels were down at least 30 dB from the peak of the beam.

5.2.1.2 Radiated Power. Measurements of the radiated power made in the far field for the VTS radars indicated that the power radiated was within 1 to 2 dB of the computed power levels based on measured transmitter power output, line losses, and antenna gain.

5.2.1.3 Transmitter and Receiver Parameters. The conclusions reached as a result of the tests on the transmitters and receivers of the VTS radars are summarized in the following paragraphs.

5.2.1.3.1 Transmitted Pulse. The narrow transmitted pulse of 50 nanoseconds as measured at PTB and YBI was found to have an exponential rise time of approximately 35 nanoseconds and a fall time of approximately 45 nanoseconds (as measured at the 3-dB amplitude points). The transmitted 200-nanosecond pulse had an exponential rise time of 45 nanoseconds and a pulse width between the 3-dB amplitude points of 190 nanoseconds.

5.2.1.3.2 Receiver Pulse Response. The receiver pulse response was measured by injecting a test signal at the radar operating frequency and observing the receiver output pulse. A test pulse with a 60-nanosecond width at the 3-dB level, a 25-nanosecond rise time, and a 20-nanosecond fall time between the 10- and 90-percent amplitude levels was used.

The observed pulse output from the logarithmic receiver had a 60-nanosecond width at the 3-dB level, a 50-nanosecond rise time, and a 40-nanosecond fall time between the 10- and 90-percent amplitude levels when measured on a logarithmic amplitude scale. The apparent output pulse characteristics when measured on a linear amplitude scale indicated a 95-nanosecond pulse width at the 3-dB level, a rise time of 65 nanoseconds, and a fall time of 55 nanoseconds. The apparent pulse stretching when the logarithmic amplifier is used is a normal characteristic of such amplifiers. By simple scaling, it would be expected that the transmitted narrow 50-nanosecond pulse would be apparently stretched to an 80-nanosecond pulse width. The apparent pulse stretching degrades intrinsic range resolution from the value of 25 feet expected for a transmitted 50-nanosecond pulse to approximately 40 feet.

The observed pulse output from the linear receiver had a 70-nanosecond pulse width at the 3-dB level, a 50-nanosecond rise time, and an 80-nanosecond fall time. Again, simple scaling would suggest that the 3-dB amplitude pulse width would be approximately 60 nanoseconds with the 50-nanosecond transmitted pulse. The corresponding intrinsic range resolution is approximately 30 feet.

5.2.1.3.3 Receiver Bandwidth. The 3-dB bandwidth of the intermediate frequency amplifiers of the radar receivers was measured at YBI and PTB. The results are tabulated in Table 5-1.

TABLE 5-1. Measured receiver system bandwidths.

Location	Transceiver Number	Amplifier Type	Transmitter Pulsewidth (nanoseconds)	Bandwidth (Mhz)	
				Expected	Measured
YBI	1	Linear		28	16*
	2	Logarithmic	50	18.6 ±2	16*
	2	Logarithmic	200	9.6 ±1.9	16*
PTB	1	Logarithmic	50	18.6 ±2	21*
	2	Logarithmic	50	18.6 ±2	17*;17.6**
	2	Logarithmic	200	9.6 ±1.9	14.2*
	2	Linear		28	18*

* 60-nanosecond test pulse
** 1.5-microsecond test pulse

It was found that the bandwidth of the logarithmic receivers for the narrow pulse mode of radar transmission at PTB were within the expected tolerance. The logarithmic receiver at YBI in transceiver number 2 was slightly smaller than the expected value for the narrow pulse mode of transmission, but this is not considered to be a serious deficiency.

The bandwidths of one logarithmic receiver at YBI and one logarithmic receiver at PTB were measured for the wide pulse mode of transmission and found to be somewhat greater than the expected limits. The excessive bandwidths observed are not considered to be significant deficiencies since they will have only a second order effect on radar detection performance.

The bandwidth of the number 1 transceiver at YBI and the number 2 transceiver at PTB were measured with the experimental linear IF amplifier installed in each. It should be noted that the measured bandwidth was considerably less than the expected value in each case. The observed values are considered acceptable, however, because they are within the expected tolerance bandwidth limits for the normally installed logarithmic amplifiers.

5.2.1.3.4 Receiver Noise Figure. The measured noise figure of the receivers indicated that all the receivers had a higher noise figure than specified by factors of 0.8 to 3.0 dB. The excess noise figures observed are not considered to be serious problems.

5.2.1.3.5 Receiver Transfer Function. The logarithmic transfer functions of the receivers at YBI and PTB were measured by injecting a pulsed signal at the operating frequency into a transmission line bidirectional coupler. The receivers were found to have an essentially logarithmic transfer function between the input levels of -85 and -40 dBm. The measured logarithmic transfer best fit to a stratight line characteristic was within ± 3 dB for one receiver and within approximately ± 2 dB for the two other receivers. (The specified allowable deviation is ± 2.0 dB.)

5.2.1.4 PPI Characteristics. Qualitative tests made on representative PPI displays at YBI indicated no apparent distortion of the displays and an apparent good relative accuracy of the movable range and bearing cursors.

5.2.1.5 Microwave and UHF Control Links. The tests of the microwave and UHF control links, conducted to determine the fade margins, indicate that the microwave link has a fade margin of at least 30 dB and the UHF control link has a fade margin of at least 23 dB.

5.2.2 Performance Measurements

5.2.2.1 YBI Antenna Elevation Coverage. The tests made to determine the operational characteristics of the cosecant-squared pattern of the YBI antenna indicated that the cosecant-squared characteristic extends from approximately 3000 to 8000 yards. Beyond 8000 yards, the echo return is essentially proportional to range to the fourth power. The normalized echo return at 1400 yards is 10 dB down from the return at 3000 yards. The radar specification requires that the elevation beamwidth of the YBI antenna be designed so that equal received signal strengths are obtained in the main lobe for equal size targets located at 1200 feet and 8.0 nmi and that received signal strength for the same size target at ranges between the limits shall not be less than these levels.

5.2.2.2 Maximum Detection Range. Maximum detection range tests were made in clear and sea state 3 conditions for the YBI radar. The experimental results show that the maximum detection range with linear polarization while the radar is tracking a 4 square meter target is 15.5 nmi, which exceeds the YBI specification requirements of 9.5 nmi and equals the PTB requirements of 15.5 nmi. With circular polarization, the maximum detection range was observed to be 13.3 nmi for a 4 square meter target and 11.8 nmi for a 1 square meter target, both measured figures exceeding the required YBI detection range of 8.0 nmi.

Sea state 3 detection measruements were made for the YBI and PTB radars using buoys whose equivalent cross section had been measured as targets. Blip-scan measurements on buoy number 1 at Hunters Point with the YBI radar averaged 0.8 for a series of tests. Buoy number 1 has an echoing cross section of 3.6 square meters and is at a range of 4.14 nmi, which is greater than the required detection range of 3.6 nmi for a 4 square meter target. Similarly, measurements from PTB of the return from channel marker number 8 has an equivalent echoing area of 1.07 square meters and is at a range of 3.6 nmi, which is greater than the required 2.5 nmi for a 1 square meter target. The system requirements in sea state 3 are therefore considered to be met.

Tests of the circular polarization mode of the antenna indicated that rain clutter was effectively reduced in amplitude and the detection of targets, which were otherwise masked with linear polarization, was possible.

5.2.2.3 Angle Resolution. The results of the angle resolution tests indicated an effective operational beamwidth discrimination of 0.35 degree.

5.2.2.4 Range Resolution. The range resolution as observed on the PPI displays was found to be nearly a direct function of the range scale in use. The resolution observed, when linear and logarithmic intermediate amplifiers and a 60-nanosecond test pulse pair were used, is tabulated in Table 5-2.

TABLE 5-2. Observed range resolution obtained on PPI displays.

Range Scale (nmi)	Observed Resolution (feet)	
	Logarithmic IF	Linear IF
2	80	60
4	90	90
6	130	130
8	180	170
16	230	290

5.2.2.5 Sensitivity Time Control. The PPI displays have three STC settings that the operator can select to best match current clutter conditions. A qualitative evaluation of the STC capabilities indicated satisfactory PPI clutter rejection performance could be achieved under most clutter conditions observed at YBI and PTB by use of at least one of the STC positions available.

5.2.2.6 Fast Time Constant. The PPI displays have an FTC option that is designed to assist the operator when sea clutter interference makes target detection difficult. Observations were made of the FTC clutter suppression on a number of occasions for the YBI and PTB radars, and a substantial reduction of clutter return was found to be obtainable.

5.2.2.7 Test Target Calibration. Four buoys were selected as test targets for the YBI radar, and five buoys were selected for the PTB radar. The return echo power from each buoy was measured, and the transmitted power was measured. The equivalent echoing cross section of each buoy was computed from the radar equation. The calibrated buoys can be used as test targets of known cross section in checking the overall performance of each radar on a regular basis.

5.2.2.8 Test Points. During the tests, it was found that the manufacturer of the radars had not provided test points on the printed-circuit cards of the radar. This makes it a very time-consuming effort to conduct routine checks on the radar. The radar must be shut down, the board placed on a card extender, and then it is necessary to wait for 3 to 5 minutes for the radar to cycle out before resuming work.

5.3 RECOMMENDATIONS

5.3.1 Antenna Sidelobes

It is recommended that specifications for future vessel traffic system radars define the sidelobe levels and feedhorn spill-over levels relative to the main beam at each elevation angle of interest when a cosecant-squared elevation pattern is required. The YBI antenna sidelobe and spill-over levels are low relative to the main beam at 0-degree elevation angle but become progressively higher relative to the main beam at higher depression angles. The high sidelobe levels are a moderately serious problem when the radar is tracking targets at short ranges.

5.3.2 Antenna Elevation

It is recommended that the antenna elevation angle of the YBI radar be mechanically adjusted upward by 0.5 degree. The magnitude of the variation of received signal strength from a fixed size target as a function of range in the range interval from 1000 to 3000 yards should be reduced by approximately 5.0 dB by this modification.

5.3.3 Test Target

It is recommended that a calibrated reflector be placed in the coverage area of each radar for daily checks of system operability. A suitable target installed at a range that returns a signal level near the MDS for normal operation would provide the operator with a quick check of the system performance.

5.3.4 Test Points and Test Equipment

It is recommended that future vessel traffic system radars include requirements for an adequate number of suitable test points such as waveguide couplers and electronic monitoring points. Specifically, it is suggested that future vessel traffic systems include the following minimun test features:

a. A 30-dB bidirectional coupler in the output of each transceiver to allow for daily routine power, MDS, and VSWR checks.

b. Each individual circuit card be provided with readily accessible test points for all critical functions of the card to allow maintenance personnel to ascertain readily if the card is performing properly or to monitor a specific function for a period of time without requiring that the radar be shut down.

c. A built-in test set be provided to enable the maintenance personnel to perform daily routine checks on the radar. (The test set should have at least the following minimum test features: I-band rf signal generator, pin diode modulator, power meter, frequency meter, and precision attenuator.)

5.3.5 Sensitivity Time Control

Consideration should be given to making the STC adjustments on the PPI displays continuously variable rather than limiting the selection to a few switch settings.

5.3.6 General Design

The AN/FPS-109 (XN-1) radars, as tested, are considered to have excellent performance characteristics. The only features that were found to be of little value at the San Francisco sites were the wide pulse (200 nanoseconds) transmission mode and the 1000 and 4000 pulse repetition rates. As previously pointed out, the narrow pulse transmission mode (50 nanoseconds) and the 2500 pulse repetition rate together with the narrow beamwidth provided excellent resolution capabilities for the area coverage and more than adequate detection performance.

Future vessel traffic system radars should include the majority of the features of the FPS-109 (XN-1) radar [i.e., short pulse transmission (50 nanoseconds), logarithmic receivers, linear and circular polarization, narrow beamwidth (0.3 degree), cosecant-squared elevation pattern, and multiple PPI displays with FTC and STC]. A most desirable additional feature would be built-in test equipment and accessible test points as recommended in Paragraph 5.3.4.

References

(a) U. S. Coast Guard report 732222.01/02, dated March 1973, "San Francisco Vessel Traffic System Comparison Tests of the Raytheon 1605 Harbor Advisory Radar With the AN/FPS-109(XN-1) Vessel Traffic System Radar - Test Results"

(b) U. S. Coast Guard report 732222.02/01, dated April 1973 "San Francisco Vessel Traffic System Test of the AN/FPS-109(XN-1) Vessel Traffic System Manual Radar - Test Plan"

(c) Airborne Instrument Laboratories document, dated 13 April 1973, "Report on Vessel Traffic System - Additional Antenna Testing"

(d) Lawson and U. H. Lenbeck, MIT Radiation Laboratory Series, Volume 24, "Threshold Signals", McGraw-Hill Book Company, Inc., 1950

(e) Radar Handbook, Merrill Skolnik, McGraw-Hill Book Company, Inc., 1979